

Department of Mechanical and Aerospace Engineering

**A Study of the Potential for Reuse of North Sea Oil
and Gas Installations for Wind Turbines**

Author:

Rory Morrison

Supervisor:

Cameron Johnstone

A thesis submitted in partial fulfilment for the requirement of the degree

Master of Science

Sustainable Engineering: Renewable Energy Systems and the Environment

2016

Copyright Declaration

This thesis is the result of the author's original research. It has been composed by the author and has not been previously submitted for examination which has led to the award of a degree.

The copyright of this thesis belongs to the author under the terms of the United Kingdom Copyright Acts as qualified by University of Strathclyde Regulation 3.50. Due acknowledgement must always be made of the use of any material contained in, or derived from, this thesis.

Signed: Rory Morrison

Date: 25/08/17

Abstract

The North Sea is host to two major projects for the UK: decommissioning of oil and gas infrastructure over the next 30-50 years and deployment of offshore wind turbines. This thesis proposes collaboration between these two projects and analyses the technical suitability of the 300+ platforms in the North Sea for retrofitting with 5MW wind turbines.

The analysis is performed via comparison of two models: an oil and gas platform and the same platform retrofitted with a 5MW wind turbine. This is conducted via finite element analysis with extreme wind and wave loads applied. Stresses in the substructure and loading on pilings were compared between models. Additionally, natural frequency differences are also investigated.

In achieving this, a representative platform was selected following the creation and analysis of a platform database which included all types of platform (jacket, floating, gravity based). The selected platform (the steel-jacket Leman BH) was within $\pm 10\%$ topside weight and water depth of 35% of platforms in the UK North Sea. The 5MW wind turbine used was the NREL reference machine.

The possibility of retrofit was found to be highly likely with results of the FEA showing reduced stress in all jacket members with an average reduction of 35% in legs. Loadings on the pilings were reduced by an average of 30%. However, possible challenges were found as natural frequency period was found to increase.

The results are extrapolated across the database and it is estimated there are 128 potential candidates for such a retrofit project.

Acknowledgements

I would like to thank my supervisor, Cameron Johnstone, for his time and involvement in this thesis.

Further thanks to my family for their support, without whom this thesis would not be possible.

Finally, thanks to the good people of the LT501 for their companionship, without whom this thesis would not have been enjoyable.

Contents

1. Introduction	12
1.1. Background	12
1.2. Project Objectives	13
1.3. Project Method Overview	14
1.4. Project Scope.....	15
2. Literature Review	16
2.1. North Sea.....	16
2.2. Wind power	17
Generation theory	18
Infrastructure	19
Substructures	20
Trends in the North Sea.....	21
2.3. Oil and Gas.....	22
Infrastructure	23
Decommissioning	26
2.4. Similar Studies	28
“Fixed Platforms at Ageing Oil Fields – Feasibility Study for Reuse to Wind Farms”, Barros et al, 2017 [30]	28
“Application of an Abandoned Jacket for an Offshore Structure Base of Wind Turbine in Bohai Heavy Ice Conditions”, Wang et al, 2009 [31]	29
2.5. Alternatives use of platforms	29
3. Methodology.....	31
3.1. Database Creation and Analysis:.....	34
3.2. Creation of Models.....	34

Oil and Gas Installation	35
Piles and Soil Conditions.....	36
Wind Turbine.....	36
3.3. Forces Acting on Structure.....	37
Gravitational Loading	37
Wind Loading	38
Wave Loading.....	39
Hydrostatic Force and Current Force	40
3.4. Simulation and Comparison of Forces	41
3.5. Verification of Models and Loading	42
4. Database and Analysis.....	43
4.1. Database creation	43
4.2. Database Analysis	43
Structure type.....	43
Water depth and topside mass	44
Field Installation Characteristics	46
4.3. Representative Installation	46
Comparison to UKCS O&G Stock.....	47
5. Modelling.....	48
5.1. Substructure.....	48
Jacket Modelling Process	49
5.2. Topside	51
5.3. Wind Turbine	52
Tower.....	54
Rotor, Blades, and Nacelle	55

Transition Piece	55
5.4. Jacket Validation	56
6. Forces Acting on Structures	61
6.1. Gravity Loads	61
Dead Loads	61
Live Loads	62
6.2. Wind Load	62
Wind Profile	63
Jacket Wind Load	63
Topside Wind Load	65
Wind Turbine Wind Load	66
Wind loading Validation	69
6.3. Wave Load	70
Wave Profile	70
Substructure Wave Load	72
Other Hydrodynamic Loads	74
Wave Loading validation	74
7. Summary and Simulation	76
7.1. Gravitational Loads	76
7.2. Wind Load	77
7.3. Wave Loading	78
8. Results	79
8.1. Mesh Convergence	79
8.2. Simulation 1 – Gravitational Loads Only	80
8.3. Simulation 2 – Transition Piece Comparison	84

8.4.	Simulation 3 – Full Simulation	86
9.	Discussion.....	92
9.1.	Database Creation and Analysis.....	92
9.2.	Simulation 1: Gravitational Loads Only.	92
9.3.	Simulation 2: Transition Piece	93
9.4.	Simulation 3: Full Simulation	95
9.5.	North Sea Potential.....	98
9.6.	Criticism and Further Study	99
9.7.	General Discussion on the Potential of Retrofit.....	100
10.	Conclusion	102
11.	References.....	104
12.	Appendix.....	107
12.1.	Appendix A - Drawings of Models	107
12.2.	Appendix B - Solidworks model verification.....	110
12.3.	Appendix C - Wind Profile Calculation	112
12.4.	Appendix D - Wave Profile Calculation.....	118
12.5.	Appendix E - Wave Equation Table used for calculation	121
12.6.	Appendix F – Simulation 1.....	122
12.7.	Appendix G – Simulation 2	124
12.8.	Appendix H – Simulation 3	125

List of figures

Figure 2.1: The North Sea with sectors indicated. Courtesy of [8]	17
Figure 2.2: Diagram of wind turbine components. Images courtesy of [11].....	18
Figure 2.3: Layout of a wind farm, image courtesy of [12].....	19
Figure 2.4: Summary of OWT foundations with relative depth, image courtesy of [18]	21
Figure 2.5: Summary of typical wind turbine characteristics with size, courtesy of [22]	22
Figure 2.6: Diagram of a typical oil and gas platform. Substructures shown are jackets. Image courtesy of [24].....	24
Figure 2.7: Supporting structure choice with relative depth for oil and gas platforms. Image courtesy of [27]	26
Figure 3.1: Summary of methodology	33
Figure 4.1: Breakdown of UKCS O&G installations by type	44
Figure 4.2: Topside weight and water depth of UKCS O&G installations with indication of North Sea area by colour	45
Figure 4.3: Leman BH platform (front) with bridge linked BT platform (rear). Image courtesy of [38].....	47
Figure 5.1: Jacket as modelled using Solidworks with the reference drawing used, courtesy of [39].....	49
Figure 5.2: Drawing of topside from decommissioning document [39]. Additional red annotations for reference during geometry simplification.....	51
Figure 5.3: Solidworks model of retrofitted Leman BH platform with 5MW NREL wind turbine	53
Figure 5.4: Properties of the NREL 5MW wind turbine	54

Figure 5.5: Hub and nacelle arrangements as per NREL document.....	55
Figure 5.6: Transition piece by Barros et al (left) with transition piece used in this project (right)	56
Figure 5.7: Simplification of model of jacket for validation	57
Figure 5.8: Dimensioning of hand-calculation model with reference to the CAD model	57
Figure 5.9: Co-ordinate system of the hand calculation model using the related diagram	58
Figure 5.10: Resultant force calculation using theory (via Mathcad).....	58
Figure 5.11: Reaction forces of support (via Mathcad)	59
Figure 5.12: Stress and strain calculation in leg member (via Mathcad).....	59
Figure 6.1: Peak wind velocity with elevation above sea level for the Lemna BH site	63
Figure 6.2: Simplification of transition piece geometry	64
Figure 6.3: Wind loading upon front leg of jacket.....	65
Figure 6.4: Simplification of topside for wind load calculation	66
Figure 6.5: Wind turbine wind load with elevation above sea level.....	67
Figure 6.6: NREL 5MW wind turbine thrust curve with wind speed.....	68
Figure 6.7: Geometry of wind turbine tower and ANSYS FLUENT simulation	70
Figure 6.8: Wave spectra data for site near Lemna BH location. Provided by [41]....	71
Figure 6.9 Maximum horizontal particle velocity and acceleration profiles with water depth (note, these do not occur at the same time).....	72
Figure 6.10: Variation of drag, inertia, and total force on the front leg.....	74
Figure 7.1: LEFT, O&G loading for simulation 1. RIGHT, OWT tower top loading for simulation 1.....	77

Figure 7.2: Full loading of OWT model	78
Figure 8.1: Numbering convention of supports.	79
Figure 8.2: Stress results (Von Mises) of the simulation of gravitational loads only on the O&G model. The result shown is undeformed. Still water level is indicated in blue.	81
Figure 8.3: Stress results (Von Mises) of the simulation of gravitational loads only on the wind turbine model. The result shown is undeformed. Still water level is indicated in orange.....	82
Figure 8.4: Stress results (Von Mises) of the full loading on the O&G transition piece model. The result shown is undeformed.	84
Figure 8.5: Stress results (Von Mises) of the full loading on the wind turbine transition piece model. The result shown is undeformed.....	85
Figure 8.6: Stress results (Von Mises) of the full loading on the O&G model. The result shown is undeformed	87
Figure 8.7: Stress results (Von Mises) of the full loading on the OWT model. The result shown is undeformed	88
Figure 8.8: Fundamental mode shapes of both models.....	91
Figure 9.1: Von Mises stress in front and rear transition pieces with height between models for simulation 3	97
Figure 9.2: Von Mises stress in front and rear legs with height between models for simulation 3.....	97
Figure 12.1: Resultant force at point A.....	110
Figure 12.2: Displacement	110
Figure 12.3: Resultant force in leg.....	111
Figure 12.4: Resultant force in member EF.....	111

Figure 12.5: Resultant force in member EG	112
Figure 12.6: Location of the Leman BH installation off the coast of Norwich.	113
Figure 12.7: Fundamental basic wind velocity map from NA to BS EN 1991-1-4...	114
Figure 12.8: Turbulence intensity of wind with elevation above sea level for Leman BH site	116
Figure 12.9: Peak velocity pressure with elevation above sea level for Leman BH site	117
Figure 12.10: Peak wind velocity with elevation above sea level for Leman BH site	117
Figure 12.11	119
Figure 12.12; From DNV RP-C205	120

List of tables

Table 4-1: Summary of statistics found from the analysis of UKCS O&G installations.	46
Table 5-1: Summary of dimensions and permissible stresses as per ISO 19902. All end conditions are fixed-fixed	50
Table 5-2: Hand and computational study results.....	60
Table 6-1: Summary of calculated gravitational loads	62
Table 6-2: Summary of wind loading and conditions.....	68
Table 6-3: Summary of wave loading.....	73
Table 8-1: Mesh convergence results	80
Table 8-2: O&G - Support reactions for gravitational loads only. Forces and moments in supports 3 and 4 mirror 1 and 2 respectively and are shown in Appendix F.....	82
Table 8-3: Wind turbine – Support reactions for gravitational loads only. Forces and moments in supports 3 and 4 mirror 1 and 2 respectively and are shown in Appendix F	83
Table 8-4: O&G – Stresses in key members for gravitational loads only	83
Table 8-5: Wind turbine – Stresses in key members for gravitational loads only	83
Table 8-6: O&G – Transition piece reactions for full loading. Forces and moments in supports 3 and 4 mirror 1 and 2 respectively and are shown in Appendix G	85
Table 8-7: OWT – Transition piece reactions for full loading. Forces and moments in supports 3 and 4 mirror 1 and 2 respectively and are shown in Appendix G	86
Table 8-8: O&G – Support reactions for full model and full loading. Forces and moments in supports 3 and 4 mirror 1 and 2 respectively and are shown in APPENDIX H.....	88

Table 8-9: OWT – Support reactions for full model and full loading. Forces and moments in supports 3 and 4 mirror 1 and 2 respectively and are shown in APPENDIX H.....	89
Table 8-10: O&G – Member stresses for full loading and full model.....	89
Table 8-11: OWT – Member stresses for full loading and full model.....	90
Table 8-12: Mode shapes and frequencies of different scenarios.....	90
Table 12-1	118

Nomenclature

CNS	Central North Sea
CoM	Centre of Mass
EIA	Environmental Impact Assessment
FEA	Finite Element Analysis
FPSO	Floating Production Storage and Offloading vessel
GBS	Gravity Based Structure
HAWT	Horizontal Axis Wind Turbine
IS	Irish Sea
LNG	Liquefied Natural Gas
MF	Moray Firth
mT	Metric tonnes
NNS	Northern North Sea
NREL	National Renewable Energy Laboratory
O&G	Oil and Gas
OWT	Offshore Wind Turbine
SNS	Southern North Sea
SOR	Statement of Requirements
TLP	Tension Leg Platform
UKCS	United Kingdom Continental Shelf
VM	Von Mises
WoS	West of Shetland

1. Introduction

1.1. Background

The United Kingdom currently finds itself with two large-scale and expensive engineering challenges: decarbonising the energy sector (whilst also increasing generation capacity), and the decommissioning of the North Sea oil and gas infrastructure.

North Sea O&G production began in the 1970s and peak oil was achieved in the year 2000.[1] Production rate in 2017 is 1.3 million barrels of oil and gas equivalent/day, approximately a third of peak oil and continues to decline. With this downturn in productivity many O&G companies are bringing forward plans for decommissioning their offshore infrastructure (which is obligatory as per the OSPAR agreement). The scale of work includes some 300 platforms, 3,000 pipelines, 5,000 wells [2] and many other infrastructures with current estimates for the cost of decommissioning in the UK's territory varying between £17.6 billion [3] and £53 billion [4]. This will result in substantial losses of earnings to the UK government through tax breaks.

Just as infrastructure is being removed from the North Sea more is being deployed. Amongst other technologies, the UK has 4.5GW of offshore wind turbines under construction, or some 1,200 turbines.[5] This is on top of its 5.4GW of already installed capacity.[6] This is part of the UK's involvement in a number of binding and non-binding agreements to reduce CO₂ emissions, of which decarbonisation of energy generation is critical component. These include the EU's 2020 Climate & Energy Package and the Paris Climate Agreement.

With these two projects considered, this leads to the question: can O&G decommissioning costs be reduced through reusing this infrastructure for wind turbines?

Could the topside be removed from the substructure and a wind turbine be put in its place?

If so, there could be significant benefits for the parties involved and the UK. Wind farm operators would benefit from reduced cost in substructure and likely a reduced need for EIA. Oil and gas installation owners would benefit from increasing revenue before decommissioning. The UK would benefit by increasing installed capacity of renewable generation and reduce the loss in earnings via tax breaks.

The potential for such retrofits would depend upon the O&G substructures' abilities to withstand the different forces imposed upon them by the wind turbines. Although the weight borne by a substructure is likely to decrease, the change in horizontal load is far more uncertain. The nacelle and hub acting at the top of wind turbine's tower are essentially point masses at the end of long arms, the stresses induced by this will differ greatly from the typically low-as-possible topside. Additionally, these changes in masses and their distribution will result in changes to the harmonic response of the structure as a whole. As these installations are located offshore, the sinusoidal nature of wave forces could be render such a retrofit infeasible. This study recognises the need for an in-depth analysis to understand if such a retrofit is possible.

1.2. Project Objectives

The objective of this study is to determine if O&G installations can be repurposed for the use of wind turbines and to what extent this is possible in the North Sea. More specifically, the objectives are:

1. Create a database of the North Sea platforms. This is to include position, water depth, and structure characteristics.

2. Determine a representative platform for the North Sea O&G stock. This is to be based on an analysis of the database.
3. Create models of the installation using FEA software and create a subsequent model with a wind turbine retrofitted.
4. Determine the differences in responses of the two models in terms of stress, support reactions, and frequencies when applied with gravitational and environmental loads.
5. Determine to what extent the findings of the analysis can be applied to the North Sea O&G database.
6. Suggest methods to improve the study for similar future analyses.

1.3. Project Method Overview

This project will compare two models: the first model will be an oil and gas installation, and the second model will be the best estimate of the previous model with the oil and gas topside removed and a wind turbine put in its place. Therefore only one O&G installation and one wind turbine will be investigated.

The O&G installation model will be modelled against a real installation which will be as representative of the entire North Sea stock as possible. To select such an installation, a database of the UKCS installations will be created. This database will be analysed for different variables such as topside mass, water depth, and substructure type. The choice in wind turbine will be the 5MW NREL [7] reference turbine. This turbine is fictional and was created by NREL to represent 5MW turbines for the purpose of research.

Following the selection of a representative installation and the subsequent creation of the wind turbine installation, the forces acting upon both structures will then be

calculated. This will consist of the force of the wind, the sea, and the gravitational loads of the structures themselves.

Both models will then be created and the forces on them simulated. The resulting response of the substructure (i.e. the part that is getting retrofitted) in both models will be compared to determine if the retrofit is possible. This will consist of a stress comparison in members, reactions and moments upon the supports, and a harmonic analysis.

If such a retrofit is possible, the results will then be extrapolated for the rest of the North Sea O&G stock. This will be achieved by revisiting the database created previously along with the analysis previously conducted to estimate the number of potential sites for retrofit.

Prior to the analysis described, this project will begin with a literature review and background reading to develop an understanding of the structures involved and how such a retrofit would work.

1.4. Project Scope

The geographic scope of this project is limited to the UK's North Sea territory. This includes the Central, Southern and Northern North Sea, the West of Shetland, and the Irish Sea. Only one installation will be included in the analysis.

The technological scope of this thesis is limited to a horizontal axis wind turbine only although other potential uses of O&G installations for RESs are discussed as alternatives. Only one wind turbine will be included in the analysis.

The analysis that will be conducted will determine if the installation can withstand the forces induced by the retrofitted wind turbine. Not included is the feasibility in terms of cost, logistics, supply chain, sustainability, or how such retrofit project would be implemented.

2. Literature Review

In order to understand the process involved in the project a literature review was conducted and the findings presented below. This can be summarized as literature on wind turbines and oil and gas installations. This literature is centred on the North Sea and a brief summary is provided first. Also investigated were similar projects of retrofitting O&G platforms with wind turbines and alternative uses for the installations.

2.1. North Sea

The North Sea lies on the East coast of the UK as indicated in Figure 2.1. As is shown, the UK shares these waters with the following countries: Norway, Sweden, Denmark, Germany, Netherlands and Belgium.

The North Sea is typically split into different sectors. These are, Northern, Southern, Central, West of Shetland, and Moray Firth. This thesis uses the terms UKCS and North Sea interchangeably although this is not strictly appropriate hence the Irish Sea is included throughout.

As shown in the diagram, water depth varies from 25m in southern regions to 200m deep in northern regions. It should be noted that Norwegian waters can be far deeper than this and reach depths of 700m.



Figure 2.1: The North Sea with sectors indicated. Courtesy of [8]

2.2. Wind power

Wind power is the leading renewable technology in the UK. As of 2016, wind power represented 30.6% of renewable energy capacity [9]. This is made up almost exactly by two-thirds onshore wind and one-third offshore wind. Total energy generation differs

due to the stronger and more stable winds offshore and the ability to build larger turbines. Onshore wind accounts for 25.2% of renewable energy generation and offshore 19.7%. In the UK energy mix, OWTs account for only 1.75% of total energy consumption. [10]

Horizontal axis wind turbines operate by converting the kinetic energy of wind into electrical energy. To do so, a wind turbine consists of the components shown and arranged in Figure 2.2.

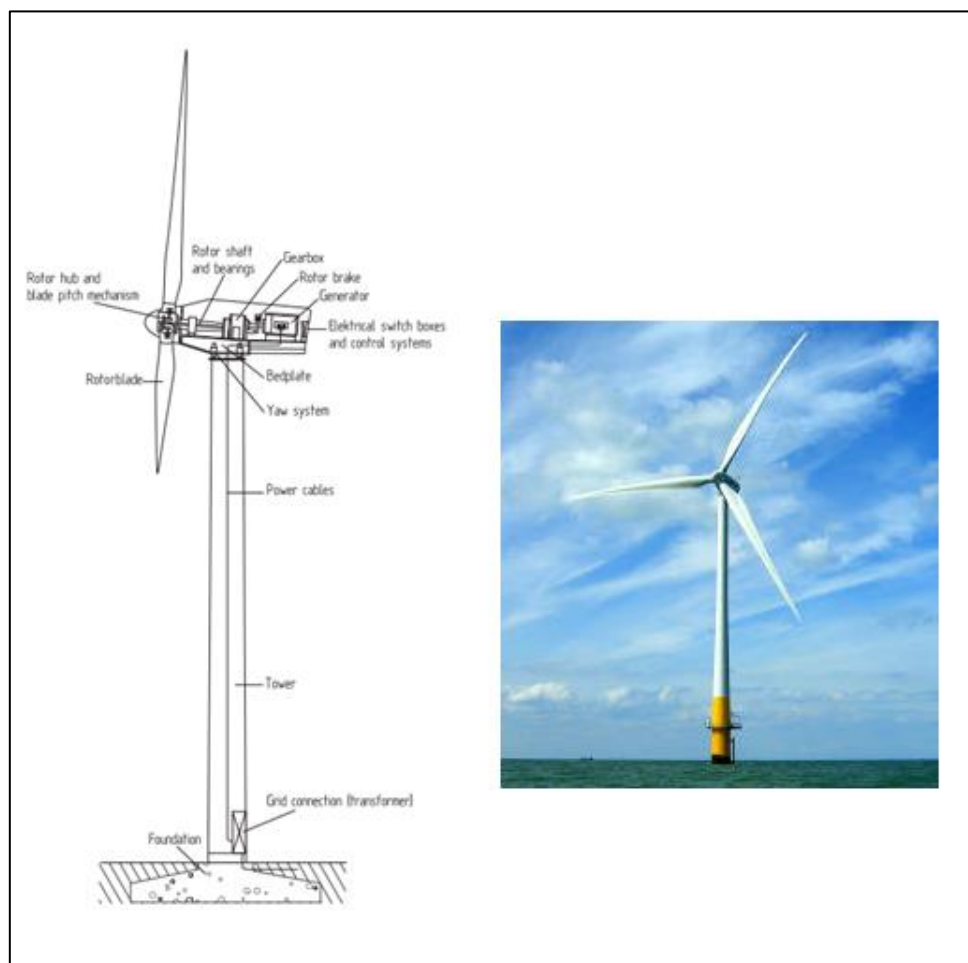


Figure 2.2: Diagram of wind turbine components. Images courtesy of [11]

Generation theory

The wind turbine is orientated such that the plane of blade rotation is perpendicular to the wind direction and the tower is downstream of the blades. Wind passes over the

blades which are aerofoils. This produces lift and the blades are orientated such that this lift results in the rotor rotating. The shaft, which the rotor is attached to and turns, also contains an induction motor. This generates power as the shaft spins the induction generator.

Using these principles, the amount of power generated by the wind turbine is proportional to the lift force. The lift force is dictated by the aerodynamic characteristics of the blades, their length, air density, velocity of the incoming wind and efficiency of the generator. This is summarised by equation (1).

$$P = \frac{1}{2} \cdot \rho \cdot A \cdot V^3 \cdot C_p \quad (1)$$

Where A is the area of swept through by the blades (equal to π multiplied by the blade length squared) and C_p is the power coefficient.

Infrastructure

Typically, offshore wind turbines are part of an array commonly known as a “windfarm”. Each turbine is often linked in series with other turbines by inter-array cabling. This cabling feeds into a substation where the electricity is transformed to a higher voltage for transmission to a recipient substation onshore to join the national grid. This is summarised in Figure 2.3.

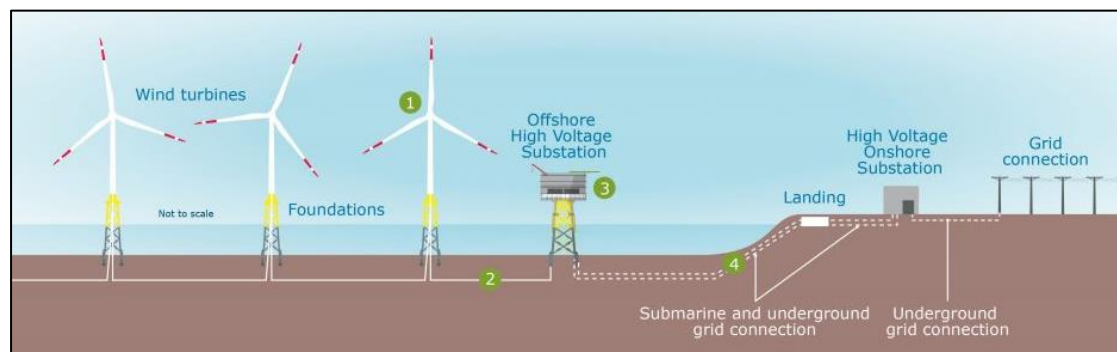


Figure 2.3: Layout of a wind farm, image courtesy of [12]

Substructures

Offshore wind foundations are either monopiles, gravity based, tripod, jacket, or floating structures. The choice of foundations is greatly dictated by the water depth as summarised in Figure 2.4.

Monopiles: Monopiles are typically used in water depths of less than 30m. They consist of simple steel pile and extend into the soil between 30 and 60m.[13]

Gravity based structure: GBSs are used in water depths between 30 and 40m. The wind turbine structure is mounted on an extremely heavy base. This is done in both single leg and triple leg variations. They operate on the principal that the overturning moment of the structure as a result of having the heavy base is far in excess of the moment it will experience from environmental forces. Gravity bases are composed of concrete and will weigh approximately 5,000mT in most cases.[14]

Tripod and jacket structures become more economical than GBS at depths between 35 and 50m.[15] The wider the base of the structure is the more resistant it is to overturning.

Floating: For water depths greater than 50m, floating wind turbines are only applicable. This technology is still within its infancy with only a handful of operating turbines in the world but is expected to become a major component of the UK's energy generation mix in the coming decades.[16] Tension Leg Platforms (TLPs) and Spar platforms are being deployed, the operation of which are discussed in greater detail in the following sections. The first and only (non-demonstrator) wind farm is the recently developed Hywind wind farm near Peterhead, Aberdeen, which uses spar platforms.[17]

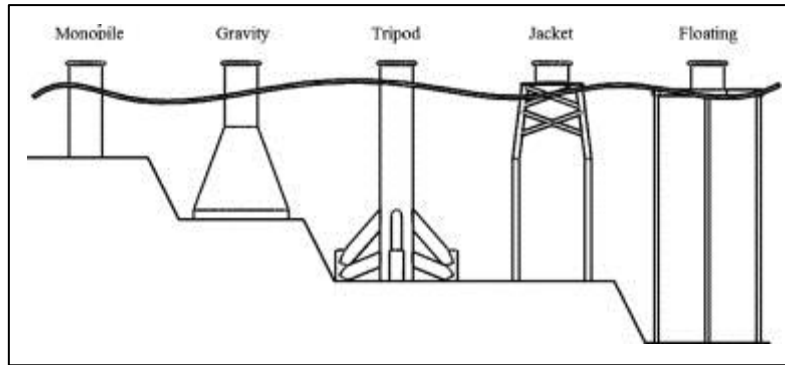


Figure 2.4: Summary of OWT foundations with relative depth, image courtesy of [18]

Trends in the North Sea

Wind turbines have steadily increased in size since their first deployment in the North Sea. The average turbine installed in 2015 was 4.2MW, whilst in 2010 it was 3.2MW.[19] In terms of future projections of capacity, this is expected to vary between 5-10MW. Two major consented projects are the Beatrice Offshore Wind Farm and the Dogger Bank wind farms which have planned turbine capacities of 7MW [20] and (up to) 10MW. [21]

The differences in physical characteristics between 5MW and 10MW (and also a 8MW) wind turbines are summarised in Figure 2.5 with data provided from IOPscience (reference [22]).

As previously mentioned, the UK currently has its 5.4GW of already installed capacity.[6]. At the time of writing, a further 4.5GW of offshore wind turbines are under construction on the UKCS which is equivalent to approximately 1,200 turbines.[5]

Turbine	NREL	LW	DTU
Rating	5 MW	8 MW	10 MW
Rotor Orientation, Configuration	Upwind, 3 blades	Upwind, 3 blades	Upwind, 3 blades
Rotor Diameter	126 m	164 m	178.3 m
Hub height	90 m	110 m	119 m
Cut-in, Rated, Cut-out wind speed	3 m/s , 11.4 m/s, 25 m/s	4 m/s , 12.5 m/s, 25 m/s	4 m/s , 11.4 m/s, 25 m/s
Rotor speed range	6.9 – 12.1 rpm	6.3 - 10.5 rpm	6 – 9.6 rpm
Hub mass	56,780kg	90,000 kg	105,520 kg
Nacelle mass	240,000 kg	285,000 kg	446,036 kg
Blade mass	17,740 kg	35,000 kg	41,716 kg
Nacelle dimensions (L x W x H)	NA ¹	20 m x 7.5 m x 7.5 m	NA ¹
Tower Mass	347,460 kg	558,000 kg	605, 000 kg
Tower Height	87.6 m	106.3 m	115.6 m
Tower top thickness, diameter	20 mm, 3.87 m	22 mm, 5 m	20 mm, 5.5 m
Tower bottom thickness, diameter	27 mm, 6 m	36 mm, 7.7 m	38 mm, 8.3 m
Overall Centre of Mass	-0.2 m , 0.0 m 64.0 m	0 m, 0 m, 77 m	NA ¹

Figure 2.5: Summary of typical wind turbine characteristics with size, courtesy of [22]

2.3. Oil and Gas

Oil and gas production in the North Sea began in 1959 in Dutch waters. The first discovery on the UKCS was in the West Sole field by BP in 1965. Production vastly increased in the 1970's with the Argyle and Forties fields. [23]

Infrastructure

Over the 50 years of North Sea O&G production a wide range of infrastructure has emerged. This project only considers the oil and gas platforms and does not consider the wider infrastructure (such as subsea wells, transport back to shore, and all midstream and downstream infrastructure). These offshore structures are similar to those found for wind turbines and include gravity based and fixed jacket structures. Other substructures which differ significantly to wind turbines are compliant towers, spar buoys, tension leg platforms (TLPs), and FPSOs.

All non-floating structures consist of a substructure (either gravity based or fixed and made from either steel or concrete) and topside as shown in Figure 2.6. The topside is where all operations are based whilst the substructure serves to keep the topside above sea level and protected from the elements.

Again, the choice in substructure is influenced by the water depth but is also influenced by the demands of the topside with different substructures preferred for different operations as shown in Figure 2.7. Economics will come into play and production companies may choose to build a number of small structures or a single large structure based upon the demands of the field and production challenges expected.

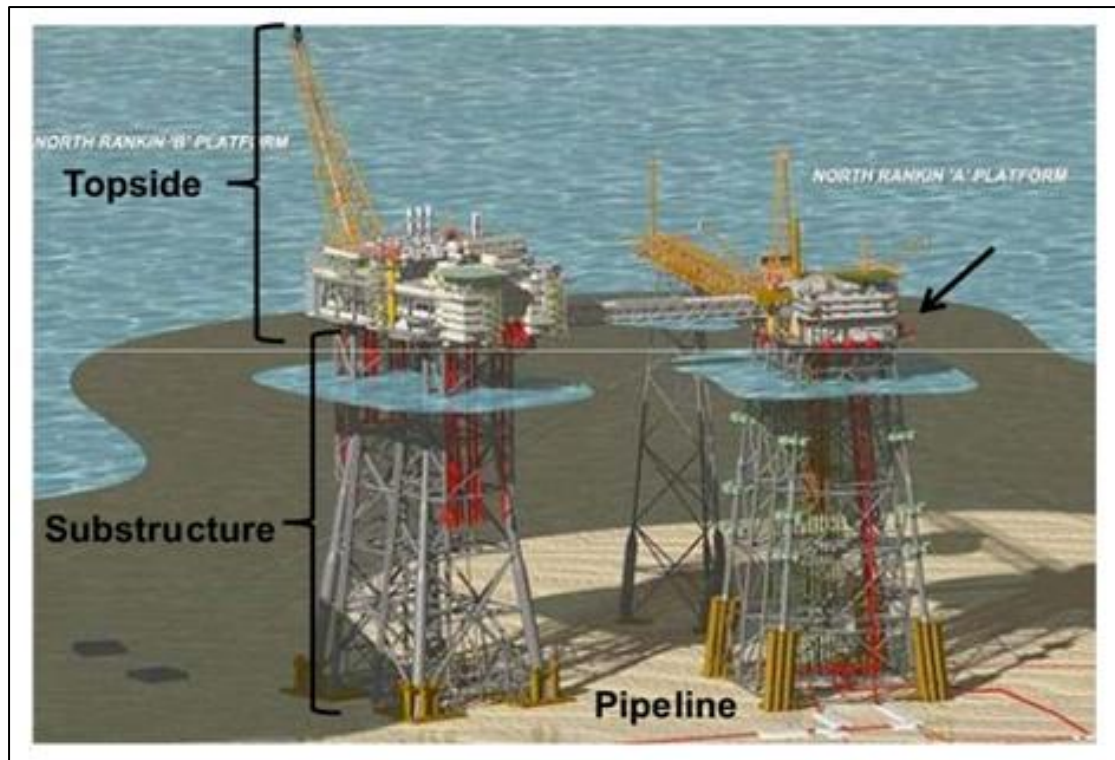


Figure 2.6: Diagram of a typical oil and gas platform. Substructures shown are jackets.

Image courtesy of [24]

Gravity based: These operate under the same principals as wind turbine GBS. Typical depths are between 110 and 160m.[25]

Jacket: These operate under the same principals as wind turbine jackets. O&G jackets are typically categorised as either “large steel” or “small steel” jackets with the range of depths occupied far greater than wind. Depths occupied in the UKCS are up to 186m (BP’s *Magnus*) although fixed platforms can occupy depths of 450m. [26]

Compliant towers: These towers are typically used in depths of 450m to 900m. Compliant towers are narrow with vertical legs as shown in Figure 2.7. This allows flexibility allowing them to withstand wind and sea conditions. The UKCS does not require such structures but are found in the Norwegian waters of the North Sea.

Spar: These platforms are shown in Figure 2.7. The bottom end of the spar is heavily weighted with basalt or similarly dense material which keeps the centre of gravity of the entire structure beneath the topside. The spar is tethered to the sea bed which fixes its position. These platforms exist in the North Sea (such as the *Brent Spar*) but are not common. They are used in depths between 300m and 1500m.

TLPs: Tension leg platforms are used in depths of between 450m and 2100m. They are vertically moored structures in which a hull creates the buoyant force. The tension in the legs allows for horizontal movement with the sea but does not permit vertical movement.

FPSOs: Floating Production, Storage and Offloading systems are not technically platforms but are ships with most of the same capabilities. They are used where the cost of piping is too great and transporting it via the vessel is more economical. They have been operated in waters up to 1,800m deep but are also used in far shallower waters where it is not cost effective to install a platform.

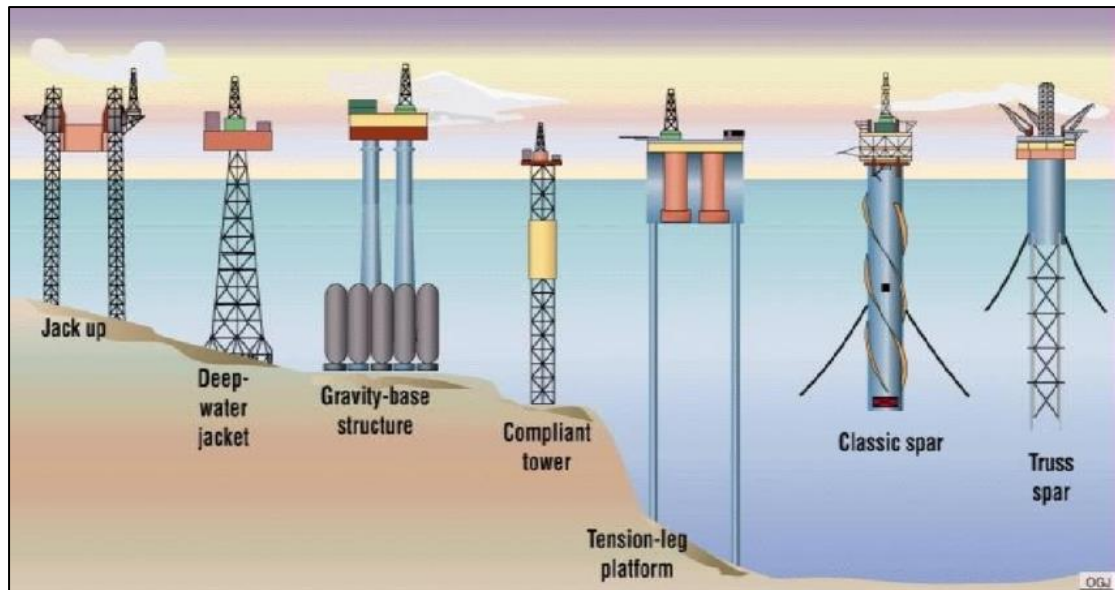


Figure 2.7: Supporting structure choice with relative depth for oil and gas platforms.

Image courtesy of [27]

Decommissioning

Although oil and gas still are a major component of the UK’s energy sector and economy (and will continue to be for some number of decades yet) the industry is now looking towards decommissioning. This is being driven by commercial and regulatory pressures. The foremost regulation is the OSPAR agreement, the following excerpt from DECOM North Sea best explains this:

“OSPAR Decision 98/3 prohibits leaving offshore installations wholly or partly in place unless further derogation are granted. However, it provides certain derogations to concrete structures and the footing of large steel jackets weighing more than 10,000 tonnes, from the fundamental principle that decommissioning should result in full removal of the installation. Derogation is not automatically available and is subject to a detailed assessment and consultation procedure to determine if there are significant reasons to allow the installation (or part thereof) to remain in situ. Furthermore, no derogation is available to steel installations constructed after 9 February 1999 (being the date that Decision 98/3 came into force)”. (Decom North Sea, 2014 [28])

As decommissioning is obligatory, commercial pressure becomes significant as companies attempt to optimize between each installation's predicted revenue, maintenance and operational costs, and the uncertain cost of decommissioning.

Ignoring the potential reuse of platforms as proposed by this thesis and other publications (see 2.4), decommissioning is predicted to become a large industry in itself in the coming years. It presents a massive infrastructural and logistical challenge with some of the following requiring decommissioning in the UKCS [2]:

- 8 installations with large concrete substructures
- 31 installations with large steel jackets (> 10,000 tonnes)
- 223 other steel jackets
- 280 subsea production systems
- 21 floating production systems
- Over 3,000 pipelines and around 5,000 wells.

With this scale of work, bottle-necking is widely predicted at the UK's already small number of facilities capable of receiving such structures with demand far exceeding capacity. Competition for these facilities from wind farm operators, as discussed previously, must also be factored in which intensifies the problem. Resulting from this costs of decommissioning services will fluctuate. O&G platform decommissioning will likely be brought forward in many cases (significantly before the design life of the platform or whilst field production is still viable) to reduce the lifetime cost of the installation and maximize profit. Alternatively, decommissioning may be brought forward as a learning experience for a company.

Decommissioning is not new to the North Sea with its history stretching back to the 1988 and Piper Alpha. More recently projects planned include *Brent Spar* and *Hutton*. Estimates of full decommissioning of UKCS O&G predict completion after 2050. It is currently estimated that another 24 billion barrels of oil are available for extraction which will take between 30 and 40 more years.[29]

2.4. Similar Studies

The concept of reusing O&G structures for wind turbines is not new and frequently occurs as a suggested alternative to decommissioning. However, the number of studies found which investigate the feasibility was limited to two results which are presented below, one from Brazil and another from China. Additionally, to the writer's knowledge only one such project has occurred in practice, the Chinese SZ36-1. This is discussed below and makes up one of the two studies presented.

Historically, close working between the industries and knowledge transfer has occurred most notably with the *Beatrice Demonstrator* project and the company *SeaEnergy Renewables*¹, both of which employed jacket designs instead of piled structures for their wind turbines.

“Fixed Platforms at Ageing Oil Fields – Feasibility Study for Reuse to Wind Farms”, Barros et al, 2017 [30]

This study was conducted for the coastal region of Brazil. O&G jackets studied used jackets situated in water depths between 13m and 41m (based upon real operational installations). The jacket with a retrofitted turbine was simulated using SACS software. The wind turbine used was the NREL 5MW reference turbine.

¹ SeaEnergy Renewables were bought by Repsol in 2011 and are no longer active.

A fatigue evaluation was performed and the jacket was aged using the software. Wind and wave regimes were calculated and applied to the structure for simulation. A stress check and fatigue analysis was conducted with the results indicating the foundation and jacket could withstand the loads induced. Researchers estimated the platform could bare the turbine for its entire design life of 20-25 years.

“Application of an Abandoned Jacket for an Offshore Structure Base of Wind Turbine in Bohai Heavy Ice Conditions”, Wang et al, 2009 [31]

The paper states that the project was funded by the Chinese government to demonstrate the viability of wind power as a technology. The installation employs a jacket situated in 31m water depth which was retrofitted with a 1.5MW wind turbine in 2007. It is not known if the installation is still in use.

The study summarised the analysis supporting the project but falls short of comparing the analysis data with any data measured on the installation. The analysis consisted of creating a model using ABAQUS finite element analysis software. Pile-soil interaction elements were used as per the software. The analysis determined the structures suitability in terms of natural frequencies and stress with the result ultimately allowing the project to proceed. Researchers estimated the retrofitted structure could withstand at least another 20 years of service (it is not stated how old the jacket was).

2.5. Alternatives use of platforms

A plethora of alternatives to decommissioning (and the proposal of this project) are available for the installations. For the installations discussed in this project the following apply:

- Rigs to reefs

- Platforms for airborne wind energy systems
- Geothermal energy
- Tidal system moorings
- Fish farms
- Other use: Research centres, military use, prisons etc.

The reader is invited to read about these options and wider decommissioning alternatives in references [32]–[36]. Wider industry alternatives make use of pipe networks, depleted wells, and other mid and downstream equipment and include:

- Synthetic gas production and storage
- Hydrogen production and storage
- Carbon sequestration storage
- LNG distribution and storage

3. Methodology

Following the literature review, the methodology used to achieve the objectives set in 1.2 are now presented. This has been based primarily upon the methodology used to design offshore O&G structures set about by El-Reedy, 2012. Other methodologies which have been influencing are that used by Barros et al and Wang et al as described in the literature review.

The methodology for this project is summarized as per the flow chart in Figure 3.1.

This can be broken into 4 main stages:

1. UKCS installation database creation and analysis
2. Model creation
3. Loading calculations
4. Simulation and comparison of forces

To summarise, a database of UKCS oil and gas installations will be created. Following this, the stock will be analysed to find an installation which is representative of a typical installation. Using the installations dimensions, it will then be modelled using CAD software. A subsequent model with the O&G topside replaced by a wind turbine will then be created.

The loads acting upon both models will then be calculated. Stress and moment analyses will then be conducted upon the members and seabed fixings and the results compared between the two models to determine the worthiness of the structure for wind turbine reuse.

This thesis will only consider one representative model of UKCS O&G installations and one wind turbine due to limited time. As every installation is of a unique design,

history, and environmental condition, ideally every installation would be modelled with multiple sizes of turbines to determine the maximum potential installed capacity. The wind turbine being used is the fictional NREL 5MW reference turbine which is discussed in later sections.

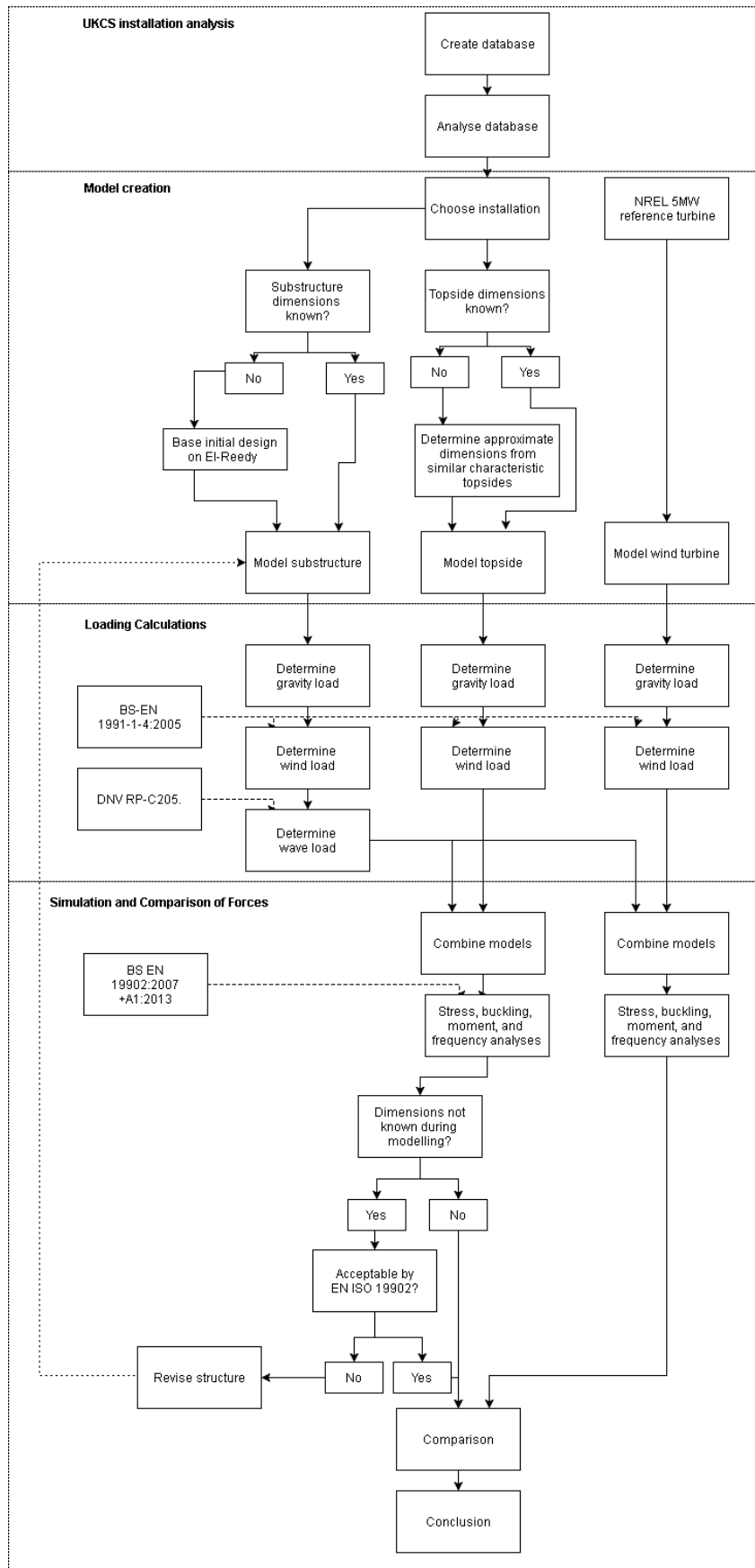


Figure 3.1: Summary of methodology

3.1. Database Creation and Analysis:

This stage is necessary as a precursor to creating an oil and gas installation which is representative of a portion of the UKCS stock. The information is to be gathered from reputable sources only. The information the database will include is as follows:

- Facility type (gravity based, jacket, FPSO, other)
- Topside dimensions and mass
- Substructure dimensions and mass
- Water depth
- Location
- Age

This database will then be analysed for trends in these variables and a suitably representative installation will be chosen for subsequent analysis based upon the findings.

Logically, the O&G topside must weigh more than the wind turbine which will replace it otherwise the gravitational load will be increased by the retrofit. As stated the NREL 5MW reference turbine will be modelled which has a total mass of 697mT (see 5.3). For this reason, only installations with topsides in excess of this mass will be considered.

3.2. Creation of Models

Once the representative installation has been determined, this installation will be modelled using Solidworks, a combined CAD and simulation package. Only the substructure will be modelled in detail and the topside will be approximated as a

distributed load (detailed 3D modelling is not required as it is only the substructure is of concern as the topside is being removed).

Using this initial model, the second model containing the wind turbine will be created. The jacket will be modelled with a transition piece and wind turbine. The transition piece and tower will be modelled in detail (unlike the topside). More detail is provided in the subsequent sections.

Oil and Gas Installation

Only the substructure will be modelled in detail, the topside dimensions are only required for calculation of loading upon the substructure.

Analysis of a real installation is preferred as this will reduce model creation time and make the findings more robust. Where possible, drawings for an installation which closely matches the characteristics of the representative installation will be used. Where the use of a real installation is not possible or information is missing (likely due to the commercially sensitive nature of the installation design) installation design will be performed iteratively with loading calculations and simulations until satisfactory results are found (using ISO 19902). This will be performed using the methods set in El-Reedy 2012 [26] in tandem with the following standards:

- API RP2A: Recommended Practice for Planning, Designing and Constructing Fixed Offshore Platforms—Working Stress Design
- BN EN ISO 19902:2007: Petroleum and natural gas industries – Fixed steel offshore structures

Only structural members of the jacket will be modelled i.e. steelwork which is either part of the oil and gas production equipment or secondary steelwork (such as walkways) will not be modelled.

Connections between members will be simplified. Welded joints (including welding bead) and joint-cans will be ignored. Joint-cans have the effect of enabling greater load to be carried so should be included in future, more detailed analyses.

Fatigue will not be modelled in the substructure.

Piles and Soil Conditions

Piles will be simplified to rigid fixings. Ideally, sea bed fixings would be simulated as non-linear springs as per the soil conditions and p-y curves.

Wind Turbine

In keeping with the O&G analysis, a representative wind turbine will be modelled. As stated in the literature review OWT are currently being deployed in the range of 5-10MW in the North Sea with the 2015 mean of 4.2MW. The chosen model, NREL's 5MW reference wind turbine, is within this range. The machine is fictional with the dimensions used based upon many real models in operation. Detail on this wind turbine are provided in 5.3.

The wind turbine consists of the tower, nacelle, blades, and rotor. The tower shall be modelled in the same manner as the substructure, all other components will be approximated as remote loads acting upon the top of the tower.

A transition piece (between turbine and substructure) will also be modelled. As retrofitting of O&G platforms for OWT is not common, transition piece design will be based upon that used by Barros et al, 2017.

The transition piece will be positioned so as to make the base of the tower at the same elevation as the base of the O&G topside. This is on the assumption that the topside was designed at the appropriate height in relation to the sea beneath it, therefore

positioning the OWT below this elevation may endanger either the OWT or personnel boarding the platform.

3.3. Forces Acting on Structure

The forces acting on offshore structures are summarised as follows with the structures which these forces act upon are included in parentheses:

- Gravitational loads (all)
- Aerodynamic loads (substructure, topside and wind turbine)
- Actuation loads (topside and wind turbine)
- Hydrodynamic loads (substructure)
- Sea ice loads (substructure)
- Other loads such as wake, ice, earthquake (substructure)

Due to time constraints of this project, only the most significant loads can be considered.

These are gravitational, aerodynamic, and hydrodynamic loads.

Gravitational Loading

Gravitational loading will be considered for all structures. Gravitational loading consists of the dead-load and live-loads and will be determined as per the guidance set by El-Reedy 2012.

Dead loads are the self-weight of structures and are calculated and simulated as such.

Live-loads are the loads imposed on a structure during its use. These will only be calculated for the O&G model only (live load upon the OWT is considered negligible).

Live loads are calculated as per platform use and geometry. A design load of 15KN/m²

will be applied to the topside surface area. The total gravitational load will be increased by 5% for contingency allowance.

Wind Loading

Wind loading will be calculated for all areas of the models exposed to the wind. These are:

- The length of substructure above water
- The topside
- The wind turbine and transition piece

Loads will be calculated as per BS-EN 1991-1-4:2005+A1, “Actions on structures: - Wind actions”. Wind loading is the sum of external forces, internal forces, and friction forces as wind flows into and around an object in its path. Internal forces will be ignored for this study. Wind force is given by equation (2):

$$F_w = C_s C_d \sum_{elements} C_f \cdot q_p(z) \cdot A_{ref} \quad (2)$$

Where $C_s C_d$ is the structural factor, C_f is the force coefficient, $q_p(z)$ is the peak velocity pressure with elevation, and A_{ref} is the reference area.

Wind loading will be calculated for the topside, wind turbine, and substructure separately. Additionally, simplified geometries will be used in all cases which best fit those described by the BS EN standard. To account for this atomistic calculation loading will be modestly increased by 10 per cent.

For this analysis, the effect of fluctuating water height from the movement of sea waves will be ignored. Furthermore only one direction of wind will be considered. This direction will be in line with the wave force.

The wind data used for these calculations will be determined from a wind profile (which consists of average and peak wind velocity with elevation above sea level and peak pressure with elevation). Wind profile will be calculated as per the site location using the method described in BS-EN 1991-1-4.

In the case of the wind turbine, wind thrust will also be considered. Thrust results from the wind action upon the blades as they pass through the air during power generation. Peak thrust will be stated by the manufacturer and considered with peak wind drag. Wind drag results from the wind passing around stationary components. This will only be calculated for the tower (and not the hub, nacelle, or transition piece). The tower will account for the vast majority of wind loading due to its wind-loading reference area in relation to other components. Future detailed analyses should include these components to increase the reliability of results.

Wave Loading

Wave loading is calculated for the substructure only. Loading will be calculated as per DNV RP-C205 “Environmental Conditions and Environmental Loads”.

Wave loads are the sum of drag forces and inertia forces. Drag forces are a result of water moving over the structure during both wave motion and current motion and is defined by equation (3):

$$F_d = \frac{1}{2} \rho \cdot C_d \cdot V^2 \cdot A \quad (3)$$

Where ρ is the water density, C_d is the coefficient of drag of the member, V is the water velocity in the horizontal direction and A is the loaded area.

Inertia forces are a result of water particle acceleration acting upon the structure and are defined by equation (4):

$$F_I = \pi \cdot \rho \cdot a \cdot C_m \cdot \frac{D^2}{4} \quad (4)$$

Where a is the water particle acceleration in the horizontal direction, C_m is the inertia coefficient of and D is the diameter of the submerged member.

Total wave load will be calculated by combining the two forces with time and the peak load found. Wave force is considered in one direction only which is in line with the wind force. Additionally, the effect of oscillating water height with wave motion will be ignored.

A simplified geometry will be used in accordance with the standard. Where multiple members exist (i.e. for all structures except GBSs) loading will be considered for each member in isolation (although shielding coefficients will be applied if necessary) and interference of flow around members resulting from connections with other members is ignored.

Wave data used will be obtained from a wave profile. This profile will be calculated using the appropriate wave theory for the site as dictated by DNV RP-C205. This consists of time-varying profiles of water velocity and acceleration with water depth.

Hydrostatic Force and Current Force

Hydrostatic force increases with water depth and is given by equation (5):

$$F_H = \rho \cdot g \cdot h \quad (5)$$

Where h is the submerged depth.

As per El-Reedy 2012, hydrostatic forces only become significant for structural members where the ratio of diameter to thickness is less than $205 / h^{0.333}$. Hydrostatic force will only be calculated and applied for the substructure if this condition is true.

Current force acts upon structures as a result of wind generated currents, tidal currents, circulation currents, loop and eddy currents, soliton currents and longshore currents. As per El-Reedy 2012 designers often account for current force by increasing water depth by 5% in their calculations (p57, [26]). As this is a relatively small difference, current force will be ignored unless the site is stated to be particularly energetic.

3.4. Simulation and Comparison of Forces

Following the creation of models and calculation of loads simulation will then be performed. Three simulations will be conducted. These will be as follow:

- Simulation 1 – Gradational Loads Only: Simulations of both models with only gravitational loads considered i.e. wind and wave loads will not be applied.
- Simulation 2 – Transition Piece Comparison: This simulation will consider the forces and moments upon the transition pieces of both models. The substructure/transition pieces connection will be simulated as rigidly fixed. All forces (gravitational, wind, and wave forces) will be applied.
- Simulation 3 - Full simulation: All loads will be applied with full models. Buckling and frequency studies will also be conducted.

All simulations will be static with only the maximum gravitational, wind, and wave loads borne by the structure considered.

For each simulation, member stress will be determined as will reaction forces about fixed joints. The stresses in members will be compared between models. In the case of the wind turbine model, they will also be compared against ISO 19902:2007 +A1:2013 - “Petroleum and natural gas industries — Fixed steel offshore structures”. Stresses considered will be as follows (with their relevant ISO 19902 section stated):

- Axial tensile (as per 13.2.2)
- Axial compressive (as per 13.2.3)
- Bending (as per 13.2.4)
- Shear (as per 13.2.5)
- Von Mises stress

The relevant design factors of safety will be applied. Buckling, and hence critical load, will also be considered. Natural frequencies of the models will be determined (using the software) and compared between models.

3.5. Verification of Models and Loading

The stresses and moments generated by the model will be verified against hand calculation. The substructure model will be isolated, simplified and simulated. The resulting stresses induced and the reaction forces will be compared against basic static structures theory.

Wind load will be verified using a single member only via comparing the result derived from the standard used against calculation via ANSYS.

Wave load will be verified by comparison to grey literature. Ideally, wave load would be verified using ANSYS or Sesam software and a full jacket simulation but this is not possible due to time constraints of the project.

4. Database and Analysis

As per the methodology, a database was created and analysed to find a representative O&G installation. The results are presented below.

4.1. Database creation

A database of O&G installations on the UKCS was created by combining data from “Oil and Gas UK” [see reference [37]] and “Oil and Gas Authority” (reference [25]). A total of 326 unique platforms were obtained including compression and riser towers, accommodation and wellhead platforms, and FPSOs (this excludes 6 flare towers which were eliminated from study due to inadequate design).

4.2. Database Analysis

Structure type

Structure type was first analysed. The majority structures (89%) are fixed-steel structures as seen in Figure 4.1. Only one TLP existed in the UKCS, Conoco Philip’s *Hutton*, which is now decommissioned.

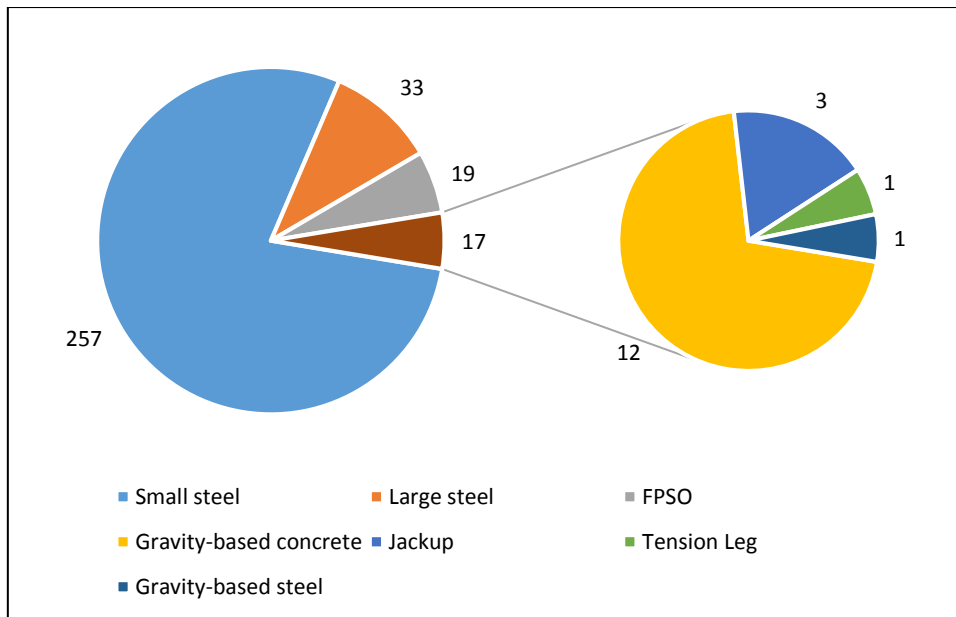


Figure 4.1: Breakdown of UKCS O&G installations by type

As they comprise the majority, small-steel structures were therefore carried forward for further analysis. Information on number of legs is scant but seems to suggest that the majority of these platforms employ 4-legs (only 24 platforms state the number of legs used, of this number 22 state using 4 legs).

Water depth and topside mass

Water depth and topside mass were plotted to investigate their relationship. This is shown in Figure 4.2. An estimated 69% of total installations are installed in a water depth of less than 60m with a topside weight less than 10,000 tonnes.

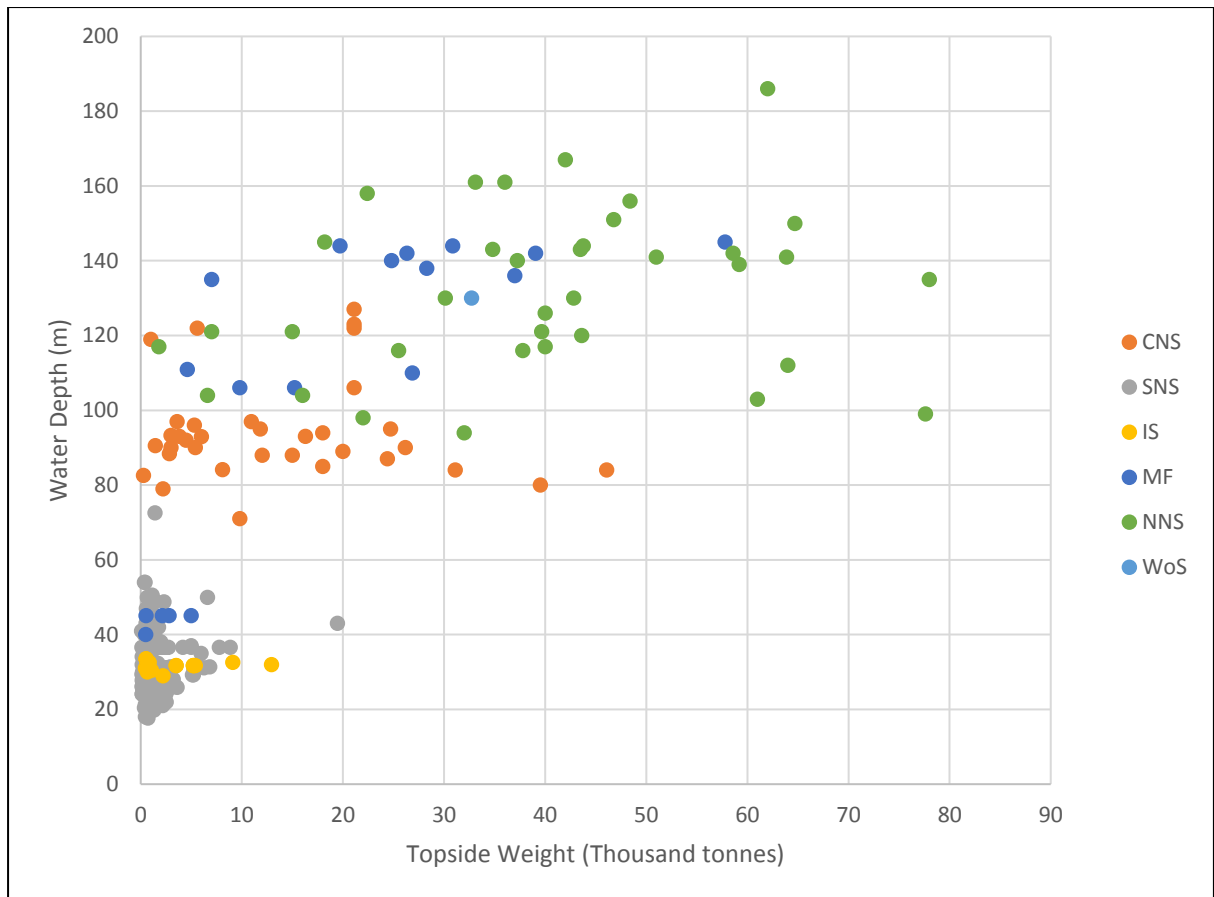


Figure 4.2: Topside weight and water depth of UKCS O&G installations with indication of North Sea area by colour

From the figures and Table 4-1 the approximate trends of the different North Sea sectors are shown. SNS make up the bulk of platforms (62%) and are typically installed in shallow water with relatively light topsides. IS installations are similar to SNS installations in their characteristics but make up only 17% of stock. Advancing northwards the spread of both depth and weight dramatically increases. CNS, NNS, and MF platforms vary greatly in topside weight however installed water depth is fairly constant at approximately 94m, 132m, and 106m respectively for the sectors.

Only two fixed steel platforms in the WoS sector were found therefore no significant trends can be discerned hence the sector is excluded from Table 4-1.

Table 4-1: Summary of statistics found from the analysis of UKCS O&G installations.

	CNS	SNS	IS	MF	NNS	Av.
No.	41	189	17	20	37	51
(%)	(13.4)	(61.6)	(5.5)	(6.5)	(12.1)	(100)
Av. Water depth, m, (Standard dev)	94.1 (33.5)	33.0 (11.2)	31.7 (10.6)	106.6 (51.6)	132.0 (30.6)	47.2 (35.4)
Av. Topside mass	6,660	1,425	3,310	9,300	19,500	4,900

Field Installation Characteristics

Further analysis of the database suggest that, for all sectors, there is a 35% chance an installation will be standalone (107 installations total). 72% of all installations are within a field of 5 installations or fewer. These trends vary from sector to sector.

4.3. Representative Installation

Based upon the database analysis the representative installation will have the following characteristics:

- Type: Small steel jacket with 4 legs
- Topside mass of less than 10,000 tonnes
- Water depth of less than 60m
- Located in the Southern North Sea in a complex size of 5 or fewer

Based upon these results the Leman BH platform was selected for analysis. The Leman BH platform was a living quarters and operations platform which served the bridge-linked and gas-producing Leman BT platform as shown in Figure 4.3. It was installed

in 1968 in UKCS quadrant 49/26 of the SNS, off the North East coast of Norwich. Owned by Shell, the topside was brought to shore in July 2017 as part of their decommissioning program.

Comparison to UKCS O&G Stock

The jacket is a 4-legged small steel structure weighing 566mT and installed at a water depth of 35.7m. The topside weighs 990mT.

At 35.7m of water depth, 60.1% of fixed-steel installations are either within ± 5 m water depth or shallower. Similarly, 69.3% of fixed steel installations are within a topside weight of $990\text{mT} \pm 100\text{mT}$ or greater. Combining the two variables, there are 96 4-legged fixed steel installations which are in a depth of 35.7 ± 5 m or less and a topside mass of $990 \pm 100\text{mT}$ or more. This is approximately 35% of all UKCS fixed installations.

Furthermore it is located in the SNS. Although it is technically part of a larger complex of 19, there is only one other platform in the immediate area which is the Leman BT discussed previously.



Figure 4.3: Leman BH platform (front) with bridge linked BT platform (rear). Image courtesy of [38]

5. Modelling

After the selection of the Leman BH installation, the following models were made as per the methodology and are presented in this section:

- Leman BH with O&G topside
- Leman BH installation with wind turbine

5.1. Substructure

The jacket substructure was modelled as shown in Figure 5.1 with a detailed drawing available in Appendix A.

The jacket was modelled using the drawing also shown in Figure 5.1 and the knowledge that the total weight of the jacket shown in the diagram is 566mT. No further information was available (this includes member cross sections).

The following assumptions were therefore made (with the guidance of El-Reedy 2012):

- All sides of the jacket are identical
- X-braces provide support between legs and are located in the horizontal planes at the same elevations as horizontal members as shown. This is extremely common practice for jackets to contain these horizontal braces.
- All material used was A36-steel
- K-joint and X-joint bracing gaps were 100mm

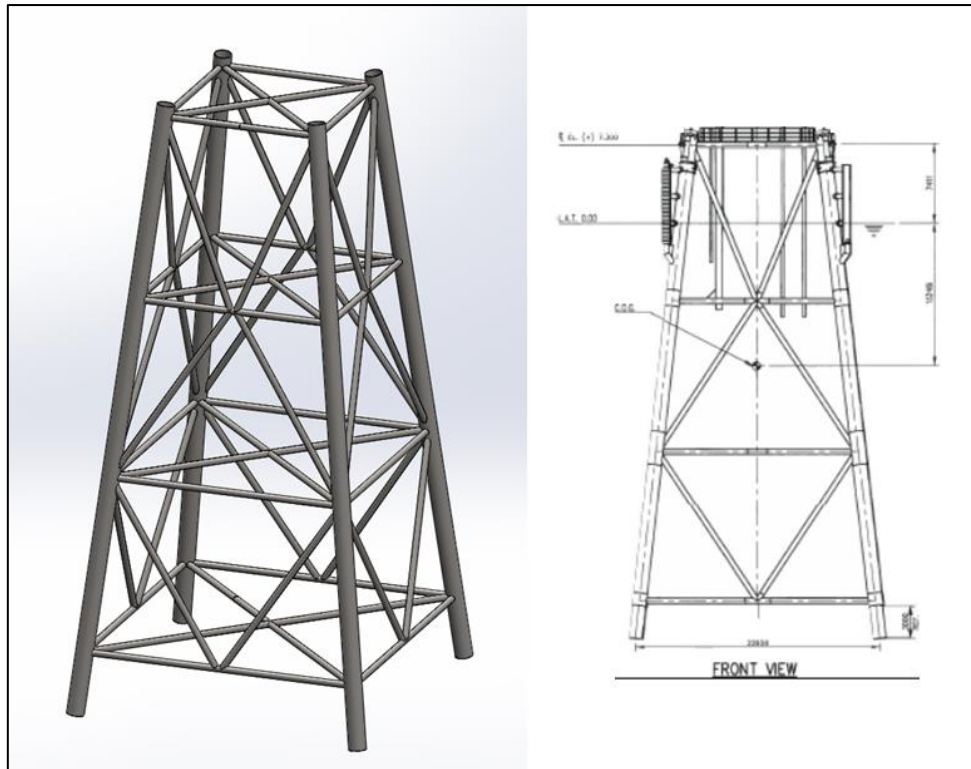


Figure 5.1: Jacket as modelled using Solidworks with the reference drawing used, courtesy of [39]

Jacket Modelling Process

Using the methodology flowchart of Figure 3.1, the jacket model was designed iteratively with the calculated loads and permissible stresses determined using EN ISO 19902. The final results of the iterations are shown in Table 5-1.

Unknown dimensions of members and their outer diameters were inferred from the drawings using graph plotting software². Thicknesses were initially estimated using guidance on diameter to thickness ratios and kept between 16 and 80. Slenderness ratios (KL/r) were kept below 90. The specified mass of the jacket of 566mT was also considered during the iterations. A 100mT margin was allocated to account for additional metalwork which was not modelled as well as paint etc.

² For interested readers, “WebPlotDigitizer” was used: <http://arohatgi.info/WebPlotDigitizer/>

As stated in the methodology, joint-cans were omitted and sea-bed fixings were represented using fixed supports. The point of fixing was modelled as the base of the jacket, these points are stated to be 5m beneath the mud-line.

Table 5-1: Summary of dimensions and permissible stresses as per ISO 19902. All end conditions are fixed-fixed

	Leg	Horizontal brace	Diagonal brace	X-brace
Outer diameter (mm)	1,400	500	500	500
Calculated wall thickness (mm)	35	20	20	35
D/t	40	25	25	20
Maximum Length (m)	14.69	19.21	16.97	15.98
Maximum slenderness ratio (KL/r)	21.3	79.0	69.9	65.7
Permissible Axial tensile stress (MPa)	238	238	238	238
Permissible axial compressive stress (MPa)	211	211	211	211
Permissible shear stress (MPa)	137	137	137	137
Euler's buckling load (MPa)	244	167	185	193

5.2. Topside

The topside is shown in Figure 4.3 with a schematic shown in Figure 5.2. The topside has the following characteristics:

- Total mass: 990mT (1039mT if the bridge to the connected Leman BT platform is included).
- Square planned, with maximum dimensions (i.e. including rails and helipad) of 28m x 35.4m x 23.5m (W x L x H).

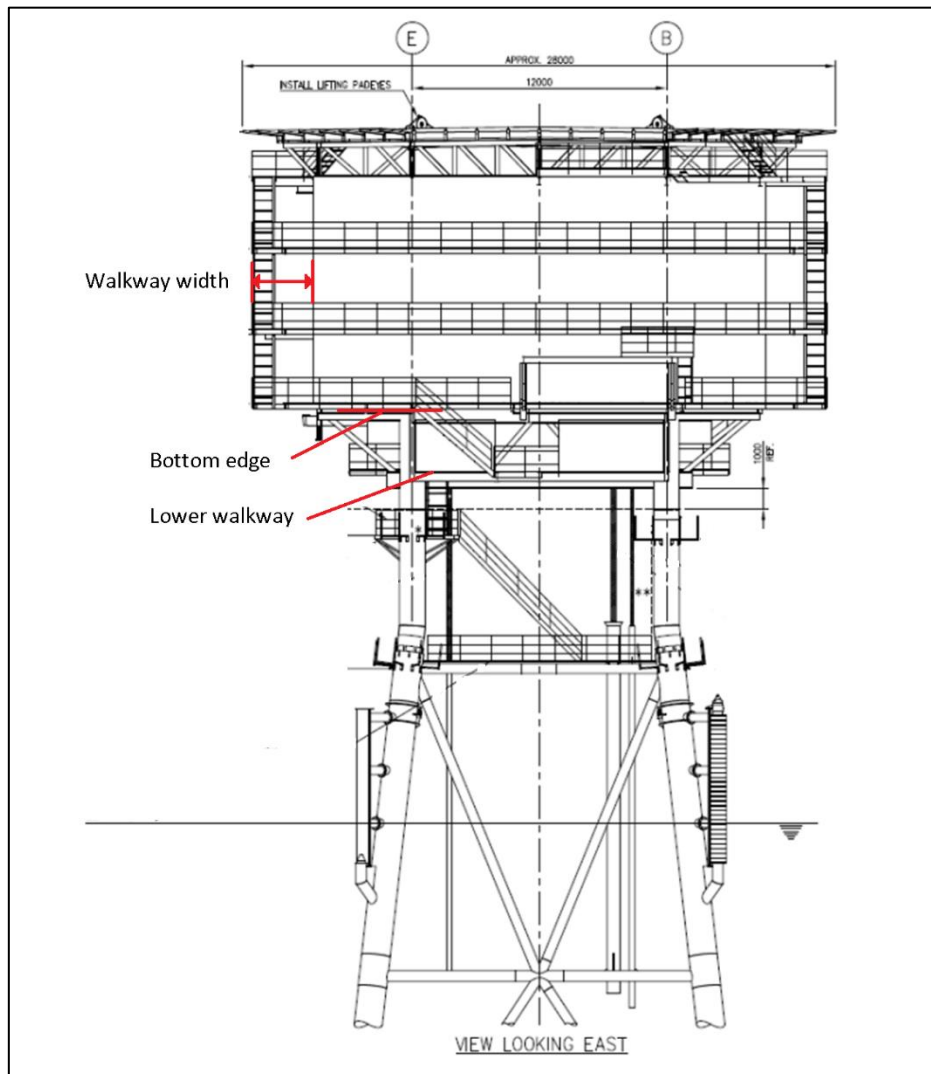


Figure 5.2: Drawing of topside from decommissioning document [39]. Additional red annotations for reference during geometry simplification

As stated, the topside was not modelled in Solidworks although the topside transition piece has been (i.e. the connection between jacket and topside). Here, “modelling” of the topside refers to determining geometries and dimensions with relation to the jacket for the purpose of hand calculation during “Wind Load”.

For modelling, the topside geometry was approximated into a cube for subsequent wind load calculations. This cube is based upon the main body of the topside. To account for peripheral metalwork, such as the railings and walkways, the width was expanded by 20% of the width of the walkways as shown in Figure 5.2. Similarly, the bottom edge was lengthened by 75% of the height of the open lower walkway. Based upon this simplified geometry, the centre of mass of the topside was set equal to the centre of the cube hence gravitational load was modelled as a remote load acting at a distance from the jacket.

5.3. Wind Turbine

As stated, the fictional “NREL offshore 5-MW baseline wind turbine” was used. The OWT model is shown in Figure 5.3 and has physical specifications as summarised in Figure 5.4. A detailed drawing is available in Appendix A. Further details can be found via [7].

The tower and transition piece were modelled in 3D in Solidworks, hub (i.e. rotor and blades) and nacelle were modelled as remote loads acting on the tower.

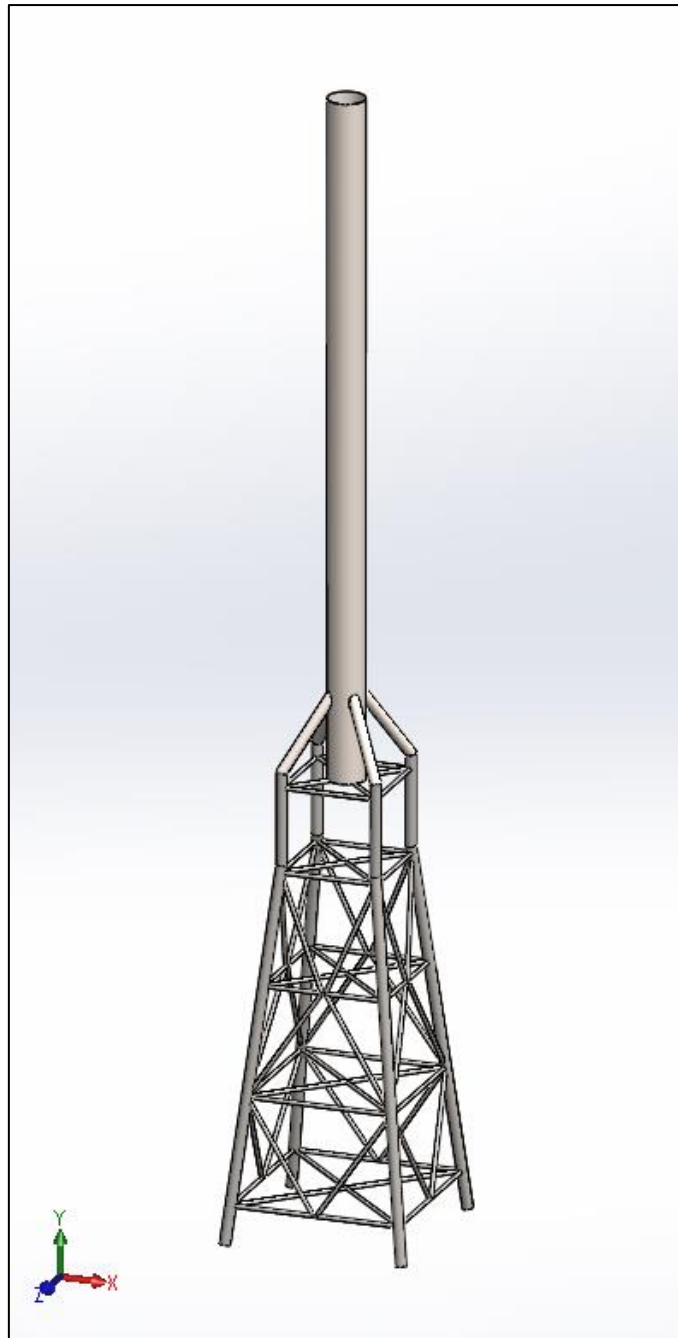


Figure 5.3: Solidworks model of retrofitted Leman BH platform with 5MW NREL wind turbine

Rating	5 MW
Rotor Orientation, Configuration	Upwind, 3 Blades
Control	Variable Speed, Collective Pitch
Drivetrain	High Speed, Multiple-Stage Gearbox
Rotor, Hub Diameter	126 m, 3 m
Hub Height	90 m
Cut-In, Rated, Cut-Out Wind Speed	3 m/s, 11.4 m/s, 25 m/s
Cut-In, Rated Rotor Speed	6.9 rpm, 12.1 rpm
Rated Tip Speed	80 m/s
Overhang, Shaft Tilt, Precone	5 m, 5°, 2.5°
Rotor Mass	110,000 kg
Nacelle Mass	240,000 kg
Tower Mass	347,460 kg
Coordinate Location of Overall CM	(-0.2 m, 0.0 m, 64.0 m)

Figure 5.4: Properties of the NREL 5MW wind turbine

Tower

The tower has a height of 90m with a base diameter of 6m and top diameter of 3.87m. Thickness is greatest at the base at 27mm and smallest at the top at 19mm. The material used throughout is an altered mild steel with Young's modulus of 210 GPa and shear modulus of 80.8 GPa. The material is marginally denser than is typical at 8,500 kg/m³, this is to account for miscellaneous tower components such as paint, bolts, welds, and flanges. The mass of the tower is 348mT. A painted surface finish is assumed (roughness factor of 0.02).

For 3D modelling, the wind turbine is approximated as a cylinder of set diameter and thickness which were equal to the average diameter and thickness (4.935m and 23mm respectively). It should be noted that this approximation slightly raises the position of the centre of mass. The base of the tower is modelled at the same elevation above sea level as the bottom edge of the approximated topside. 3D modelling differs from wind-load hand calculation modelling in which the taper of the tower is maintained.

Rotor, Blades, and Nacelle

The rotor and blades were combined into a single mass of the hub. The hub and nacelle arrangements are shown in Figure 5.5. Hub and nacelle masses are shown along with dimensions of CoM relative to the tower. Masses of are given in Figure 5.4.

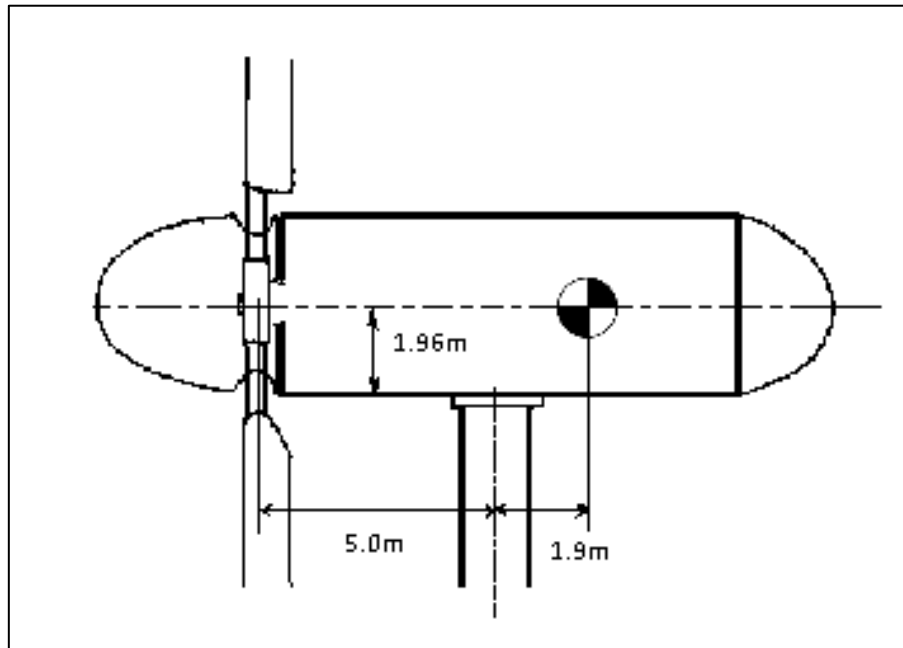


Figure 5.5: Hub and nacelle arrangements as per NREL document

Transition Piece

A transition piece between the tower base and the substructure was created as shown in Figure 5.6. This was modelled upon transition pieces used for similar studies conducted by Barros et al, also shown in the figure. The material used throughout was the same as the jacket (A36 structural steel). As shown in Figure 5.6 the lateral supports were extensions of the legs, the horizontal X-brace was the same cross section as used previously for the jacket X-braces. As before, joint-cans are ignored.

The transition piece was designed as to make the bottom of the tower at the same elevation above sea level as the bottom of the topside.

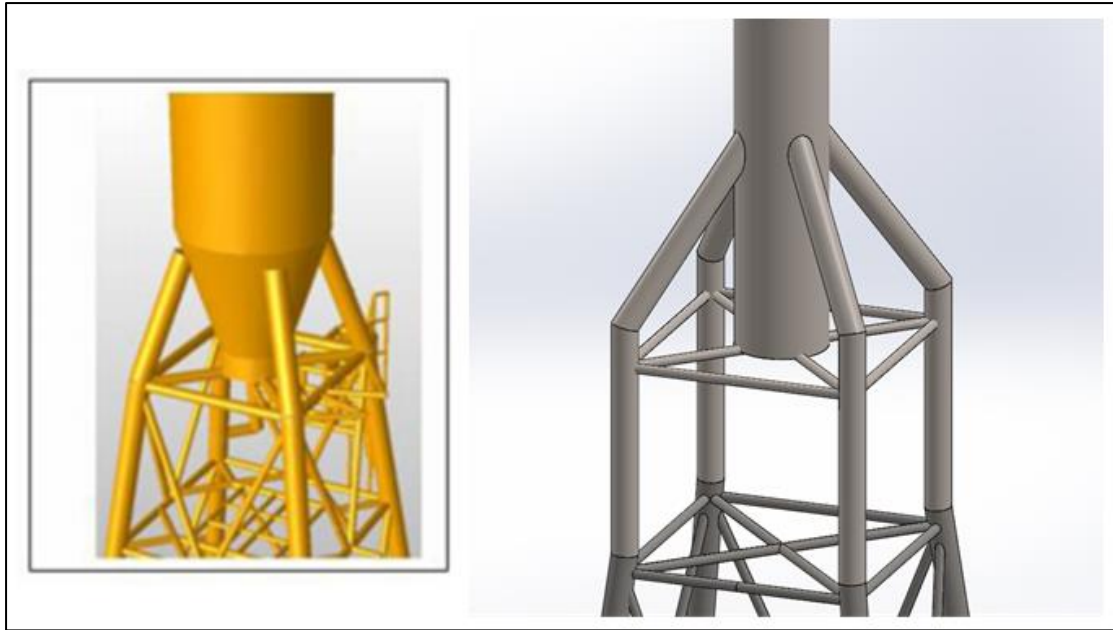


Figure 5.6: Transition piece by Barros et al (left) with transition piece used in this project (right)

5.4. Jacket Validation

Prior to simulation, the jacket was validated for stress and strain.

The model was verified with a 3-dimensional static calculation. The final jacket used for analysis was simplified as shown in Figure 5.7. This was achieved by removing K and X-braces

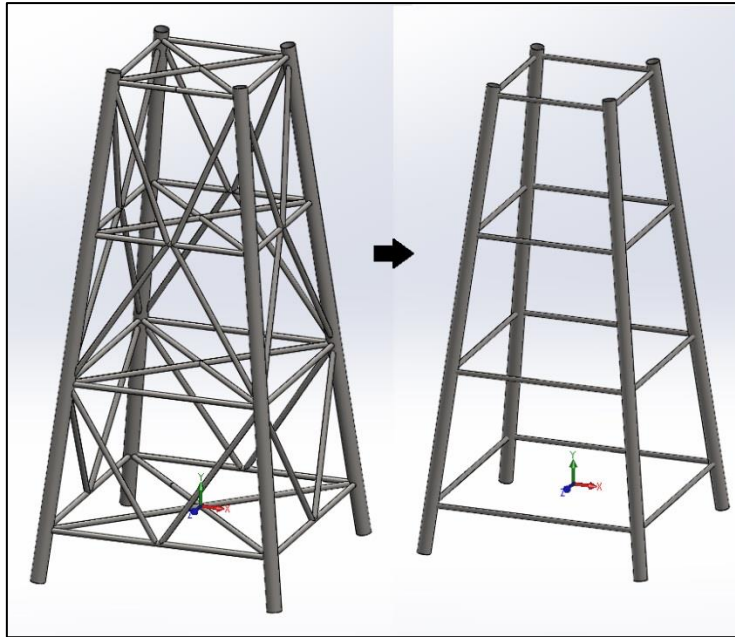


Figure 5.7: Simplification of model of jacket for validation

A pin-jointed linear elastic spring model was assumed. Sea bed fixings were rigidly fixed in keeping with the CAD model. Using *Mathcad* (an advanced calculation software) a co-ordinate and resulting vector system was established as per Figure 5.8 and Figure 5.9 which faithfully reproduced the geometry of the simplified jacket.

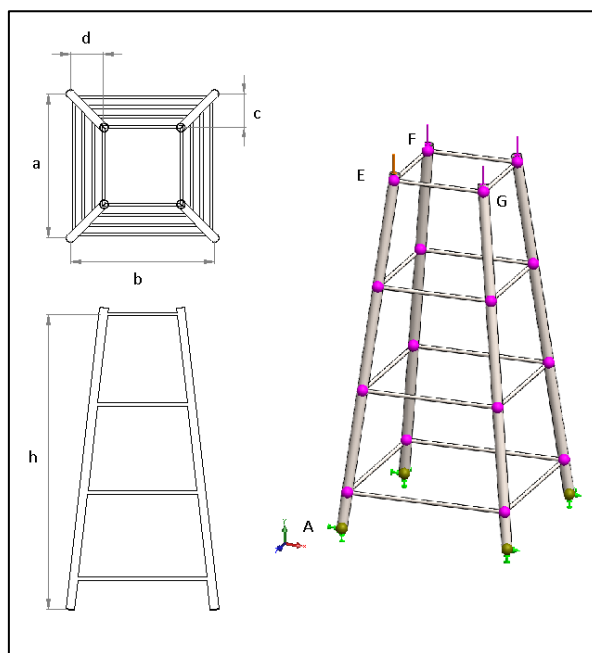


Figure 5.8: Dimensioning of hand-calculation model with reference to the CAD model

Dimensions (meters) as per diagram

a := 23.46 b := a h := 48.08 c := 5.37 d := c

Coordinates of Vertices

$$\vec{A} := \begin{pmatrix} 0 \\ 0 \\ 0 \end{pmatrix} \quad \vec{G} := \begin{pmatrix} a - c \\ b - d \\ h \end{pmatrix} = \begin{pmatrix} 18.09 \\ 18.09 \\ 48.08 \end{pmatrix}$$

$$\vec{E} := \begin{pmatrix} c \\ d \\ h \end{pmatrix} = \begin{pmatrix} 5.37 \\ 5.37 \\ 48.08 \end{pmatrix} \quad \vec{F} := \begin{pmatrix} c \\ b - d \\ h \end{pmatrix} = \begin{pmatrix} 5.37 \\ 18.09 \\ 48.08 \end{pmatrix}$$

Figure 5.9: Co-ordinate system of the hand calculation model using the related diagram

Forces were applied in the downward direction on the vertices as shown in the diagram. The combined force was equal to the topside and simplified jacket weight (i.e. gravity loading on each member was ignored and approximated as a combined force acting on the jacket). This force was equal to 1546mT (15,170 KN).

Resulting forces in the legs and top braces were calculated as shown in Figure 5.10.

Force Per Joint (N)

Load := 1546.1000 Kg

$$F_1 := \begin{pmatrix} 0 \\ 0 \\ \text{Load} \cdot 9.81 \cdot 0.25 \end{pmatrix} = \begin{pmatrix} 0 \\ 0 \\ 3.792 \times 10^6 \end{pmatrix}$$

Member directional vectors, as per diagram

$$\vec{EA} := \vec{E} - \vec{A} = \begin{pmatrix} 5.37 \\ 5.37 \\ 48.08 \end{pmatrix} \quad \vec{EH} := \vec{H} - \vec{E} = \begin{pmatrix} 12.72 \\ 0 \\ 0 \end{pmatrix} \quad \vec{EF} := \vec{F} - \vec{E} = \begin{pmatrix} 0 \\ 12.72 \\ 0 \end{pmatrix}$$

Sum of vectors about point E are equal to zero

$$F_1 + F_{EA} \frac{\vec{EA}}{|\vec{EA}|} + F_{EH} \frac{\vec{EH}}{|\vec{EH}|} + F_{EF} \frac{\vec{EF}}{|\vec{EF}|} = 0 \text{ solve } F_{EA}, F_{EH}, F_{EF} \rightarrow \left(-3.839 \times 10^6 \quad 4.235 \times 10^5 \quad 4.235 \times 10^5 \right)$$

Inputting the calculated values

$$F_{EA} := 3.839 \times 10^6 \quad F_{EH} := -4.235 \times 10^5 \quad F_{EF} := -4.235 \times 10^5$$

$$F_{EA} \frac{\vec{EA}}{|\vec{EA}|} = \begin{pmatrix} 4.235 \times 10^5 \\ 4.235 \times 10^5 \\ 3.792 \times 10^6 \end{pmatrix} \quad F_{EH} \frac{\vec{EH}}{|\vec{EH}|} = \begin{pmatrix} -4.235 \times 10^5 \\ 0 \\ 0 \end{pmatrix} \quad F_{EF} \frac{\vec{EF}}{|\vec{EF}|} = \begin{pmatrix} 0 \\ -4.235 \times 10^5 \\ 0 \end{pmatrix}$$

Figure 5.10: Resultant force calculation using theory (via Mathcad)

Reaction support forces were subsequently calculated. Owing to the symmetry of the structure and that horizontal members support no vertical load in pin jointed structures, the reaction forces are equal and opposite to the forces in the legs.

Reaction Forces

$$\begin{pmatrix} R1_x \\ R1_y \\ R1_z \end{pmatrix} + F_{EA} \cdot \frac{EA}{|EA|} = 0 \text{ solve, } R1_x, R1_y, R1_z \rightarrow \left(-4.235 \times 10^5 \quad -4.235 \times 10^5 \quad -3.792 \times 10^6 \right)$$

Figure 5.11: Reaction forces of support (via Mathcad)

Finally, stress and strain in the leg member was calculated as shown in Figure 5.12.

Stress in Member

Dia := 1.400

thic := 0.035

$$\text{Area} := \frac{\pi}{4} \cdot [\text{Dia}^2 - (\text{Dia} - 2 \cdot \text{thic})^2] = 0.15 \quad \text{m}^2$$

$$\text{Stress} = \text{Force} / \text{Area} \quad \sigma := \frac{F_{EA}}{\text{Area}} = 2.558 \times 10^7 \quad \frac{\text{N}}{\text{m}^2}$$

Strain in member

YoungsModulus := $210 \cdot 10^9$ Pa

Length := 49.69 m

Youngs Modulus = Stress / Strain

$$\delta L := \text{Length} \cdot \frac{\sigma}{\text{YoungsModulus}} \cdot 1000 = 6.052 \quad \text{mm}$$

Figure 5.12: Stress and strain calculation in leg member (via Mathcad)

The results from both hand and computational studies are presented in Table 5-2. Additionally, the *Solidworks* results are presented via screen captures in Appendix B. The results show extremely close correlation.

Table 5-2: Hand and computational study results

Member	Method	F _{res} (MN)	% Difference
EA	Hand	3.8439	0.073
	SW	3.8467	
EF	Hand	0.4235	0.425
	SW	0.4217	
EH	Hand	0.4235	0.425
	SW	0.4217	

Calculated stress in the leg was 25.58 MPa, the Solidworks result was found to be 25.56. This is less than a 1% difference. Similarly, strain was calculated to be 6.052mm by hand, Solidworks found it to be 6.212mm, a minor difference. This is accounted for as Solidworks calculated the total displacement of the element rather than strain in the entire beam.

6. Forces Acting on Structures

Following the creation of the models for the substructure, topside, and wind turbine, forces acting upon the structures were then calculated. These loads are summarised as gravitational loads, wind loads and hydrodynamic loads.

6.1. Gravity Loads

Gravity load is the sum of dead weight and live weight for all the structures. These are summarised for all structures in Table 6-1.

Dead Loads

Topside: Dead weight for the topside is taken as 990mT as previously specified (with bridge to adjacent platform excluded). Included in this weight is the transition piece modelled in Solidworks which connects to the topside.

Jacket: Dead weight of the jacket (without transition pieces, as shown in Figure 5.1) was set to 566mT. However, the mass calculated by the program for the given dimensions and using A36 steel (density 7,850kg/m³) was 428mT. Therefore, the density of the material used in the simulation was manually changed to 10,200kg/m³ to increase the mass to the specified mass of 566mT. As previously stated, this difference accounts for non-modelled components such as paint and non-structural steelwork.

Wind Turbine: Wind turbine dead load is equal 751mT, the sum of the components stated in 5.3 and does not include the transition piece.

Wind Turbine Transition Piece: The designed transition piece is calculated to weigh 166mT when the same alerted-density A36 steel is used.

Live Loads

Live load was calculated for the topside only. A design load of 15KN/m² (as recommended by El-Reedy, 2012) was applied to the area (non-simplified) of the topside. This area was calculated to be 455.8m². This results in a force of 6,837MN which is equivalent to 697mT. An additional 5% of gravity load was applied to all structures as contingency to cover variation in loads.

Table 6-1: Summary of calculated gravitational loads

	Dead load, mT	Live Load, equivalent mT	Total, equivalent mT (including 5% contingency)
Jacket	566	N.A.	584
Topside (including transition piece)	990	697	1,771
Wind turbine (excluding transition piece)	751	N.A.	788
Wind turbine transition piece	166	N.A.	175

6.2. Wind Load

Wind load was calculated as per the methodology for the following:

- The length of substructure above water
- The topside

- The wind turbine and transition piece

For both the wind profile and wind loading on structures, calculations were performed at 1m increments of elevation (i.e. Z step size of 1m).

Wind Profile

Wind speed with elevation, $V(z)$, was calculated for the site and is presented in Figure 6.1. Turbulence and peak velocity pressure were also calculated. Full calculation of these parameters is presented in Appendix C.

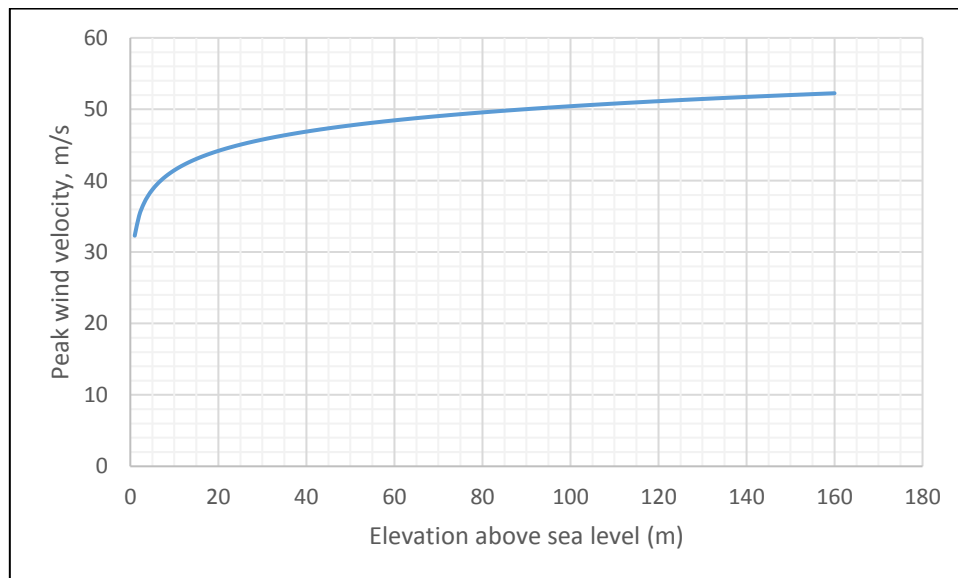


Figure 6.1: Peak wind velocity with elevation above sea level for the Leman BH site

Jacket Wind Load

Using BS-EN 1991-1-4:2005+A1, “Actions on structures: - Wind actions”, wind loads acting upon the exposed section of the jacket and transition pieces are calculated using the wind profile and the geometry of the jacket. As previously stated, the O&G topside and wind turbine elevations above sea level are modelled as equal. Additionally, the effect of the topside or transition piece upon wind flow around the jacket is simplified

with a compensatory coefficient. Therefore, wind loading on the jacket and transition piece for both scenarios was equal.

Jacket and transition piece geometry was simplified to the 4 legs arranged in a square with wind acting perpendicular to a side of the square as shown in Figure 6.2. Using the simplified geometry, the front legs were considered as being in-line with the rear legs.

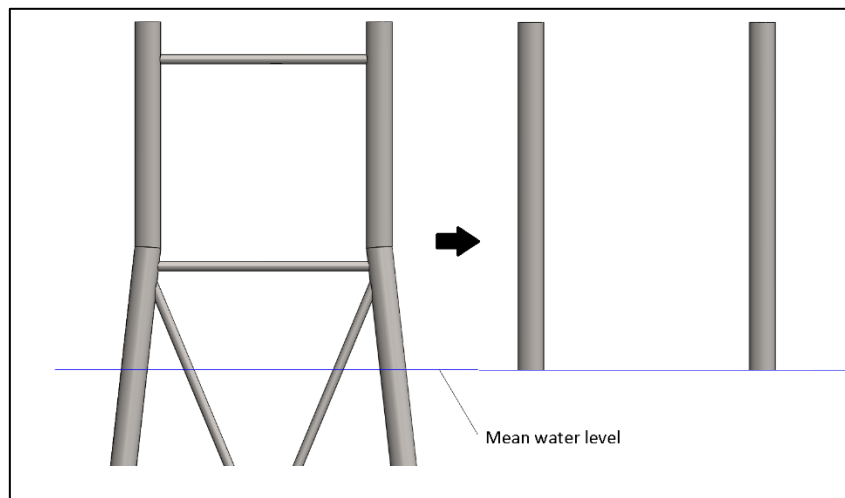


Figure 6.2: Simplification of transition piece geometry

Wind force is calculated using equation (2) which is reproduced here for convenience:

$$F_w = C_s C_d \sum_{elements} C_f \cdot q_p(z) \cdot A_{ref}$$

For all members, structural factor, $C_s C_d$, was determined to be equal to 1.15 and A_{ref} was equal to the leg diameter (1,400mm) multiplied by step size. Force coefficient with elevation, C_f , was determined for the front and rear legs separately using their circular cross section.

Loading results are presented in Figure 6.3 and Table 6-2.

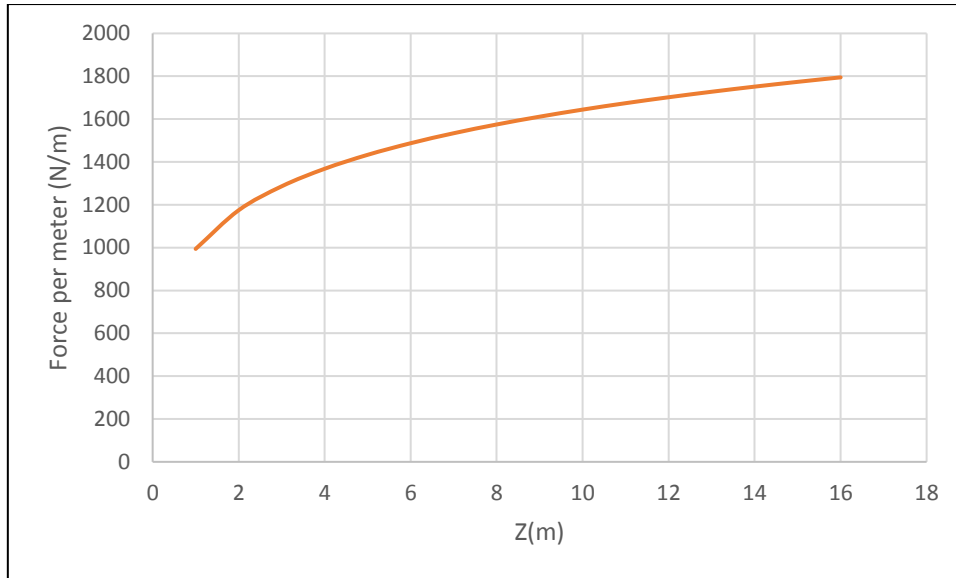


Figure 6.3: Wind loading upon front leg of jacket

Topside Wind Load

The dimensions of the topside are simplified as per 5.2 and shown in below in Figure 6.4. The topside is considered as a point-like structure (i.e. with wind flow both above and below the structure). Force acting on the structure is calculated using equation (2). It should be noted that friction along the sides of the structure is negligible (as per section 7.5 of the standard).

Structural factor is taken as equal to 1.0 (as per 6.2.1.c³). Force coefficient is taken as 1.80 (as per 7.4.3 – 1). Reference area is equal to the simplified width (22.37m) multiplied by the step size.

Loading results are presented in Table 6-2.

³ “For framed buildings which have structural walls and which are less than 100 m high and whose height is less than 4 times the in-wind depth, the value of c_{sfd} may be taken as 1.”

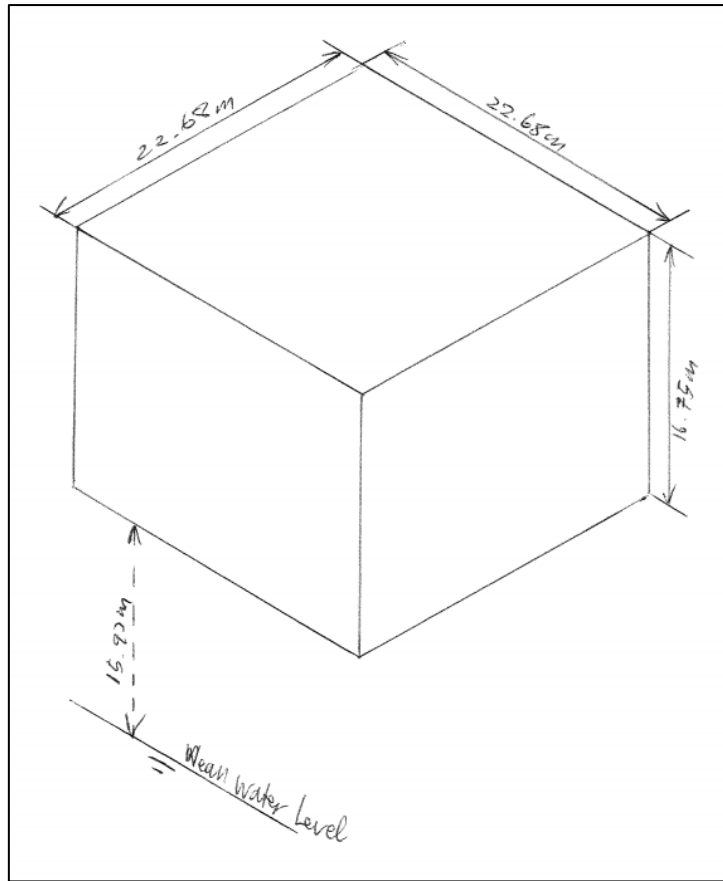


Figure 6.4: Simplification of topside for wind load calculation

Wind Turbine Wind Load

Using the generated wind profile and the dimensions given in Figure 5.4 of the modelling section wind force acting on the tower was calculated.

The wind loading is considered on the tower only and not the inclined members of the transition piece, hub, or nacelle which are likely negligible with respect to the tower loading. Furthermore, their effect of the transition piece and jacket upon wind flow around the tower base is neglected. The tower is considered as a vertical cylinder with both ends free located at elevation above the water level.

Loading is calculated using equation (2). Structural factor was taken to be 1.15. Force coefficient was calculated with elevation as per the circular geometry. Reference area

was calculated as the average diameter of the elevation step size multiplied by elevation step size.

Loading results are presented in Figure 6.5 and Table 6-2.

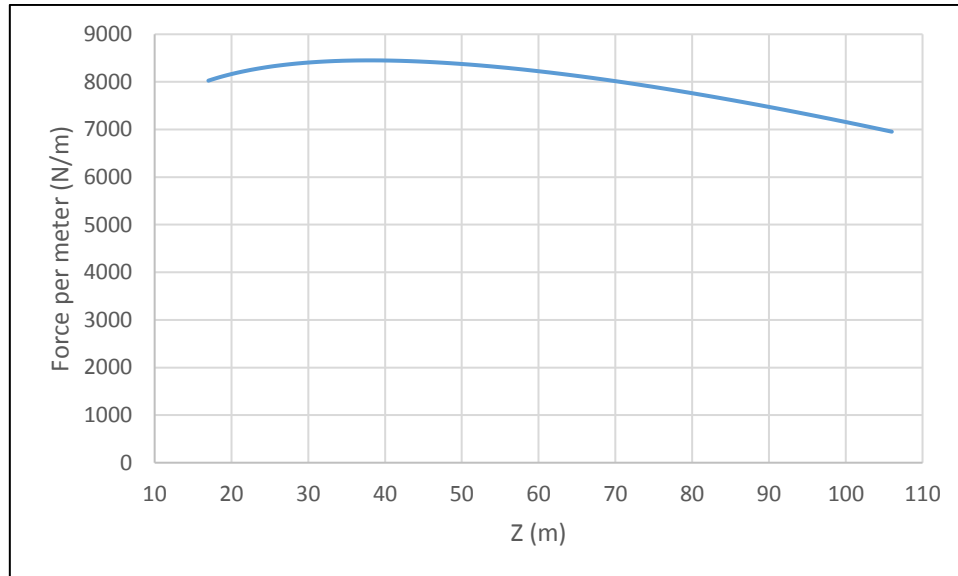


Figure 6.5: Wind turbine wind load with elevation above sea level

Thrust

As per the methodology, thrust force was also considered in addition to wind drag around the tower. Thrust produced with wind speed is given by the NREL turbine specifications as shown in Figure 6.6.

Peak thrust recorded occurs at 11.3 m/s wind speed and produces 831 KN. Although the tower drag forces are calculated at wind speeds greater than 11.3 m/s this peak thrust force will only be considered.

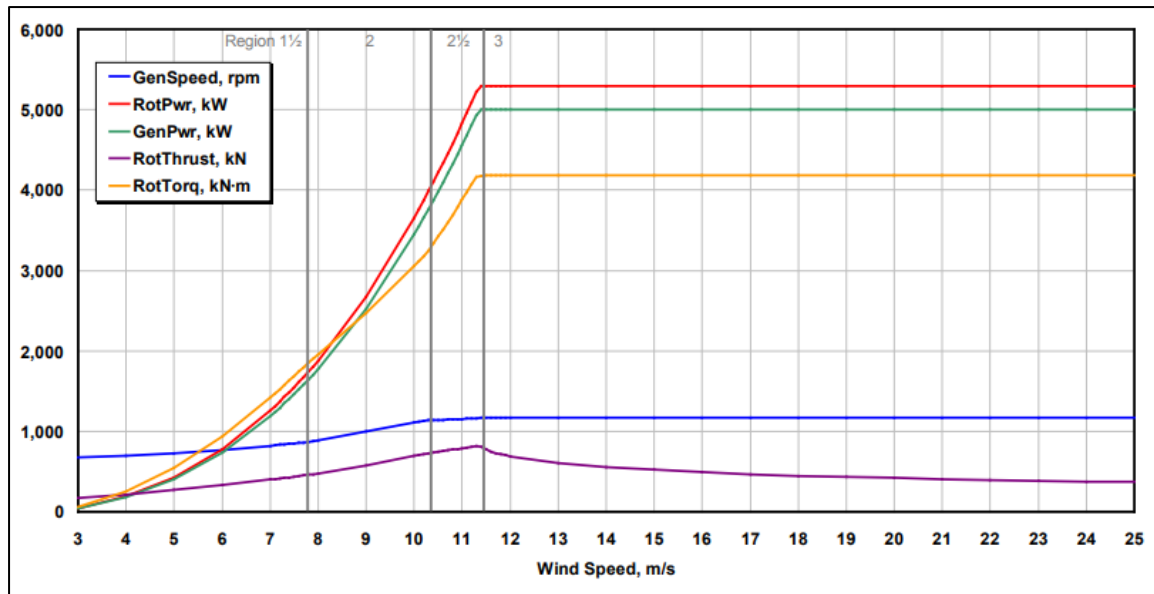


Figure 6.6: NREL 5MW wind turbine thrust curve with wind speed.

Table 6-2: Summary of wind loading and conditions

	Total force description	Total Force magnitude, KN
Simplified jacket and transition piece, all legs combined	2 front and 2 in-row rear legs with compensatory coefficient of 1.2	173.3
Topside	Point-like structure similar to signboard	1745
Wind turbine drag	Cylinder with reducing diameter with elevation. Free flow about both ends	718
Wind turbine thrust	Obtained from NREL specifications	831

Wind loading Validation

Wind load was validated using ANSYS software. Validation occurred for the wind turbine tower only. Ideally, validation would occur for all members subjected to wind load together but, due to time constraints of the project, this was not possible.

The tower was modelled as a solid body and replicated in full geometry with base diameter of 6m and top diameter of 3.87m (height of 90m) as shown in Figure 6.7.

Using ANSYS FLUENT an enclosure for wind flow was set around the tower. A minimum clearance of 5m between enclosure and model was used. A uniform wind profile was established entering one face of the enclosure and exiting in the same direction as shown in Figure 6.7.

Wind speed was set to 48.0m/s, equal to the average wind speed derived from the profile.

This makes the assumption that wind profile derived is correct and calculated correctly.

Although an inter-standard comparison is not performed, the wind profile calculated via the standard is verified against grey literature. The study used can be found in reference [40] and, when the appropriate values were substituted into the calculation, the profiles agreed.

The wind force on the tower was found to be 904KN. This value is 26% greater than the value derived previously and shown in Table 6-2. This significant difference is likely due to the uniform wind profile assumed. As the wind profile derived by BS-EN 1991-1-4 is non-linear, as shown in Figure 6.1, there is a significantly greater wind speed acting on the lower sections of the tower during the ANSYS simulation. As the lower section of the tower is far wider than upper sections, it is likely that the force received is disproportionately large.

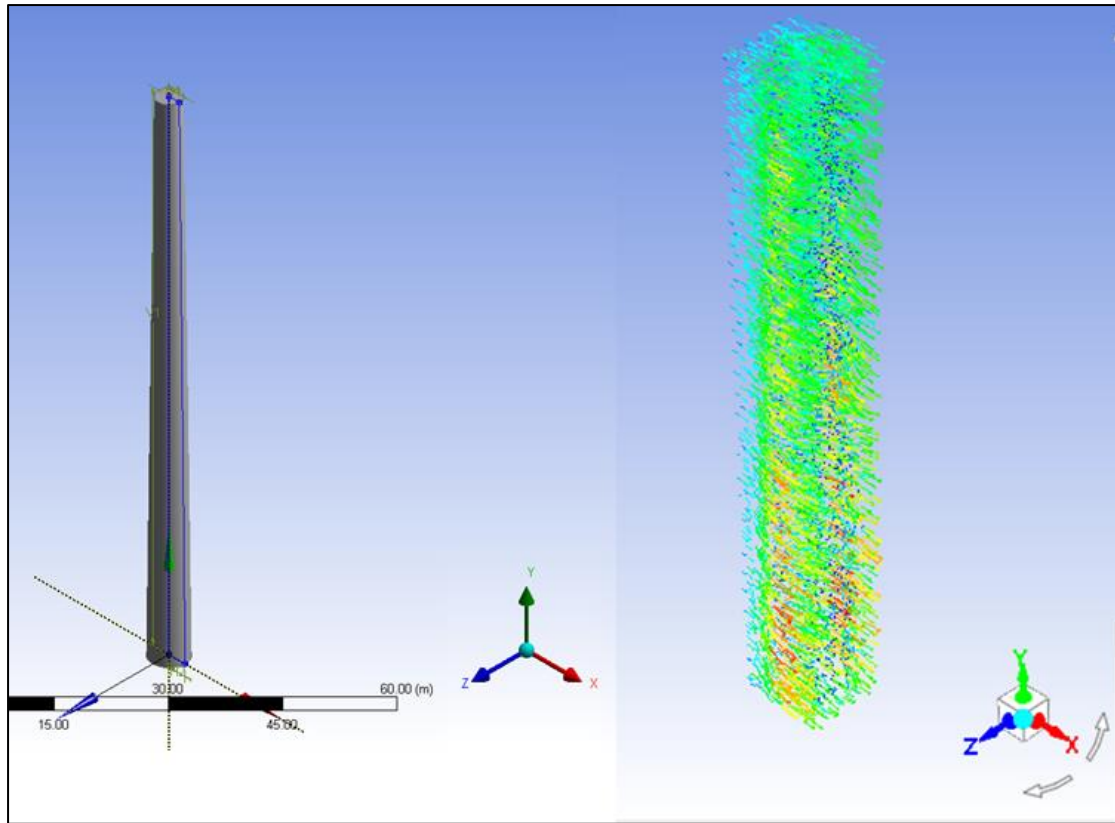


Figure 6.7: Geometry of wind turbine tower and ANSYS FLUENT simulation

6.3. Wave Load

Wave loading is calculated as per the methodology with DNV RP-C205 “Environmental Conditions and Environmental Loads”. Loading is considered for the substructure only. Throughout, wave profile and loading was calculated with elevation in 1m step sizes.

Wave Profile

A full calculation of wave profile is provided in Appendix D. Wave profile is estimated using linear wave theory (Airy). Wave spectral data gathered, shown in Figure 6.8, from a nearby site and was used and assumed to be of a similar water depth.

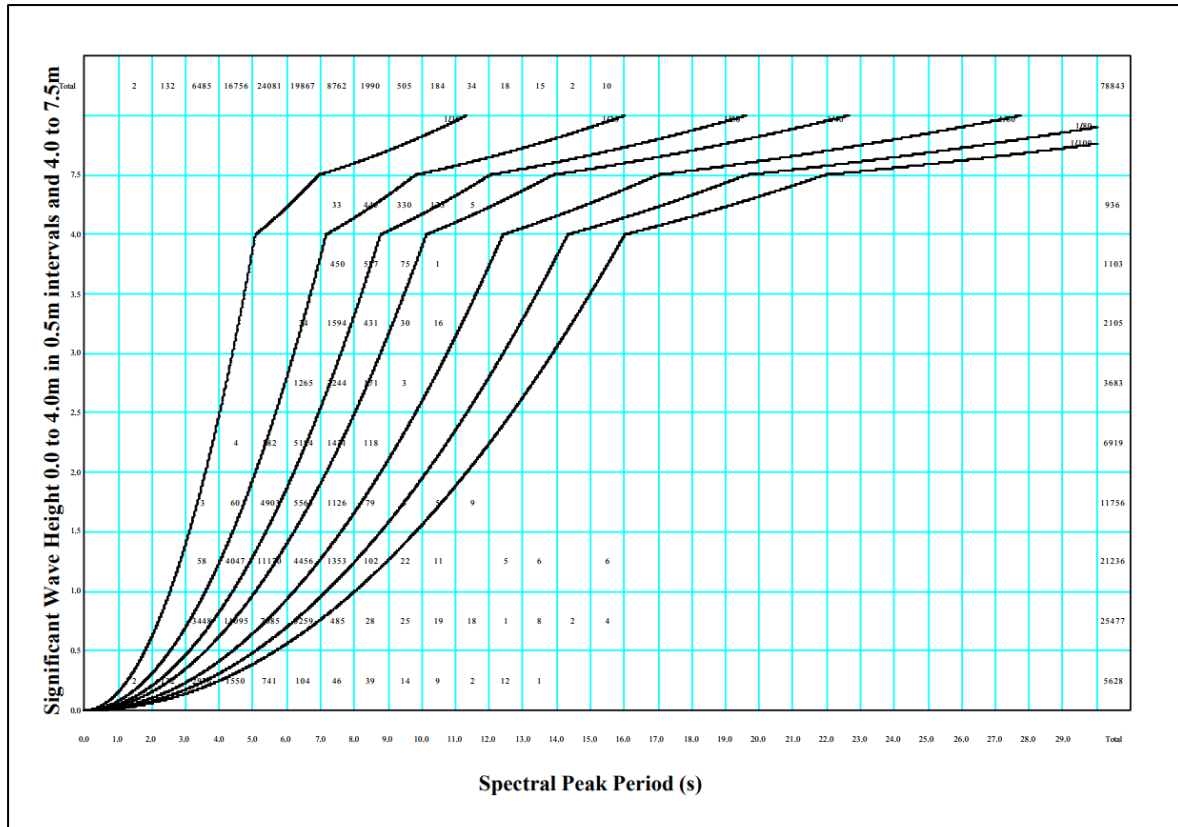


Figure 6.8: Wave spectra data for site near Lemau BH location. Provided by [41]

Wave velocity was calculated using equation (6) and acceleration was calculated using equation (7). The results are shown in Figure 6.9

$$V = \frac{\pi H \cosh(k(z + d))}{T \sinh(kd)} \sin(\theta) \quad (6)$$

$$a = \frac{-\pi^2 H \cosh(k(z + d))}{T^2 \sinh(kd)} \cos(\theta) \quad (7)$$

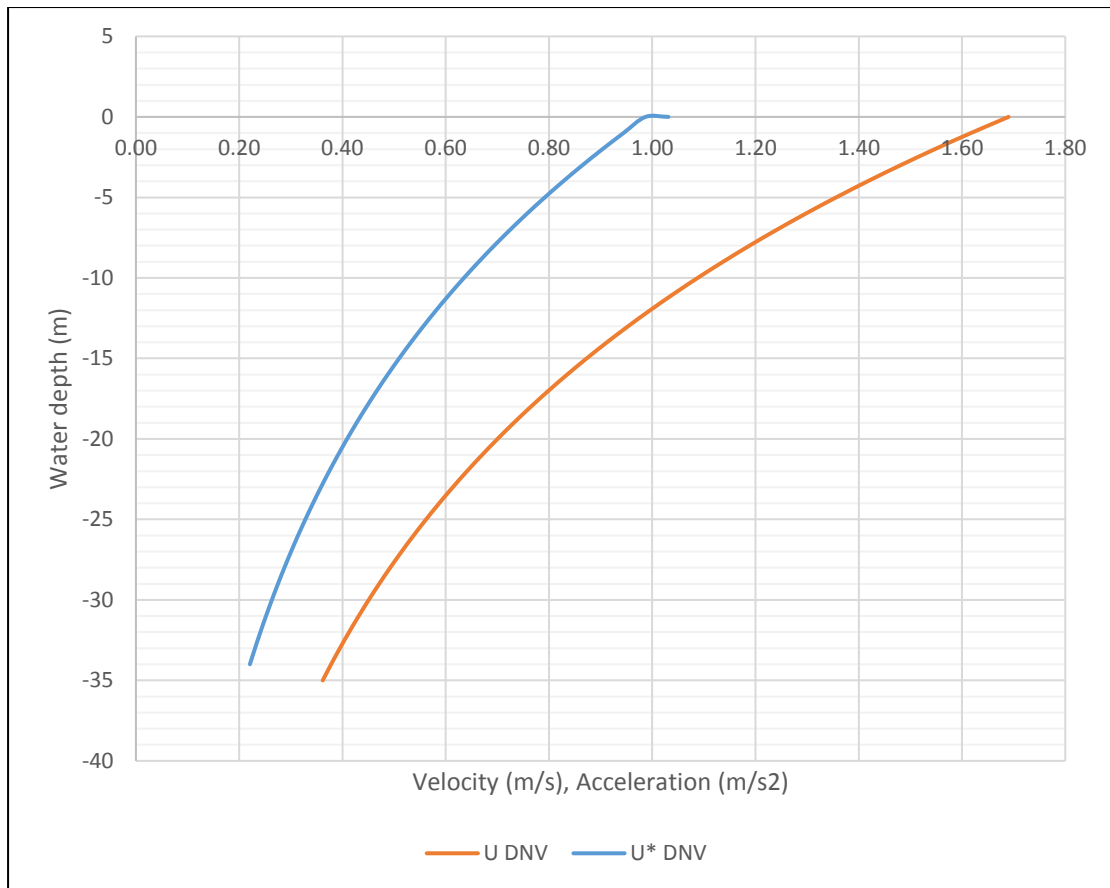


Figure 6.9 Maximum horizontal particle velocity and acceleration profiles with water depth (note, these do not occur at the same time)

Substructure Wave Load

For wave load calculation, the geometry of the jacket was simplified as follows:

- Legs were simplified to vertical members
- All diagonals were calculated as (separate) vertical and horizontal components.
As load generated with elevation is non-linear, the horizontal members forces were calculated at an elevation where loading on the vertical member was balanced above and below that elevation.
- Horizontal members behind leading members are ignored (i.e. all X-braces and horizontal braces members on the left and right sides)

- A compensatory coefficient of 1.1 was applied to wave loading magnitudes

Loading is considered in 1 direction only, perpendicular to a side of the substructure (which is symmetrical). All members are considered slender as per the standard.

Drag force, F_D on slender members as a result of wave action is given by equation (3):

$$F_D = \frac{1}{2} \cdot \rho \cdot C_d \cdot V^2 \cdot A$$

For all members coefficient of drag, C_d , was taken to be 1.05 as per API recommendations for rough surfaces. A rough surface was assumed as marine growth is likely to have accumulated over the 49-year lifespan of the Leman BH installation.

Inertia force was calculated for members as per equation (4).

$$F_I = \pi \cdot \rho \cdot a \cdot C_m \cdot \frac{D^2}{4}$$

For all members coefficient of inertia, C_m , was taken to be 1.20 as per API recommendations for rough surfaces. Total drag and inertia force for the leading leg with time is shown in Figure 6.10. Maximum force was found to occur at a phase angle of 0.8 rad (45.8°). Loading on members is summarized in Table 6-3.

Table 6-3: Summary of wave loading

Member	Elevation (m)	Total F_D max (KN)	Total F_I max (KN)	Total F_{total} max (KN)
Leg	0-35.7	47.5	51.7	60.5
Topmost diagonal braces (combined)	26.7-35.7	12.5	3.7	13.1
Horizontal members	26.4	3.2	1.5	3.7
Middle diagonal braces (combined)	13.9-26.2	6.0	2.9	7.4

Horizontal members	13.7	1.1	0.9	1.7
Lower diagonal braces (combined)	0-13.5	1.9	1.6	3.0

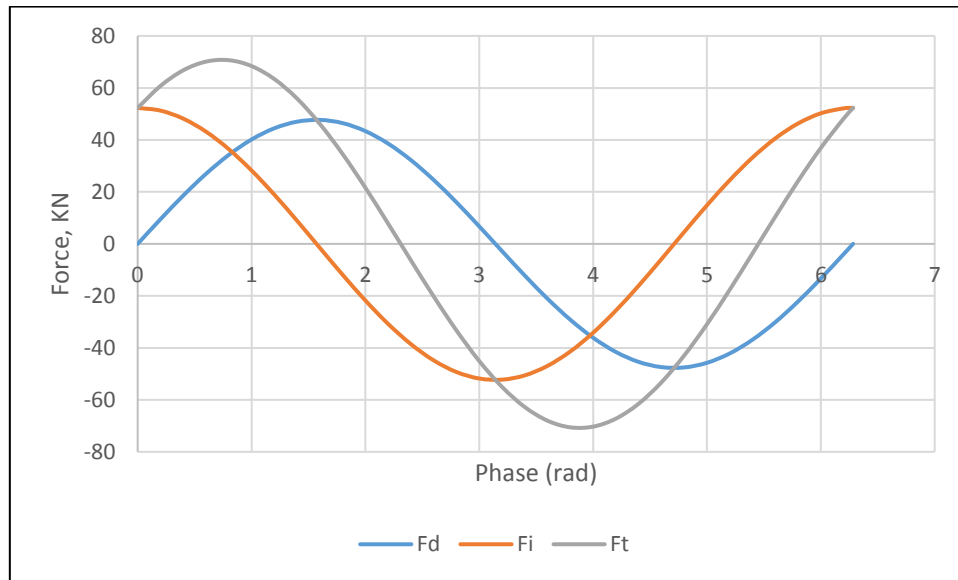


Figure 6.10: Variation of drag, inertia, and total force on the front leg

Other Hydrodynamic Loads

The site was not found to have a significant current, Therefore, as per the methodology, current force was neglected altogether.

Hydrostatic force was also ignored as all members the diameter to thickness ratio was greater than the result of $205 / h^{0.333}$.

Wave Loading validation

A proper validation of the calculated wave load was not conducted due to the time constraints of the project. However, comparison to grey literature was performed. This was achieved by replacing the values used in calculating wave loading on the leg with the values used for the grey literatures study and comparing the results. The grey

literature used can be found in [40]. This team also used the DNV RP-C205 and results showed agreement.

Ideally, a different method of calculation would be employed and the entire structure would be considered. This would be performed using software such as SESAM (also produced by DNV), ANSYS, or ABAQUS (which is made by the same developers as Solidworks).

7. Summary and Simulation

Following the creation of both models and the calculation of loading upon them, loading was then applied to the models prior to simulation. This is summarised and presented in this section.

Throughout the simulations the following is assumed:

- Changes in temperature of both wind and sea throughout the year have negligible differences on performance of the structures and the default temperature of Solidworks is appropriate
- Effect of sea level variation as a result of tide and season are negligible
- Fatigue in the structure at the time of retrofit is not significant in its performance
- All structures behave elastically

7.1. Gravitational Loads

Jacket: Gravitational load was applied to the jacket by altering the density of the material used by the program until the desired mass was achieved.

Topside: Gravitational load (both dead and live load) was applied as a distributed mass acting on the joints indicated in Figure 7.1. Note: the material's density of the transition piece for the topside was the same as the jacket and the distributed mass of the topside was reduced accordingly.

Wind turbine: Gravitational loading of the hub and nacelle were applied as remote forces acting upon the topmost joint of the tower as indicated in Figure 7.1. As with the O&G topside, the wind turbine transition pieces were composed of the same material as the jacket with greater density.

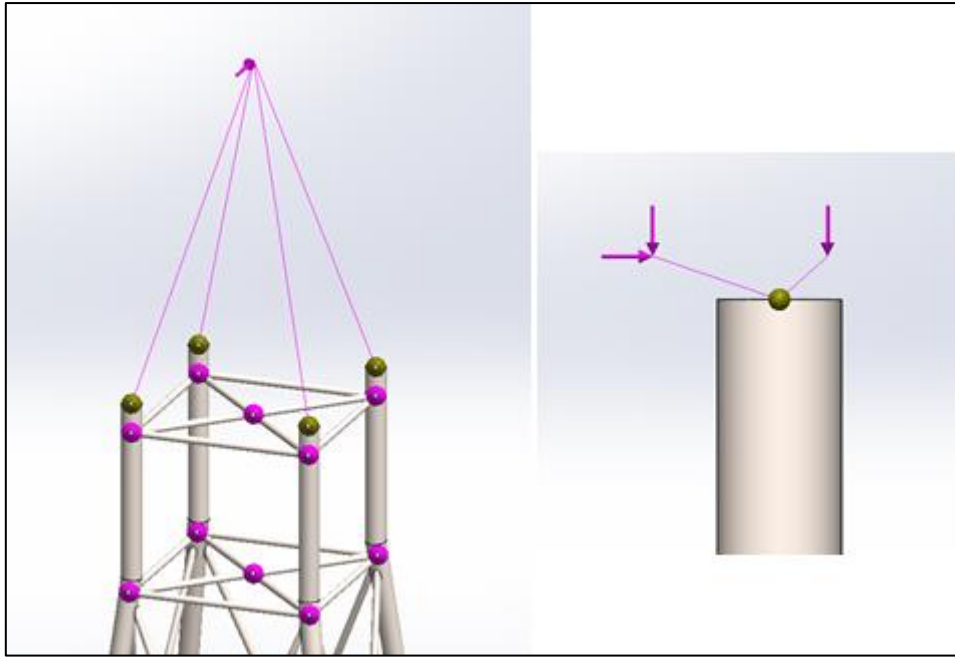


Figure 7.1: LEFT, O&G loading for simulation 1. RIGHT, OWT tower top loading for simulation 1

7.2. Wind Load

Wind load direction for all structures is kept consistent throughout. Wind load was applied as a static force.

Jacket: Wind loading was applied to the exposed length of jacket as a non-uniform load upon each of the jacket's legs as shown in Figure 7.2. Additionally, the wind loading on the transition pieces for both models are equal and applied as distributed loads.

Topside: Wind load was applied as a remote force equal to the total wind load. This force acted upon the transition piece joints at a distance equal to the centre of mass of the topside as indicated in Figure 7.1.

Wind Turbine: Wind loading on the tower was applied as a non-uniform load. Thrust from the blades was modelled as a remote force acting a point equal to the centre of the hub as shown in Figure 7.1.

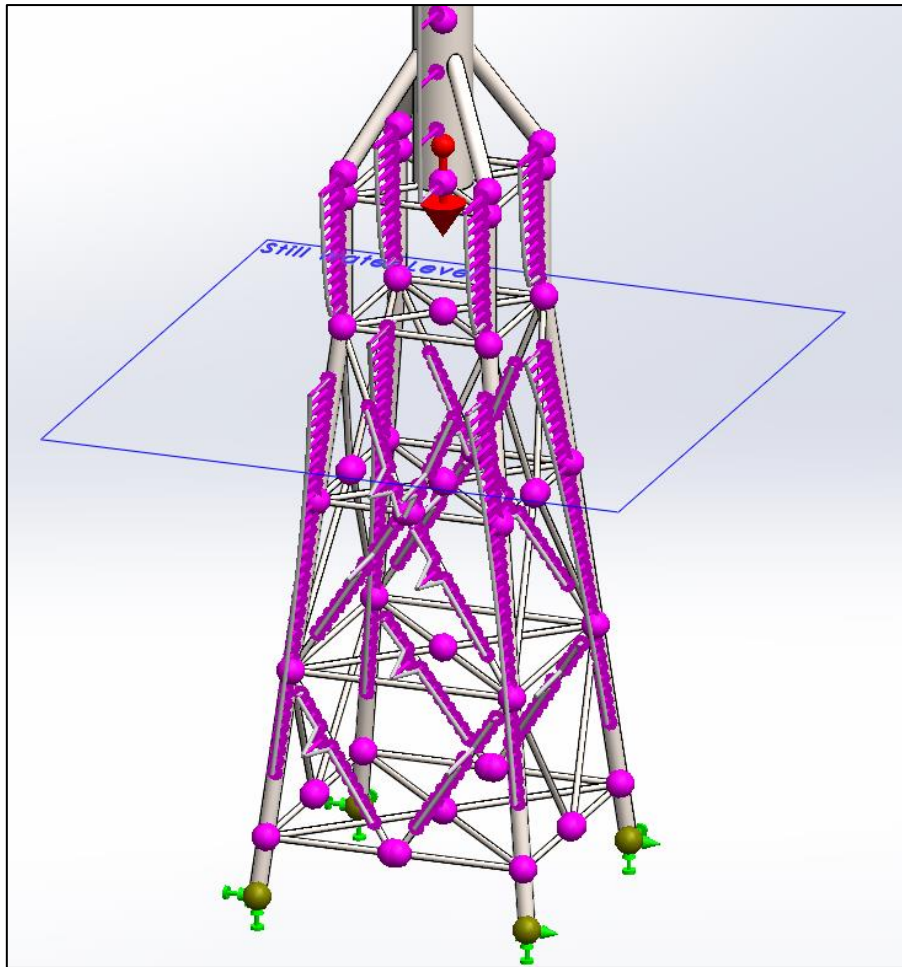


Figure 7.2: Full loading of OWT model

7.3. Wave Loading

Wave loading on the jacket was modelled as a static force equal to the maximum force in the positive wave direction. This force was modelled on the members of the jacket as a non-uniform load as shown in Figure 7.2.

8. Results

Simulations were performed with the models created in section 5 and the loading calculated in section 6 as per the methodology. Results are presented in this section.

Note on numbering convention

For all simulations, supports are always numbered from 1-4 in a clockwise fashion starting and ending at the model's front face. This is illustrated in Figure 8.1.

The front is face of models is taken to be the face which faces the incoming wind and wave forces.

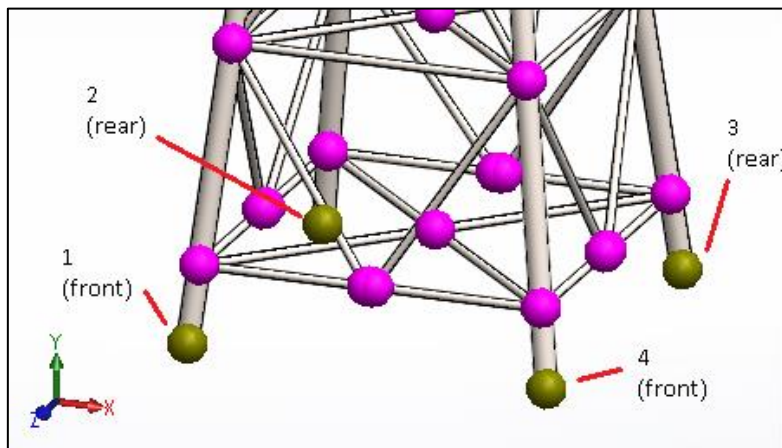


Figure 8.1: Numbering convention of supports.

8.1. Mesh Convergence

Prior to simulations, the model was first converged. The O&G model was applied with the loads as used by Simulation 1 (gravitational loads only). Different element lengths were investigated as summarised in Table 8-1. The Von Mises stress was investigated for two locations: front leg mid-point and front lower horizontal brace mid-point. Appropriate element size was found to be 250mm.

Table 8-1: Mesh convergence results

Element size (mm)	No. elements	Front leg-mid VM stress (MPa)	% difference	Front horizontal mid VM (MPa)	% difference
1000	1,224	27.54	/	14.26	/
500	2,422	27.47	0.25	14.32	0.42
250	4,829	27.39	0.29	14.34	0.14
100	12,113	27.36	0.11	14.35	0.07

8.2. Simulation 1 – Gravitational Loads Only

The study of gravitational loads only was conducted as per the methodology.

Both referenced figures show the resultant Von Mises stress from the loading (note that the resultant deformation is not shown). Key stresses and reaction forces are provided from Table 8-2 to Table 8-5.

Additional results which are not used for subsequent discussion are included in Appendix F.

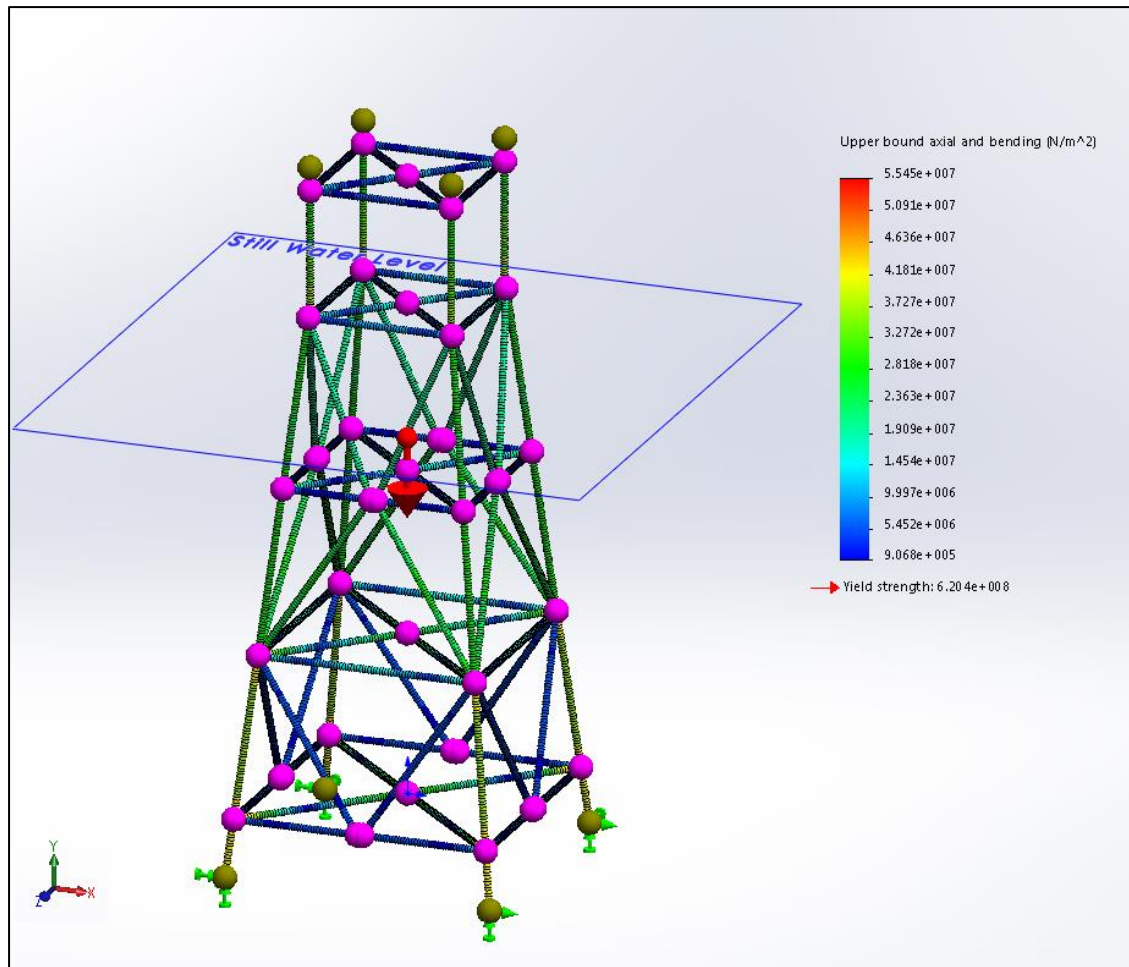


Figure 8.2: Stress results (Von Mises) of the simulation of gravitational loads only on the O&G model. The result shown is undeformed. Still water level is indicated in blue.

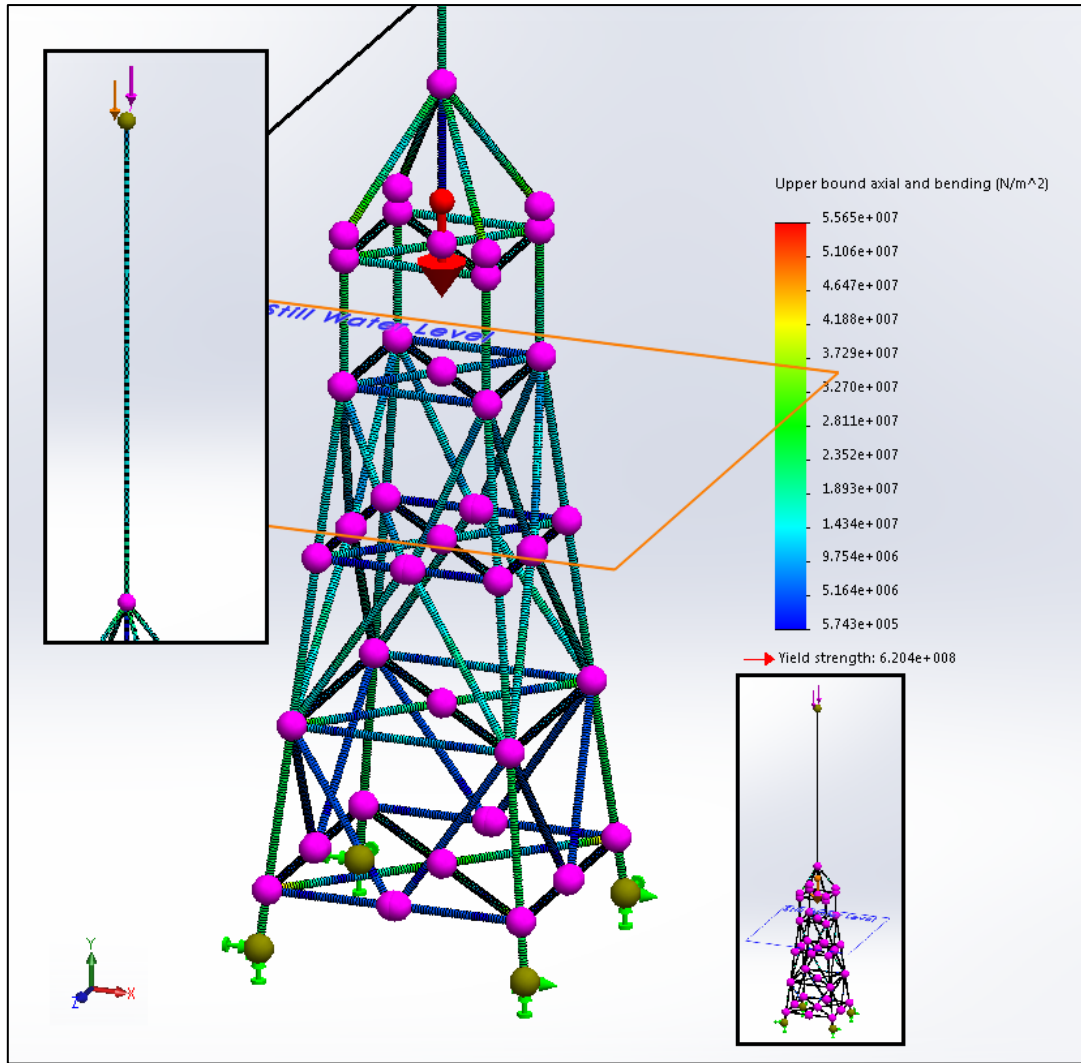


Figure 8.3: Stress results (Von Mises) of the simulation of gravitational loads only on the wind turbine model. The result shown is undeformed. Still water level is indicated in orange.

Table 8-2: O&G - Support reactions for gravitational loads only. Forces and moments in supports 3 and 4 mirror 1 and 2 respectively and are shown in Appendix F

Support	F_x (MPa)	F_y (MPa)	F_z (MPa)	F_{res} (MPa)	M_x (KNm)	M_y (KNm)	M_z (KNm)	M_{res} (KNm)
1	0.63	5.62	-0.63	5.69	57.4	0	57.4	81.2
2	0.63	5.62	0.63	5.69	-57.4	0	57.4	81.2

Table 8-3: Wind turbine – Support reactions for gravitational loads only. Forces and moments in supports 3 and 4 mirror 1 and 2 respectively and are shown in Appendix F

Support	F_x (MPa)	F_y (MPa)	F_z (MPa)	F_{res} (MPa)	M_x (KNm)	M_y (KNm)	M_z (KNm)	M_{res} (KNm)
1	0.398	3.49	-0.396	3.53	40.5	-1.16	32.1	51.7
2	0.394	3.45	0.396	3.49	-23.2	-1.16	31.6	39.2

Table 8-4: O&G – Stresses in key members for gravitational loads only

Desc	Axial (MPa)	Bending Dir1 (MPa)	Bending Dir2 (MPa)	Torsional (MPa)	Von Mises (MPa)
Leg, front, upper	-25.09	0.85	0.87	0.00	26.31
Leg, rear, upper	-25.08	-0.94	0.95	0.00	26.42
Leg, front, middle	-26.54	-0.60	-0.61	0.00	27.39
Leg, front, lower	-36.52	-0.01	-0.01	0.00	36.53

Table 8-5: Wind turbine – Stresses in key members for gravitational loads only

Desc	Axial (MPa)	Bending Dir1 (MPa)	Bending Dir2 (MPa)	Torsional (MPa)	Von Mises (MPa)
Leg, front, upper	-13.78	0.91	0.99	-0.01	15.13
Leg, rear, upper	-13.44	-1.01	0.95	-0.01	14.84
Leg, front, middle	-15.24	-0.63	-0.64	0.00	16.14
Leg, front, lower	-22.12	-0.02	0.00	0.00	22.14

8.3. Simulation 2 – Transition Piece Comparison

The study of full loading on the transition pieces was conducted as per the methodology.

Identical wind loads were applied to the legs of the transition pieces.

Again, both figures show resultant Von Mises stress and no resultant deformation. Key stresses and reaction forces are provided in Table 8-6 and Table 8-7.

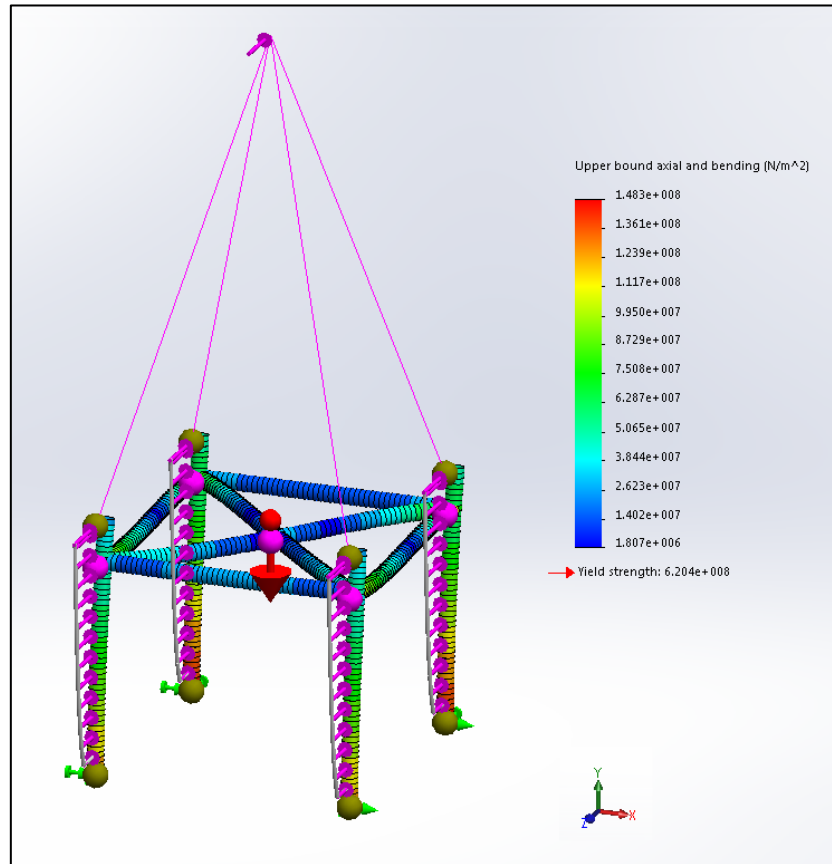


Figure 8.4: Stress results (Von Mises) of the full loading on the O&G transition piece model. The result shown is undeformed.

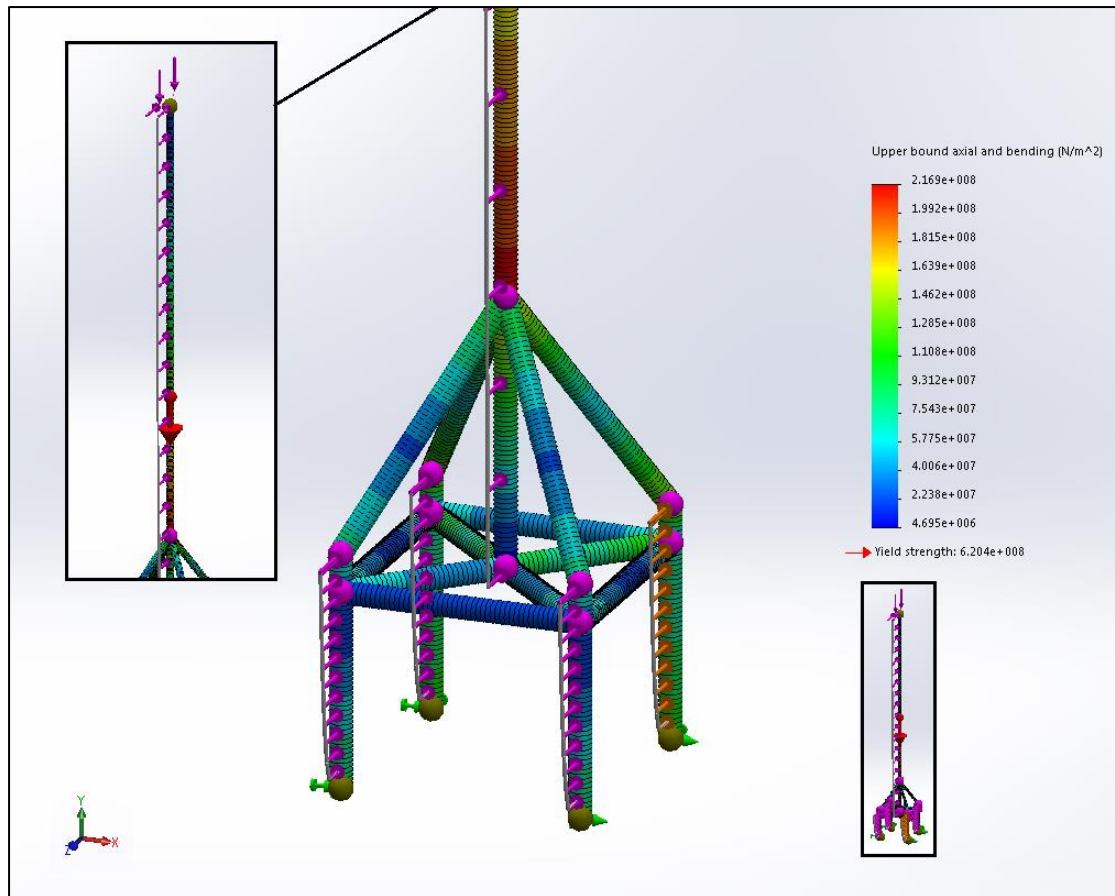


Figure 8.5: Stress results (Von Mises) of the full loading on the wind turbine transition piece model. The result shown is undeformed.

Table 8-6: O&G – Transition piece reactions for full loading. Forces and moments in supports 3 and 4 mirror 1 and 2 respectively and are shown in Appendix G

Support	F_x (MPa)	F_y (MPa)	F_z (MPa)	F_{res} (MPa)	M_x (MNm)	M_y (MNm)	M_z (MNm)	M_{res} (MNm)
1	0.0874	2.64	0.442	2.68	5.4	-0.10	-0.206	5.41
2	-0.065	5.82	0.465	5.84	5.47	-0.10	0.137	5.48

Table 8-7: OWT – Transition piece reactions for full loading. Forces and moments in supports 3 and 4 mirror 1 and 2 respectively and are shown in Appendix G

Support	F_x (MPa)	F_y (MPa)	F_z (MPa)	F_{res} (MPa)	M_x (MNm)	M_y (MNm)	M_z (MNm)	M_{res} (MNm)
1	0.0835	-2.11	0.468	2.16	3.92	0.305	-0.215	3.94
2	-0.212	6.65	0.34	6.66	3.64	0.305	0.5	3.68

8.4. Simulation 3 – Full Simulation

The study of full loading on the full models was conducted as per the methodology. Again, both figures show resultant Von Mises stress and no resultant deformation. Key stresses and reaction forces are provided from Table 8-8 to Table 8-11. Frequency analyses for the first five mode shapes were conducted on both models using the simulation software. The fundamental mode shapes of both models are shown in Figure 8.8. The five mode shapes found are summarised in Table 8-12.

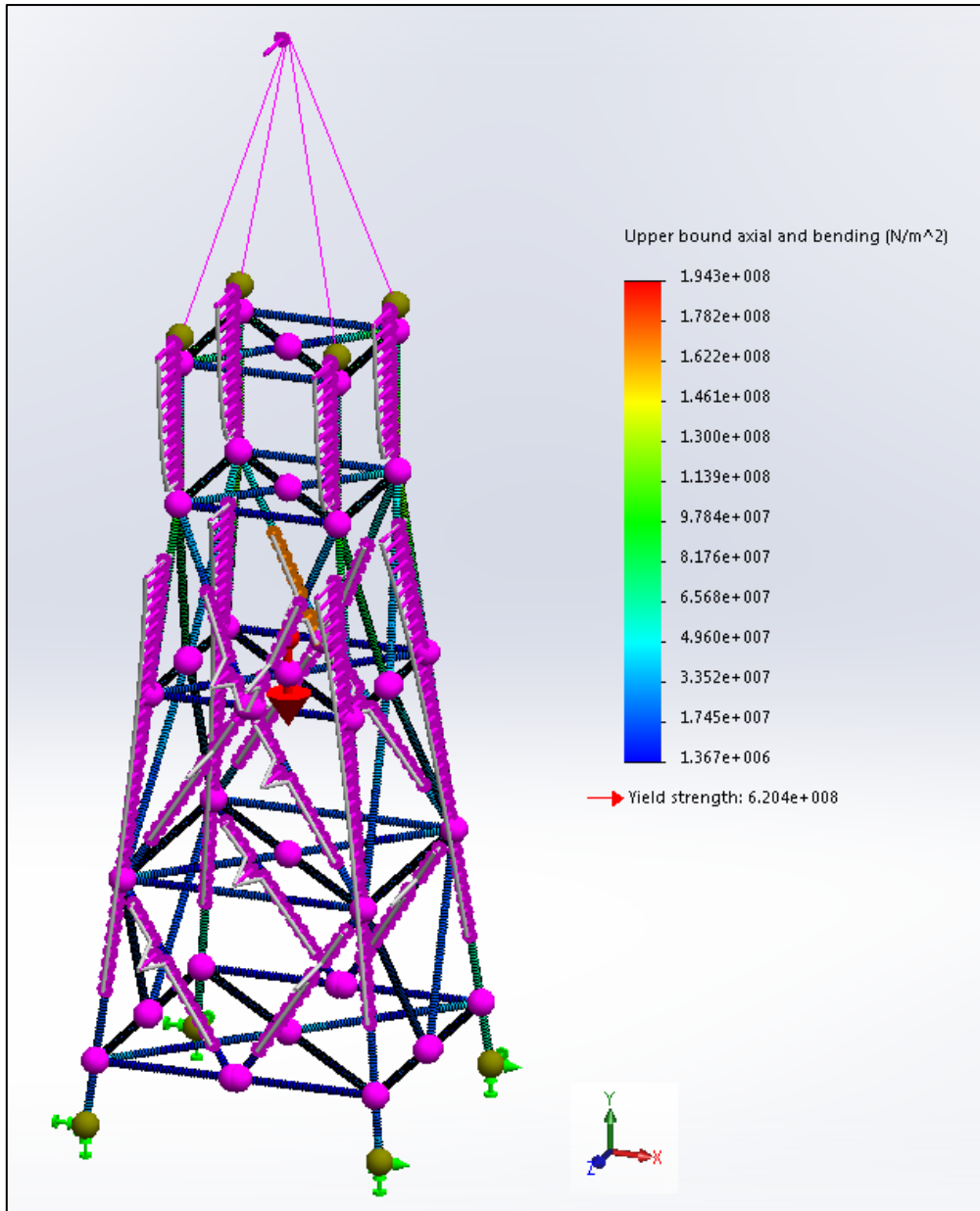


Figure 8.6: Stress results (Von Mises) of the full loading on the O&G model. The result shown is undeformed

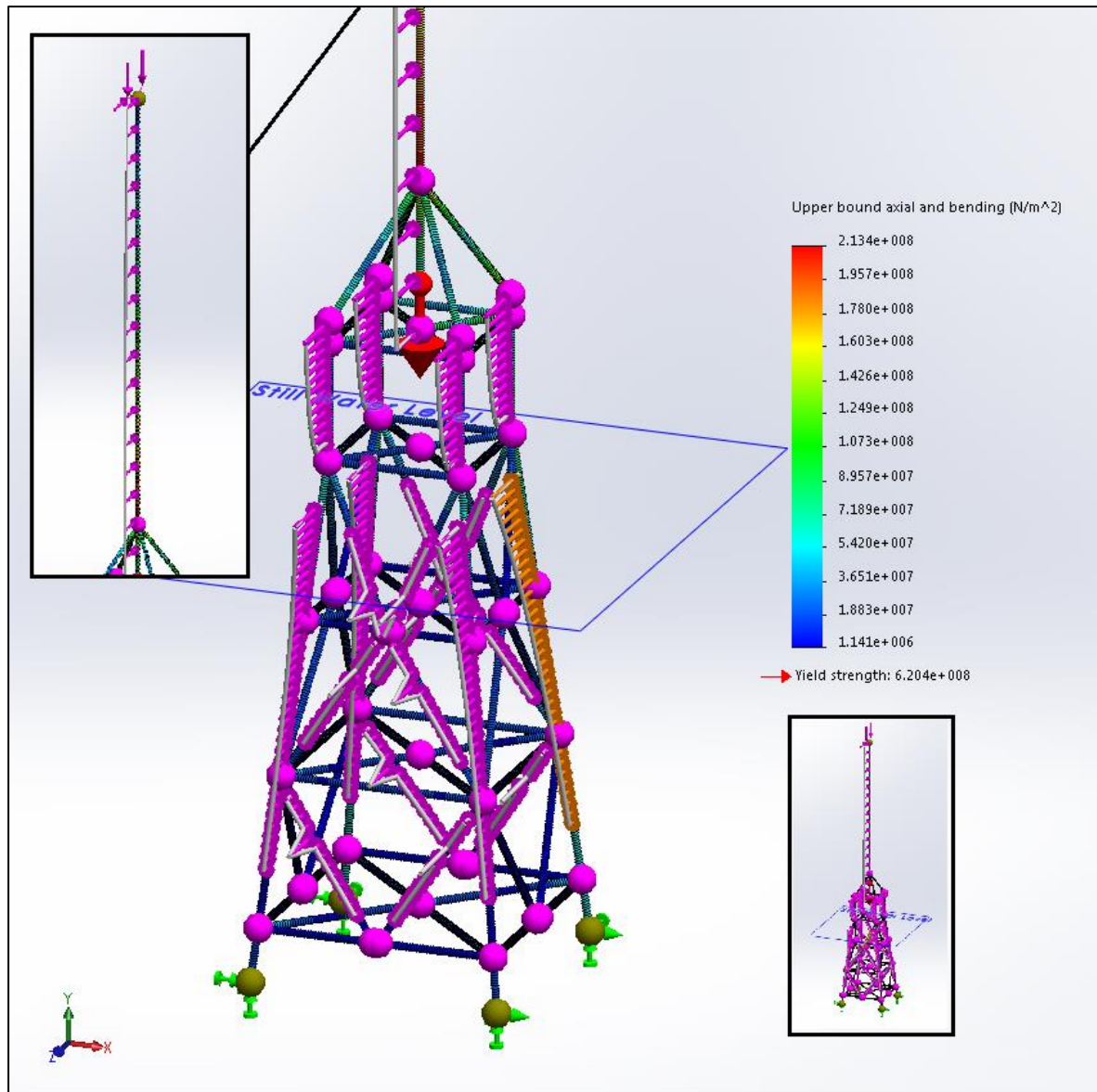


Figure 8.7: Stress results (Von Mises) of the full loading on the OWT model. The result shown is undeformed

Table 8-8: O&G – Support reactions for full model and full loading. Forces and moments in supports 3 and 4 mirror 1 and 2 respectively and are shown in APPENDIX H.

Support	F _x (MPa)	F _y (MPa)	F _z (MPa)	F _{res} (MPa)	M _x (KNm)	M _y (KNm)	M _z (KNm)	M _{res} (KNm)
1	0.266	2.28	-0.103	2.3	815	-41.6	28.6	817

2	0.995	8.97	1.16	9.1	700	-41.8	86.2	707
---	-------	------	------	-----	-----	-------	------	-----

Table 8-9: OWT – Support reactions for full model and full loading. Forces and moments in supports 3 and 4 mirror 1 and 2 respectively and are shown in APPENDIX H.

Support	F _x (MPa)	F _y (MPa)	F _z (MPa)	F _{res} (MPa)	M _x (KNm)	M _y (KNm)	M _z (KNm)	M _{res} (KNm)
1	-0.092	-1.05	0.0824	1.05	103	39.3	-13.4	111
2	0.884	7.98	0.875	8.08	39.5	39	77.1	95.1

Table 8-10: O&G – Member stresses for full loading and full model

Description	Axial (MPa)	Bending Dir1 (MPa)	Bending Dir2 (MPa)	Torsional (MPa)	Von Mises (MPa)
Transition piece, front	-16.63	-6.47	40.63	-1.63	57.78
Transition piece, rear	-38.76	45.52	-9.03	-1.64	85.17
Leg, front, upper	-7.82	42.51	0.40	1.73	50.33
Leg, rear, upper	-42.35	42.47	1.46	1.74	84.84
Leg, front, middle	-9.26	-5.60	-0.43	0.93	14.88
Leg, front, lower	-13.96	1.05	-0.10	0.50	15.01
Top horizontal	-1.90	-4.16	-3.58	0.00	7.39

Table 8-11: OWT – Member stresses for full loading and full model

Description	Axial (MPa)	Bending Dir1 (MPa)	Bending Dir2 (MPa)	Torsional (MPa)	Von Mises (MPa)
Transition piece, front	16.29	-6.38	2.97	1.44	23.33
Transition piece, rear	-42.95	13.68	-19.33	1.44	66.64
Leg, front, upper	14.08	25.90	-0.29	2.08	39.98
Leg, rear, upper	-41.31	23.99	2.24	2.08	65.40
Leg, front, middle	12.66	-1.88	-0.44	1.08	14.59
Leg, front, lower	8.44	1.52	-0.15	0.58	9.97
Top horizontal	6.50	-3.34	-6.13	0.00	13.48

Table 8-12: Mode shapes and frequencies of different scenarios

Mode No.	O&G		OWT	
	Frequency (Hz)	Period (Sec)	Frequency (Hz)	Period (Sec)
1	0.51404	1.9454	0.25077	3.9877
2	0.51404	1.9454	0.25078	3.9876
3	0.5699	1.7547	1.4837	0.674
4	3.115	0.32103	1.4837	0.67398
5	3.3205	0.30116	2.3502	0.4255

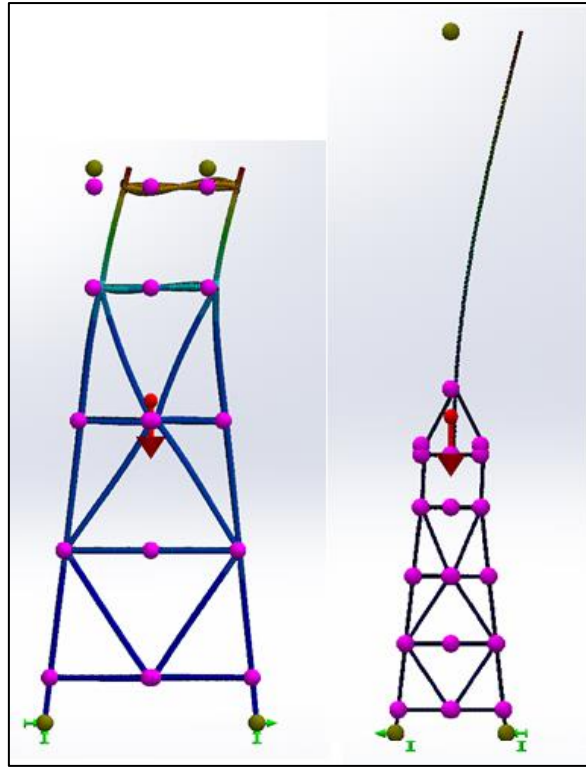


Figure 8.8: Fundamental mode shapes of both models

9. Discussion

Following the simulations, the results presented in the previous section were analysed with findings discussed in this section. The database analysis is first discussed. Each of the three simulations are then discussed followed by a discussion on the wider applicability of findings for the North Sea and criticism of the project.

9.1. Database Creation and Analysis

As per objectives 1 and 2 of this project, a database was created and analysed to find a representative model for subsequent analysis.

This database is determined to be accurate in terms of the number of platforms included as it draws from two independent lists. The data contained is found to be accurate for the Leman BH installation with the stated topside mass, jacket mass, and water depth all corresponding with the decommissioning document produced for the installation.

Both the number of platforms and accuracy of data contained may be improved by including more databases. This will likely only be possible by paying for access to more sophisticated databases. It can be reasonably assumed that the difference this would make would be marginal considering the large sample size already being used.

9.2. Simulation 1: Gravitational Loads Only.

Simulation 1 investigated the scenarios with only gravitational loads considered. The key data acquired was the stresses induced in the jacket and the (seabed) support reactions.

Jacket member stresses: For both scenarios all stresses are well within the permissible stresses as calculated in 5.1. Axial stresses are even across the four legs for the O&G model and slightly greater towards the front legs in the OWT scenario, this is in keeping

with the logic of the model and further validates it is performing correctly (wind turbines are typically weighted forward to compensate for wind thrust).

As shown in Table 8-4 and Table 8-5, Von Mises and axial stresses are reduced after retrofit by an average of 42% and 57% respectively for the jacket legs. Between scenarios, bending stresses are of negligible difference in all members except the transition pieces. This agrees with the result of the marginally forward position of the wind turbine centre of mass. In terms of stress induced by gravitational load only, the retrofit is shown to be possible.

Support Reactions and Moments: Support reaction forces calculated in this simulation are practically the same as that experienced by the models in still water and no wind. It is shown that support reaction forces are reduced by approximately 63% in all directions after retrofit. Additionally, moments in all directions are reduced by approximately the same percentage.

In this simulation, soil conditions are not considered. Considering that soil is usually modelled as non-linear springs, a 63% reduction in resultant forces will likely be of concern and a detailed study should be conducted in future. Where this is problematic, it is possible that this could be remedied by additional mass being added to the structure. This additional mass may also serve as a tuned mass damper as discussed in the subsequent discussion.

In terms of pile forces induced by gravitational load only, the retrofit is shown to be possible.

9.3. Simulation 2: Transition Piece

Simulation 2 investigated the action of the transition pieces on the jackets for wind and gravitational loading. In this simulation, joints between transition pieces and jackets were fixed to allow calculation reaction forces and moments at these points.

Transition piece member stresses: Again, left-hand and right-hand forces in members and supports are equal (as expected of the model) and well within the permissible stresses.

Jacket-Transition Piece Reaction Forces: Between scenarios, reaction forces in the X and Z (left/right, front/back respectively) are not significantly different.

As shown in Table 8-6 and Table 8-7, support reactions in the Y direction (upwards) are significantly different between scenarios. In the O&G scenario, both front and rear supports react in the positive Y direction whilst in the OWT scenario front supports react in the negative direction (i.e. tensile loading on the joints). The magnitude of this downward reaction is approximately a third of the upward reaction of the front joints. This creates a significant overturning force about the top of the jacket but, as shown in Simulation 3 results, the mass of the Leman BH jacket reduces this effect on the pilings. For future retrofits with lighter jackets than the Leman BH, this may be problematic. Although stress range is now greater on the jacket-transition piece joints (3.18MPa^4 compared to 8.76MPa^5 although stress magnitude has only marginally increased), it is unlikely to be problematic in terms of fatigue. The number of cyclic loads induced per day will be low due to the nature of wind changing direction slowly. Additionally, dynamic loading on these joints will not be of concern due to the quasistatic nature of wind loading.

Jacket-Transition Piece Moments: Differences in the moments about the joints are not notable for the Y and Z axes. Moment about the X axis is reduced by 30% as is the resulting moment consequentially. This reduced moment is encouraging for the

⁴ $5.82 - 2.64 = 3.18\text{MPa}$

⁵ $6.65 - (-2.11) = 8.76\text{MPa}$

prospect of retrofit and suggests that larger (both heavier and taller) wind turbines should be studied in future analyses.

9.4. Simulation 3: Full Simulation

Simulation 3 considered the full models with full loading. As before, for both scenarios all stresses are well within the permissible stresses as calculated in 5.1. Fixed supports are found on the seabed only (and not about the jacket-transition piece joints as in the previous simulation).

Jacket Stresses: From Table 8-10 and Table 8-11, significant differences between scenarios are observed. Figure 9.1 below visualises this difference for the transition pieces and Figure 9.2 for the legs. Von Mises stress in the legs is significantly lower for the OWT scenario across almost the entire length. Major divergence in stresses is shown above the third lowest elevation horizontal braces in which O&G stress far exceeds OWT stress.

This reduction in VM stress is found in every other member (including transition pieces) however axial stress varies. As found in the previous simulations, front leg and transition piece members are found to be in tension for OWT scenario whilst they are in compression for O&G scenario. The retrofit is shown to be possible in these terms.

Support Reactions and Moments: Following from the jacket stresses this results in front support reactions to be negative in the Y direction for the OWT scenario. As with the Simulation 2, if this is deemed to be problematic, additional mass could be added (although further study is required). Rear support resultant forces and moments are significantly reduced after retrofit therefore the jacket will likely be able to withstand more gravitational load than is currently modelled. The direction change is unlikely to be problematic as piles are typically in the order of hundreds of tonnes and length are typically tens of meters deep.

Natural Frequencies: The frequency analysis of the structures shows the fundamental frequency almost halves after retrofit which therefore increases the period required for excitation from 1.95s to 3.99s. The fundamental mode shapes are shown in Figure 8.8. These figures demonstrate what logically follows from adding masses at great lengths. This is problematic for the retrofit given the sea conditions it experiences. As shown in Figure 6.8, 4s waves are both far more common and more energetic than 2s waves. Again, an additional mass could be added on the retrofitted platform and act as a tuned mass damper so reducing the effect of this harmonic motion.

Furthermore, the blades passing the tower during power generation also introduces the possibility of harmonic motion. Cut in and rated rotor speeds are 6.9 and 12.1rpm respectively which, for the 3-bladed turbine, introduces a fluctuating load at a period between 2.9 to 1.65s. Although harmonic frequencies are not contained within this range, blade acceleration may be problematic.

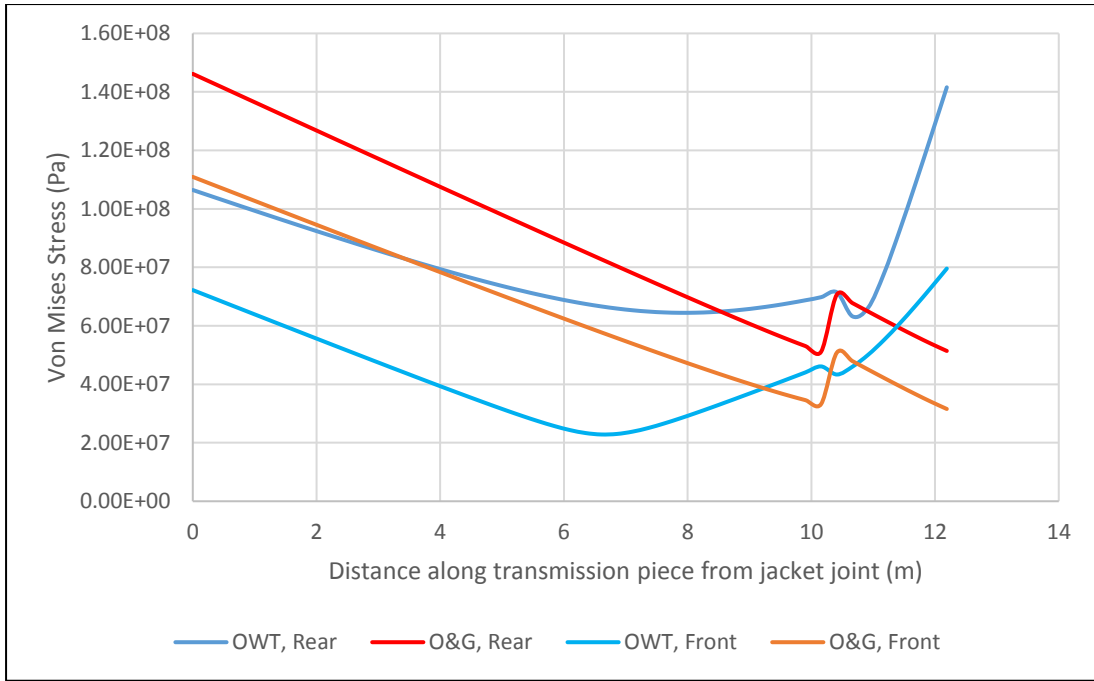


Figure 9.1: Von Mises stress in front and rear transition pieces with height between models for simulation 3

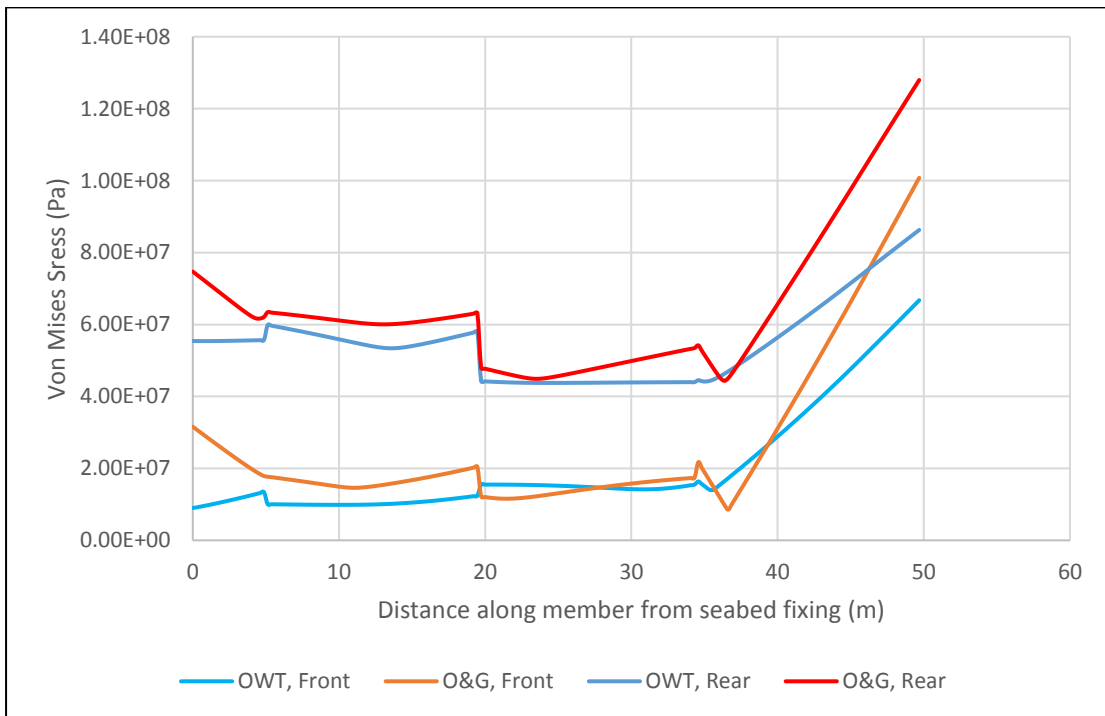


Figure 9.2: Von Mises stress in front and rear legs with height between models for simulation 3

9.5. North Sea Potential

Following the results of the simulations, retrofitting of the Lemman BH installation with a 5MW wind turbine appears possible although additional modification will likely be required. This is concluded from the reduced stresses experienced by the jacket after retrofit and the reduced reaction forces and moments on supports.

As discussed in 4, there are many similar or possibly better suited installations for retrofit. The database of installations suggests there are 96 4-legged fixed steel installations which are in a depth of $35.7\pm 5\text{m}$ or less and a topside mass of $990\pm 100\text{mT}$ which would be highly likely to better withstand the same forces generated by a 5MW site.

As shown in Simulation 2, the moment about the transition piece is lowered after retrofit. This therefore shows that jacket height is not a significant factor in retrofit suitability which allows an additional 101 installations to be added to the list of potential installations. This number makes a clearly invalid assumption that all topsides are of the same shape as the Lemman BH (hence the same wind and gravitational loading is produced). For the purposes of this approximate analysis, this number can be halved to 50.

This leaves a total of 146 potential installations. It must also be considered that many installations are too close to one another for them to both support turbines (due to the increased turbulence downstream of wind turbines due to wake effects). The database suggests that approximately a third of installations (109) are stand-alone. Other installations range in sets of between 2 and 17. It is assumed that these statistics are representative of the potential retrofit candidates. If all standalone installations are used and 1 in every 2 non-standalone installations then a total of 128 installations remain.

A more thorough analysis is clearly required (especially for non-jacket foundation structures). If a margin of error of 20% is taken, the analysis suggests there is a potential for 128 ± 25 5MW turbines or 640 ± 125 MW additional capacity.

It is highly likely that installations with far heavier topsides than the Leman BH could support larger capacity wind turbines which could greatly increase the potential installed capacity.

9.6. Criticism and Further Study

The study presented is lacking in many regards. A major area of improvement is in the calculation of wind and wave loading. Ideally, the models of both scenarios should be considered as single structures as opposed to members being studied separately or even compensated for with coefficients. A relevant software package would be used such as ANSYS, Sesam, or similar.

More loading conditions should also be considered. In this study, both wind and wave acted together perpendicular to a face of the installation. Future study should consider a greater number of angles of attack on the structure and include non-concurrent directions. This study would be greatly aided using the software packages indicated previously.

Wind turbine analysis can be improved in future by including actuation loading and the effect of the blades passing the tower during power generation.

Most critically, future analyses should consider soil conditions and p-y curves. This is a major consideration in the design of offshore structures and approximation as fixed points is reductive.

Generally, the study can be improved by considering a greater variety of platforms and wind turbines. Additionally, sensitivity analysis can be conducted in which loads are scaled up.

9.7. General Discussion on the Potential of Retrofit

Determining the potential for reuse of oil and gas installations for retrofitting with wind turbines is a study which requires far more than just technical suitability which is presented in this thesis.

The greatest driver is likely to be economic, which is not explored in this thesis. For oil and gas installation owners the revenue generated the wind turbines is likely to be a fraction of the previous revenue from oil and gas. Incentive to undergo such a retrofit would likely not be based on money but other factors such as green credentials. For wind turbine manufacturers, the bespoke nature of each project goes against the trend of mass producing wind turbines into farms so lowering costs. Additionally, the cost of the retrofit would have to include transmission of power to shore (very few installations are powered from shore so cabling would need to be installed). The cost of cabling is usually shared between turbines when installed in farms so it may be prohibitive for a stand-alone platform. Conversely, wind operator's costs may be further reduced by not needing to perform data gathering (sea, soil, and wind conditions) and a reduced environmental impact assessment.

Furthermore, the OSPAR agreement must be considered. This states that the responsibility of returning the seabed to its original state lies with the owner. Complications would arise between parties when considering liability and that retrofitting of these substructures does not mitigate the need to eventually decommission them but only delays it. Wind operators may be unwilling to buy the land due to the oversized decommissioning work the site may entail (ironic as this aspect is what makes the project possible). Oil and gas operators may be unwilling to lease the site as it would require 25 years (lifetime of a typical wind turbine) more of liability. It should be noted that this does not completely rule out the potential of these

installations for wind turbine use. In deeper waters where only floating platforms are applicable these O&G installations could possibly be used for housing substations. A modern substation topside may weigh around 2,000mT [42], the database contains 134 platforms with O&G topsides weight equal to or greater than this mass.

10. Conclusion

The potential for UKCS O&G installations for reuse as wind turbine support structures is presented.

A database containing over 300 platforms is presented. Of this database, it is estimated that there are 128 platforms suitable for retrofit with a 5MW wind turbines.

This number was arrived at through a theoretical retrofit of the Leman BH platform and FEA analysis. The Leman BH platform was chosen for study after analysis of the database and shown to be representative of the UKCS O&G stock in terms of jacket type, topside weight, and water depth.

Retrofit is shown to be likely possible using the simulations presented. These show:

- Decreased stress in all members of the jacket and permissible as per EN ISO 19902
- Decreased magnitudes of resulting forces and moments on pilings
- Decreased magnitudes of forces and moments about the joints between substructure and transition piece

However, two major concerns may prevent retrofit. These are: piling concerns and natural frequency concerns. It was found that all pilings are constantly compressed during O&G topside installation however, after retrofit and during extreme loading, upwind and downwind pilings are in tension and compression respectively. The effect of reversing reaction direction is unlikely to be problematic due to the mass of pilings. A possible solution of additional masses is suggested, both of which will require more study.

Fundamental period of the installation was found to increase from 1.95s to 3.99s. This is discussed to be potentially problematic but mitigatable (via tuned mass damper) but will also require additional study.

Finally, the project methods were critiqued. The following is cited as improvements for future studies:

- Increase sample sizes for both installations and wind turbines
- Perform full model wind and wave analyses with a greater number of loading directions considered
- Improve model accuracy by including joint-cans, include structure fatigue, and replace seabed rigid fixings with spring models with the appropriate p-y curves

The work presented is narrowly focused to a single installation and wind turbine but the conservative choice in installation produces promising results.

11. References

- [1] BBC News, “North Sea oil: Facts and figures,” 2014. [Online]. Available: <http://www.bbc.co.uk/news/uk-scotland-scotland-politics-26326117>. [Accessed: 22-Aug-2017].
- [2] Royal Academy of Engineering, “Decommissioning in the North Sea,” 2013.
- [3] Oil & Gas Authority, “Decommissioning Strategy,” 2016.
- [4] Wood Mackenzie, “Total Decom - UK North Sea decommissioning overview,” 2016.
- [5] “Offshore wind energy,” *The Crown Estate*, 2017. [Online]. Available: <https://www.thecrownestate.co.uk/energy-minerals-and-infrastructure/offshore-wind-energy/>. [Accessed: 24-Aug-2017].
- [6] “Wind Energy Statistics - RenewableUK,” 2017. [Online]. Available: <http://www.renewableuk.com/page/UKWEDhome>. [Accessed: 24-Aug-2017].
- [7] J. Jonkman, S. Butterfield, W. Musial, and G. Scott, “Definition of a 5-MW Reference Wind Turbine for Offshore System Development,” 2009.
- [8] “North Sea Image Gallery - Industry Projects - Offshore Technology.” [Online]. Available: http://www.offshore-technology.com/projects/north-sea_gallery.html. [Accessed: 25-Aug-2017].
- [9] GOV UK, “Digest of UK Energy Statistics (DUKES): renewable sources of energy, "Capacity of, and electricity generated from, renewable sources (DUKES 6.4)",” 2017. [Online]. Available: <https://www.gov.uk/government/statistics/renewable-sources-of-energy-chapter-6-digest-of-united-kingdom-energy-statistics-dukes>. [Accessed: 25-Aug-2017].
- [10] “Digest of UK Energy Statistics (DUKES) 2017: main report,” *Dukes/GOV.UK*, 2017. [Online]. Available: <https://www.gov.uk/government/statistics/digest-of-uk-energy-statistics-dukes-2017-main-report>. [Accessed: 25-Aug-2017].
- [11] E. Hau, *Wind Turbines: Fundamentals, Technologies, Application, Economics*, 2nd ed. Berlin Heidelberg: Springer , 2006.
- [12] “Offshore Wind Farms Diagram,” *A-Z Photo Gallery*, 2017. [Online]. Available: <http://www.praca-w-niemczech.info/imalodrm-offshore-wind-farms-diagram.html>. [Accessed: 25-Aug-2017].
- [13] “Monopiles Support Structures - 4C Offshore.” [Online]. Available: <http://www.4coffshore.com/windfarms/monopiles-support-structures-aid4.html>. [Accessed: 21-Aug-2017].
- [14] CarbonTrust, “Offshore wind industry review of GBSs,” 2015.
- [15] OffshoreWind.net, “Offshore Wind Turbine Foundations- Current & Future Prototypes | OffshoreWind.net.” [Online]. Available: <http://offshorewind.net/offshore-wind-turbine-foundations-current-future-prototypes/>. [Accessed: 21-Aug-2017].
- [16] CarbonTrust, “Floating Offshore Wind Market Technology Review,” 2015.
- [17] “World’s first floating wind farm emerges off coast of Scotland - BBC News,” 2017. [Online]. Available: <http://www.bbc.co.uk/news/business-40699979>. [Accessed: 22-Aug-2017].
- [18] P. Higgins and A. Foley, “The evolution of offshore wind power in the United Kingdom,” *Renew. Sustain. Energy Rev.*, vol. 37, pp. 599–612, 2014.
- [19] European Wind Energy Association, “The European offshore wind industry -

- key trends and statistics 2015,” 2016.
- [20] 4Coffshore, “Beatrice Offshore Wind Farm,” 2017. [Online]. Available: <http://www.4coffshore.com/windfarms/beatrice-united-kingdom-uk53.html>. [Accessed: 22-Aug-2017].
- [21] 4Coffshore, “Dogger Bank - Teesside A,” 2017. [Online]. Available: <http://www.4coffshore.com/windfarms/dogger-bank---teesside-a-united-kingdom-uk1f.html>. [Accessed: 22-Aug-2017].
- [22] C. Desmond, J. Murphy, L. Blonk, and W. Haans, “Description of an 8 MW reference wind turbine,” *J. Phys. Conf. Ser.*, 2016.
- [23] University of Aberdeen, “The Project: Brief History of North Sea Oil and Gas Industry,” 2006. [Online]. Available: <http://www.abdn.ac.uk/oillives/about/nsoghist.shtml>. [Accessed: 22-Aug-2017].
- [24] P. A. Risanto, “Introduction to Offshore Oil and Gas Surface Facilities.” [Online]. Available: <https://www.slideshare.net/PuputAryanto/introduction-to-offshore-oil-and-gas-surface-facilities>. [Accessed: 25-Aug-2017].
- [25] Oil and Gas Authority, “Current UKCS Installations,” ogaauthority, 2017.
- [26] M. A. El-Reedy, “Chapter 3 – Offshore Structure Platform Design,” in *Offshore Structures*, 2012, pp. 93–211.
- [27] S. Gourvenec and M. Cassidy, “New Frontiers in Offshore Geotechnics and Foundation Design,” Taylor & Francis, 2016.
- [28] Scottish Enterprise and Decom North Sea, “Decommissioning in the North Sea: Review of Decommissioning Capacity,” 2014.
- [29] Y. English, “The past, present and future of the North Sea Oil & Gas industry,” *Fircroft*, 2017. [Online]. Available: <https://www.fircroft.com/blogs/the-past-present-and-future-of-the-north-sea-oil-and-gas-71391914124>. [Accessed: 25-Aug-2017].
- [30] J. C. Barros, G. C. Fernandes, M. M. Silva, R. P. Da Silva, and B. Santos, “Fixed Platforms at Ageing Oil Fields - Feasibility Study for Reuse to Wind Farms,” in *Offshore Technology Conference*, 2017.
- [31] Y. Wang, M. Duan, and J. Shang, “Application of an Abandoned Jacket For an Offshore Structure Base of Wind Turbine In Bohai Heavy Ice Conditions,” Jan. 2009.
- [32] Scottish Enterprise, “Oil and Gas ‘Seize the Opportunity’ Guides: Offshore Wind,” 2015.
- [33] GOV.UK, “Peterhead Carbon Capture and Storage Project - GOV.UK,” 2014. [Online]. Available: <https://www.gov.uk/government/news/peterhead-carbon-capture-and-storage-project>. [Accessed: 25-Aug-2017].
- [34] R. A. Caulk and I. Tomac, “Reuse of abandoned oil and gas wells for geothermal energy production,” *Renew. Energy*, vol. 112, pp. 388–397, 2017.
- [35] PWC, “As decommissioning looms, it’s time to think outside the box: is it better to reuse, repurpose, recycle – or just remove?,” 2015. [Online]. Available: http://pwc.blogs.com/energy_spotlight/2015/12/as-decommissioning-looms-its-time-to-think-outside-the-box-is-it-better-to-reuse-repurpose-recycle-o.html. [Accessed: 25-Aug-2017].
- [36] B. B. Bernstein *et al.*, “Evaluating Alternatives for Decommissioning California’s Offshore Oil and Gas Platforms: A Technical Analysis to Inform State Policy.”
- [37] “North Sea Decommissioning Database,” *Oil & Gas UK*, 2012. [Online]. Available: <http://oilandgasuk.co.uk/product/north-sea-decommissioning-database/>. [Accessed: 25-Aug-2017].

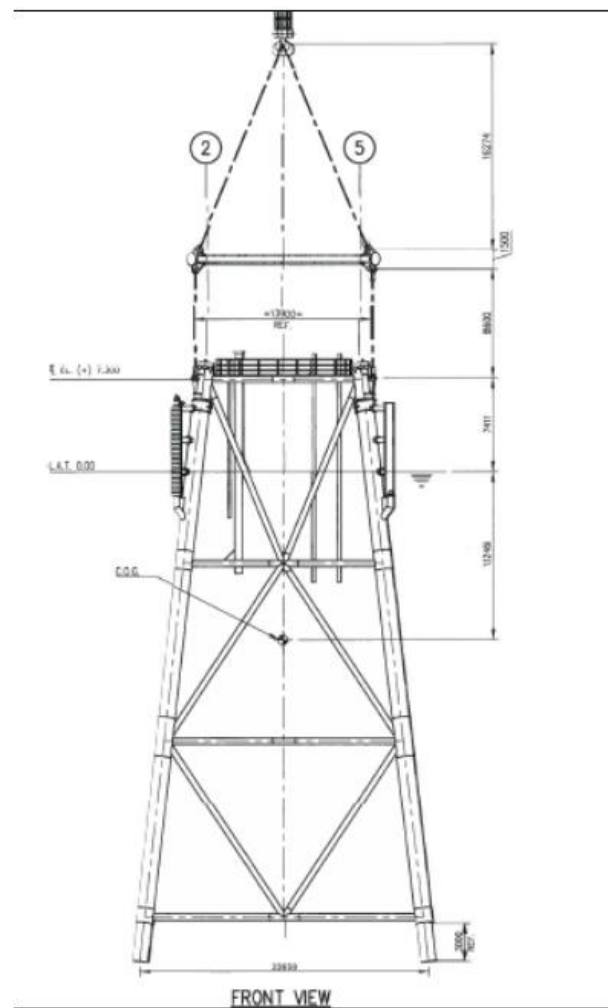
- [38] ShellUK, “leman-bh.jpeg (800×450).” [Online]. Available: http://www.shell.co.uk/sustainability/decommissioning/leman-bh-decommissioning/_jcr_content/pagePromo/image.img.800.jpeg/1438278592545/leman-bh.jpeg. [Accessed: 25-Aug-2017].
- [39] R. Sparreboom, “Leman BH Decommissioning Programme,” 2015.
- [40] Urra et al, “HOWaT | Hybrid Offshore Wind and Tidal.” [Online]. Available: http://www.esru.strath.ac.uk/EandE/Web_sites/16-17/windandtidal/index.html. [Accessed: 25-Aug-2017].
- [41] Fugro GEOS, “Wind and wave frequency distributions for sites around the British Isles,” 2001.
- [42] “Rampion Offshore Substation Jacket In Place,” *offshoreWIND.biz*, 2017. [Online]. Available: <http://www.offshorewind.biz/2017/01/13/rampion-offshore-substation-jacket-in-place/>. [Accessed: 24-Aug-2017].

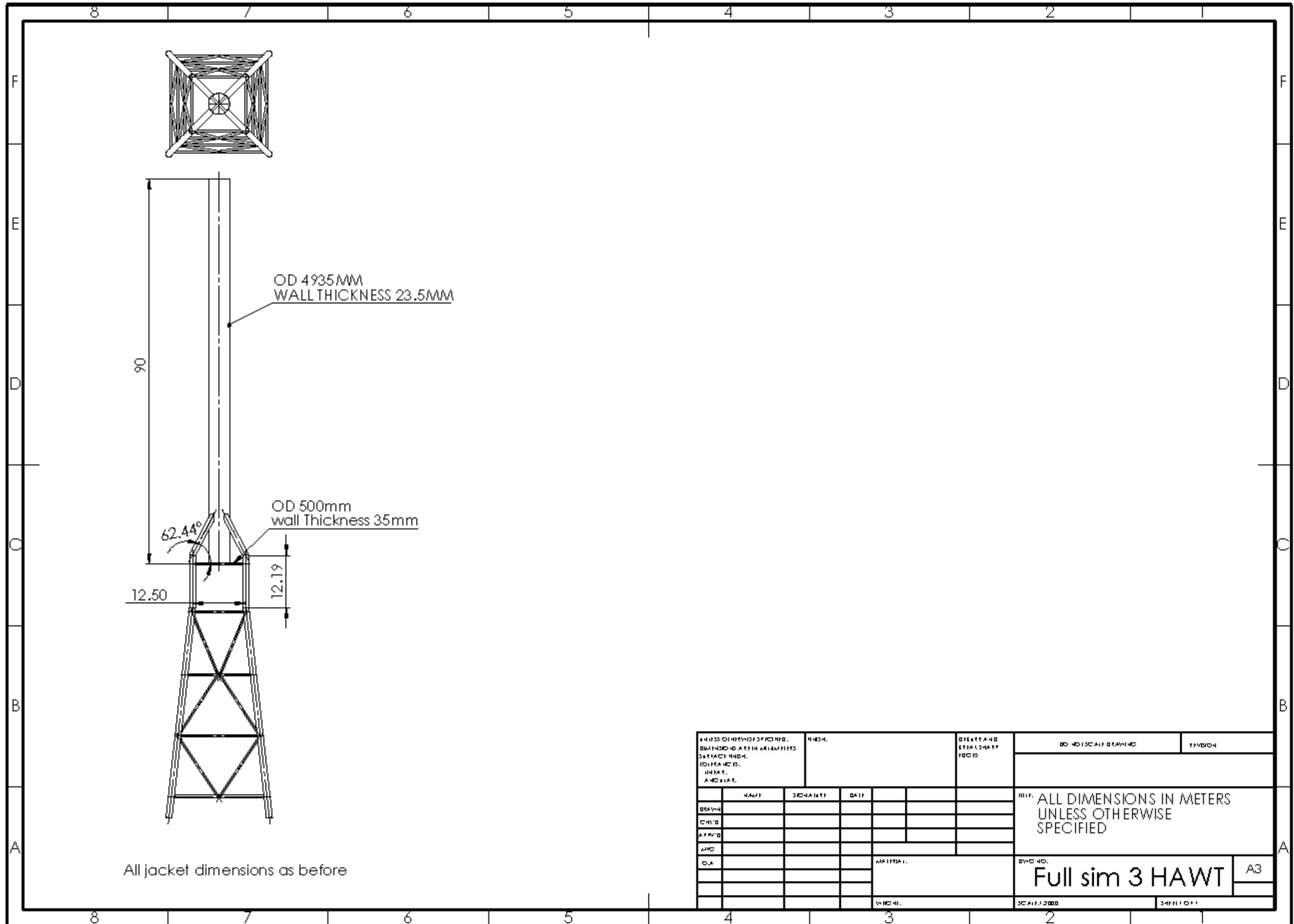
12. Appendix

12.1. Appendix A - Drawings of Models

Original drawing from the Leman BH decommissioning document

Figure 3.4 Jacket Elevation





UNLESS OTHERWISE SPECIFIED, DIMENSIONS ARE IN METERS. SURFACE FINISH, TOLERANCES, UNITS, AND ETC.		MESH		OPERATOR AND SPECIAL MARKINGS		DO NOT SCALE DRAWING		REVISION	
DESIGN		DATE				ALL DIMENSIONS IN METERS UNLESS OTHERWISE SPECIFIED			
CHK'D									
APP'D									
AWD									
DIA									
				MATERIAL		BYC NO.		A3	
				INSTR.		SCALE: 1:2000		SHEET NO. 1	

12.2. Appendix B - Solidworks model verification

The following are screen captures via Solidworks for the simulations described in 5.4

Jacket Validation.

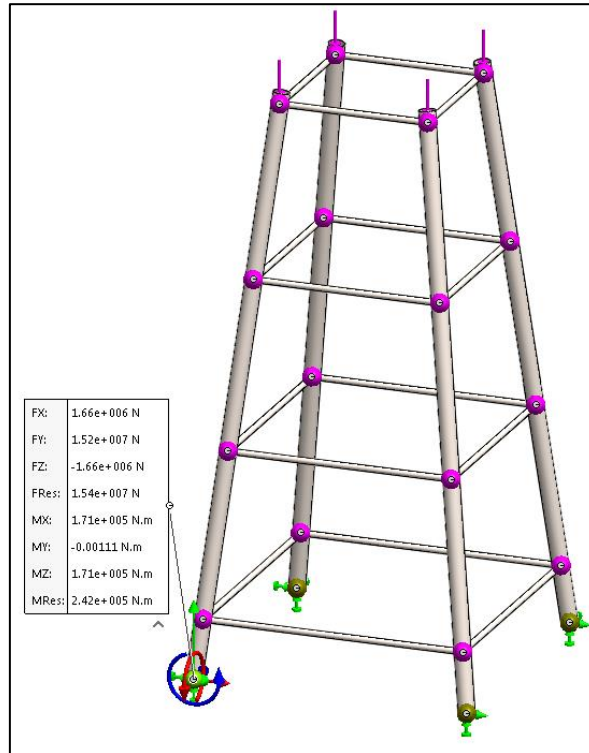


Figure 12.1: Resultant force at point A

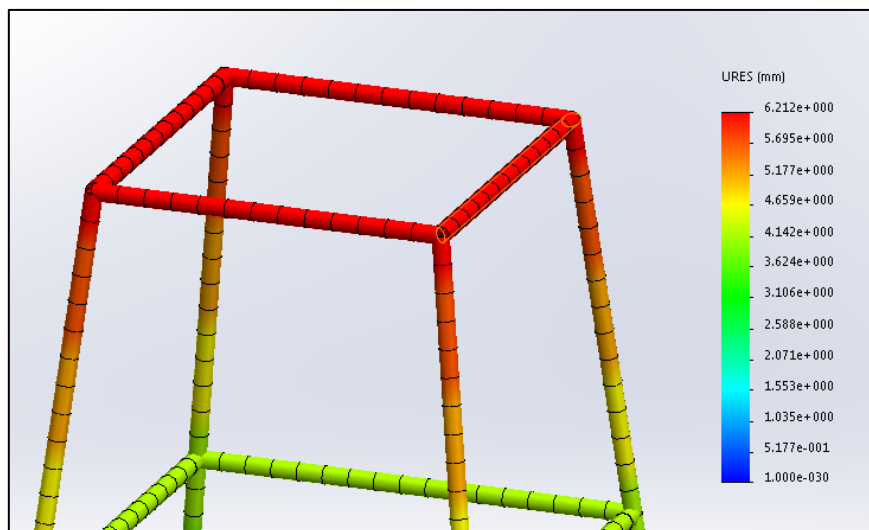


Figure 12.2: Displacement

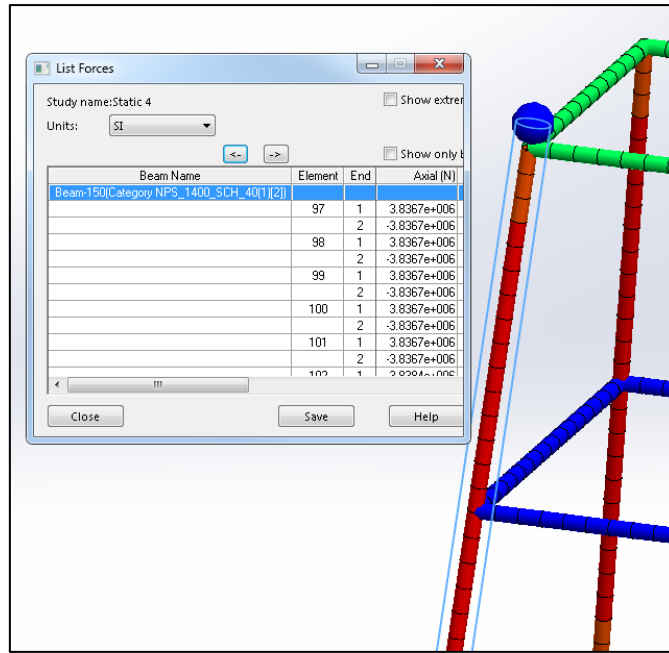


Figure 12.3: Resultant force in leg

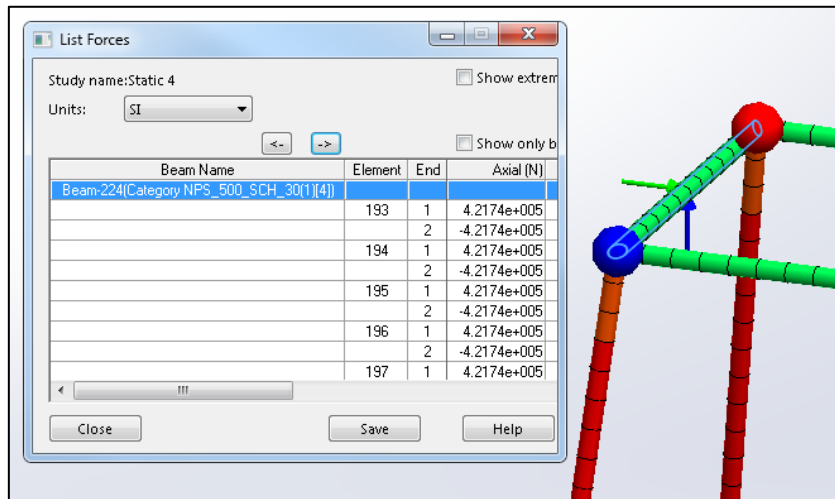


Figure 12.4: Resultant force in member EF

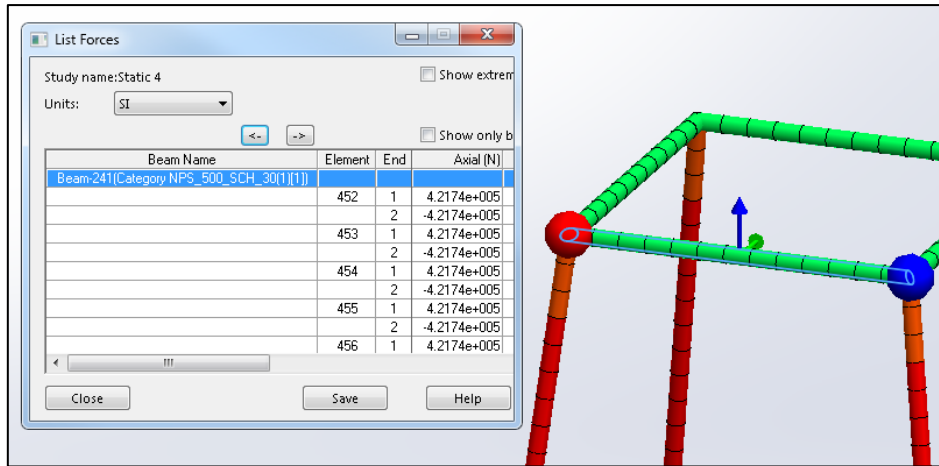


Figure 12.5: Resultant force in member EG

12.3. Appendix C - Wind Profile Calculation

The fundamental basic wind velocity was determined from the National Annex for the standard used. The Lemn complex is located 50Km North East of the Norwich coast (UKCS quadrant 49/26) as indicated in Figure 12.6. This corresponds to a fundamental basic wind velocity, $V_{b,0}$, of 24m/s as per Figure 12.7.

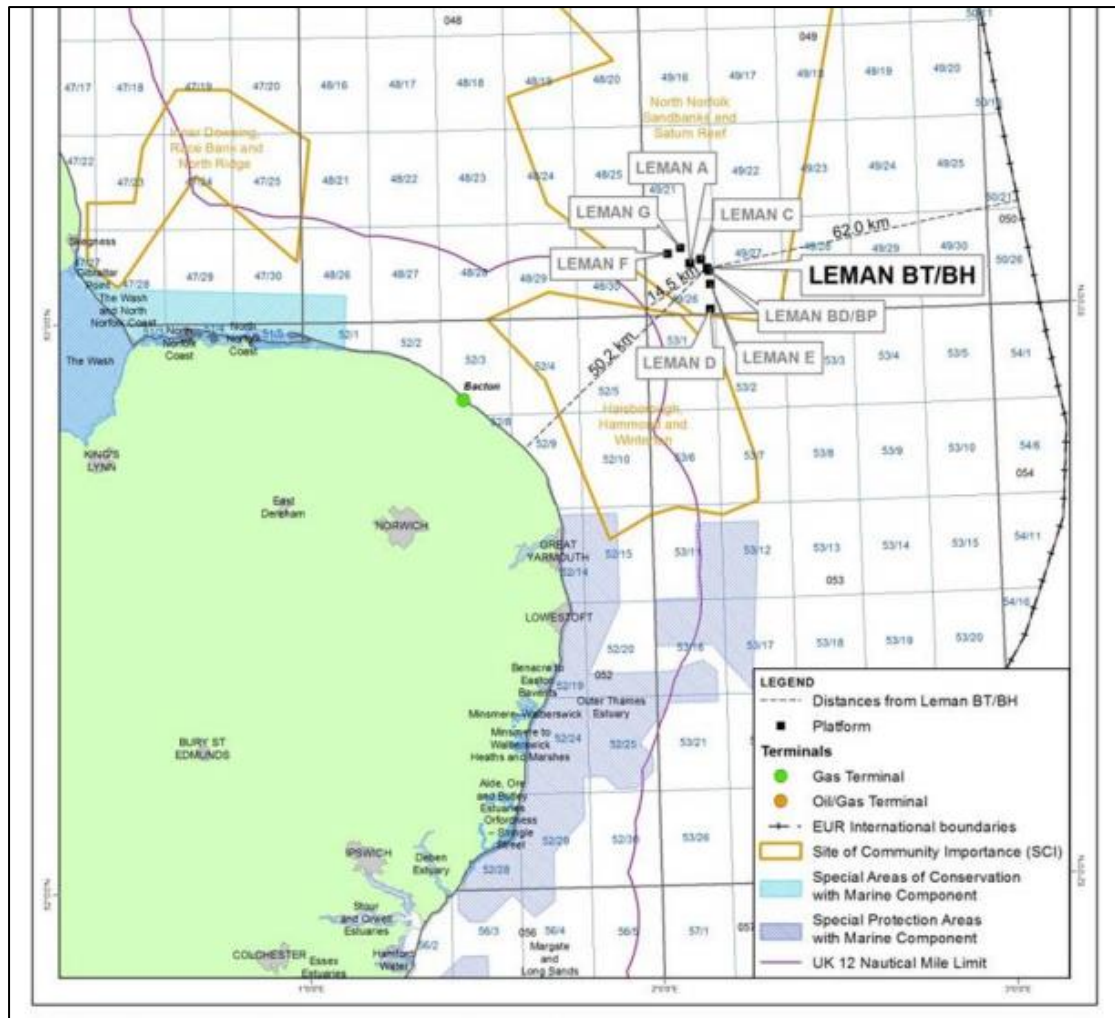


Figure 12.6: Location of the Leman BH installation off the coast of Norwich.

Figure NA.1 Value of fundamental basic wind velocity $v_{b,map}$ (m/s) before the altitude correction is applied

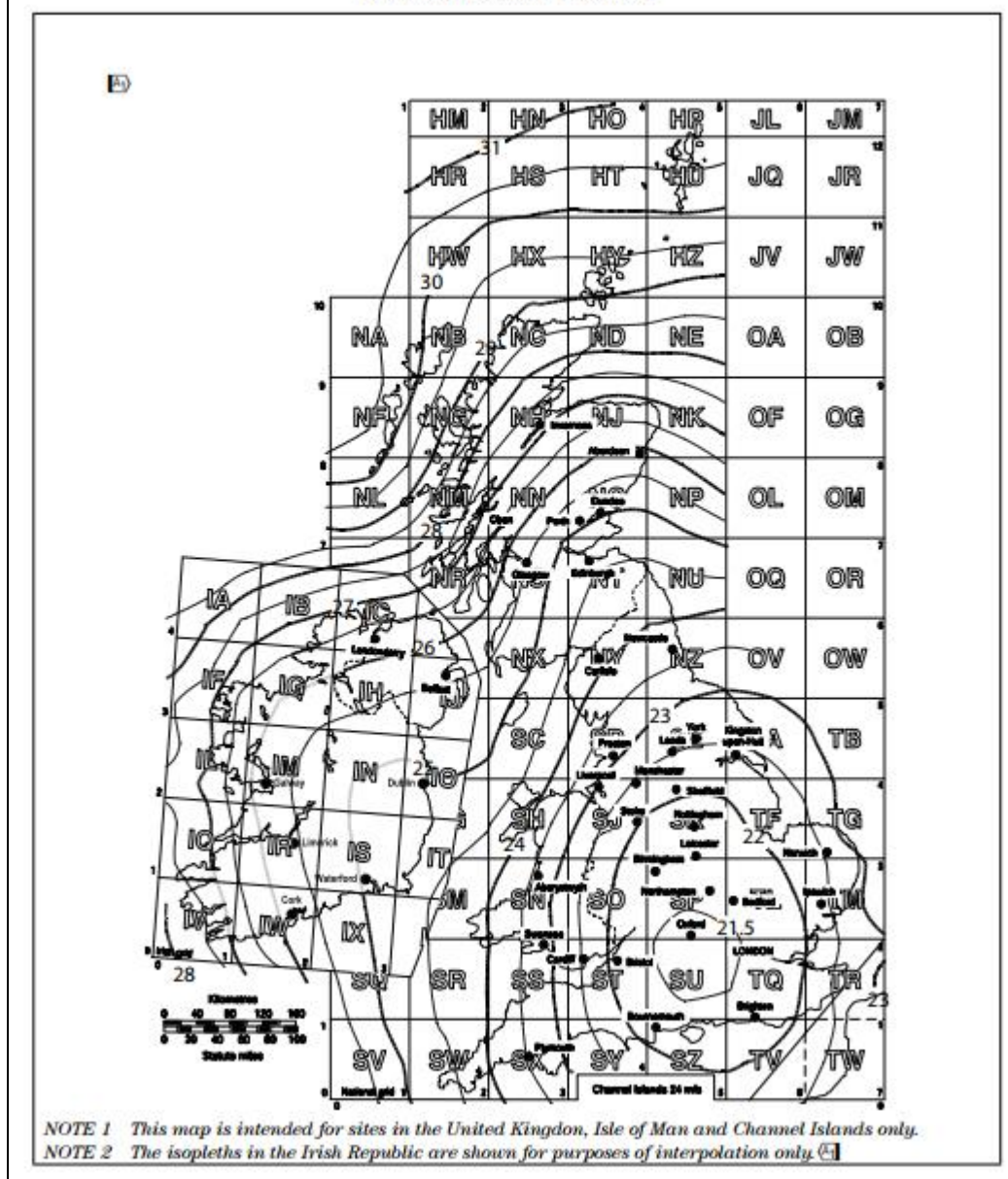


Figure 12.7: Fundamental basic wind velocity map from NA to BS EN 1991-1-4

$V_{b,0}$ is usually adjusted for site altitude as per NA 2.4 using the equation :

$$V_{b,0} = V_{b,map} \cdot C_{alt}$$

Where C_{alt} is the altitude factor and $V_{b,map}$ is the fundamental basic wind velocity found from Figure 12.6. For the site C_{alt} was set to 1 which corresponds to an altitude of at 0m (i.e. sea level) hence for the Leman site $V_{b,0}$ is equal to $V_{b,map}$.

Following on from obtaining the fundamental basic wind velocity, the basic wind velocity is determined using equation X:

$$V_b = C_{dir} \cdot C_{season} \cdot V_{b,0}$$

Where C_{dir} is the directional factor and C_{season} is the season factor. Both values are taken as 1.0 for conservative calculation of forces thereby resulting in the basic and fundamental basic wind velocities being equal.

Mean wind as a function of height, $V_m(z)$, is then calculated using equation x:

$$V_m(z) = C_r(z) \cdot C_0(z) \cdot V_b$$

Where $C_r(z)$ is the roughness factor as a function of height (given by equation the equation below) and $C_0(z)$ is the orography factor which is taken as 1.0 due to the site:

$$C_r(z) = K_r \cdot \ln\left(\frac{z}{Z_0}\right)$$

Roughness factor is the determined by the terrain factor, K_r , (given by equation the equation below) and the roughness length. Roughness length, Z_0 , is taken as 0.003 for open sea areas [as per table 4.1 of standard]:

$$K_r = 0.19 \cdot \left(\frac{z}{Z_{0,II}}\right)^{0.07}$$

Where $Z_{0,II}$ is the roughness length for category II areas (areas of low vegetation) and is equal to 0.05. Therefore:

$$K_r = 0.19 \cdot \left(\frac{0.003}{0.05}\right)^{0.07} = 0.1560$$

Turbulence

Turbulence intensity as a function of height, $I_v(z)$, was calculated as using the following equation:

$$I_v(z) = \frac{k_t}{c_0(z) \cdot \ln\left(\frac{z}{Z_0}\right)}$$

Where K_1 is the turbulence factor which is taken as 1.0 due to the low-turbulence seascape of the site. $L_v(z)$ is plotted in Figure 12.8.

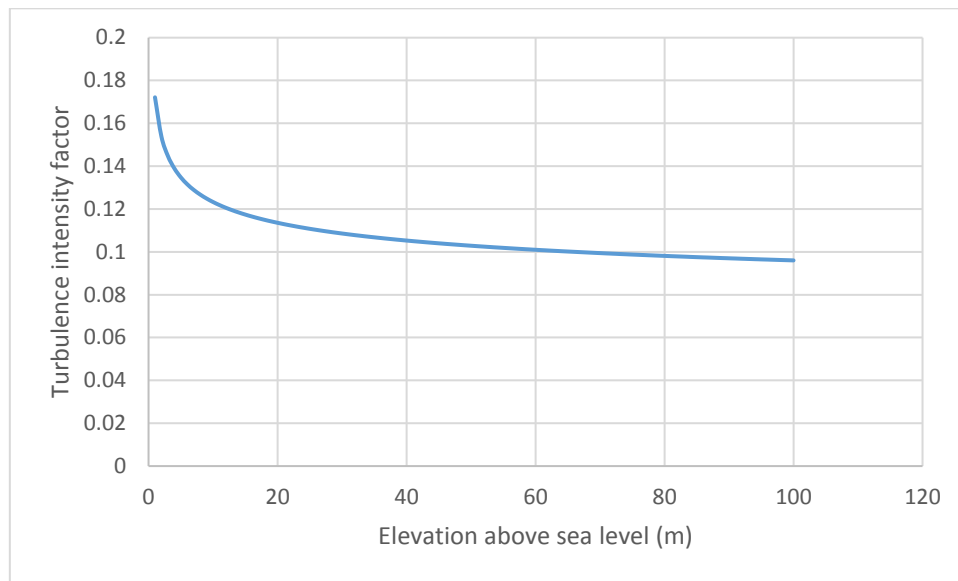


Figure 12.8: Turbulence intensity of wind with elevation above sea level for Lemna BH site

Peak Velocity Pressure

Next, peak velocity pressure with elevation, $q_p(z)$, was calculated using the equation:

$$q_p(z) = [1 + 7 \cdot l_v(z)] \cdot \frac{1}{2} \cdot \rho \cdot v_m^2(z)$$

Air density is taken to be 1.226kg/m^3 as per the National Annex. Peak velocity pressure is plotted with turbulence intensity and height in Figure 12.9.

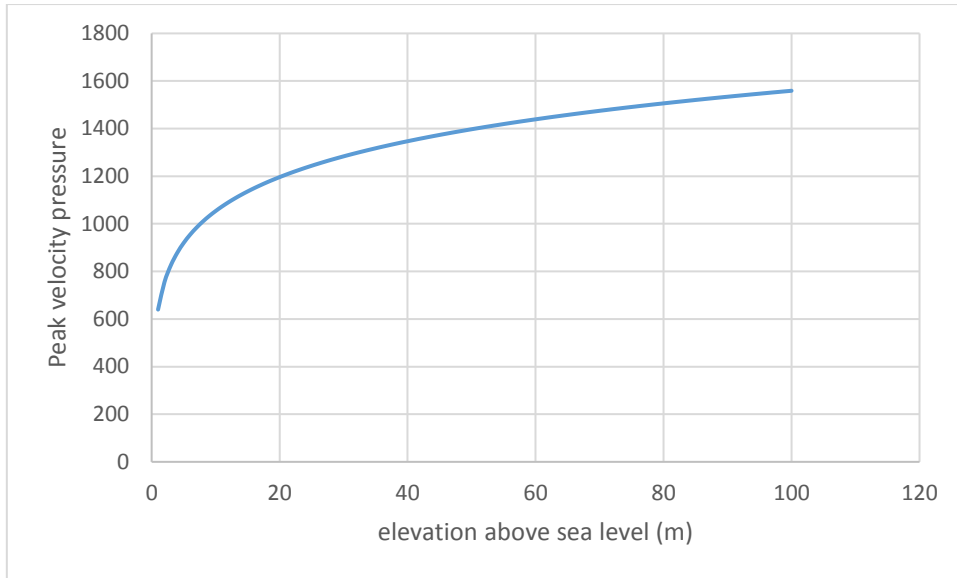


Figure 12.9: Peak velocity pressure with elevation above sea level for Lemnan BH site

Peak Wind Speed

Peak wind speed with elevation is then calculated is calculated from peak velocity pressure using the equation below and is presented in Figure 12.10:

$$V_m(z) = \sqrt{\frac{2 \cdot q_p(z)}{\rho}}$$

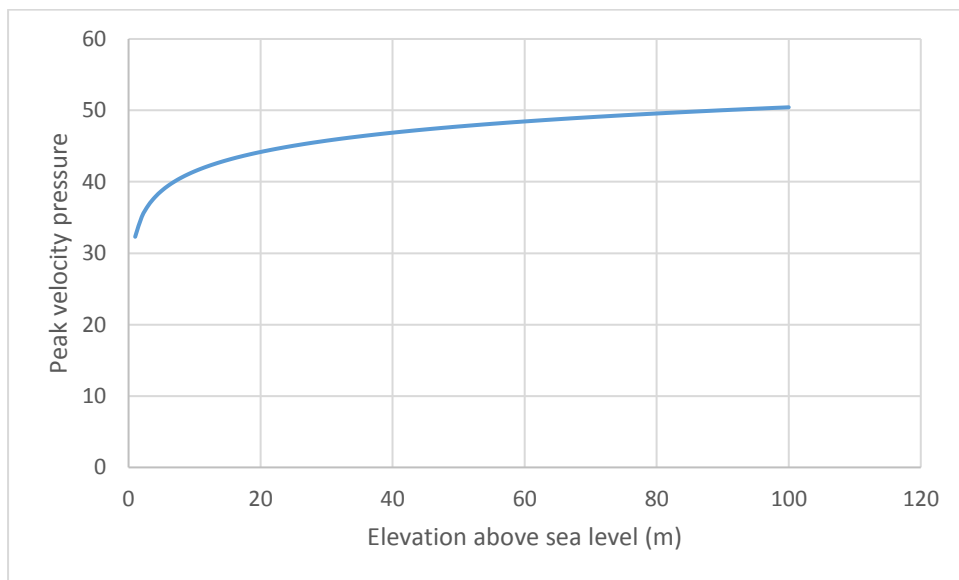


Figure 12.10: Peak wind velocity with elevation above sea level for Lemnan BH site

12.4. Appendix D - Wave Profile Calculation

Wave profile for the site was calculated as per DNV RP-C205 “Environmental Conditions and Environmental Loads”.

For the Lemna BH installation, water depth is 37.5m. The literature suggests that there are no significant seabed features to effect the propagation of waves (such as reefs) hence regular waves are assumed. A range of significant wave heights, H, and wave periods, T, were taken are presented in Table 12-1. These values were obtained from HSE wave spectra data shown in Figure 6.8 from a site 15512 as shown in Figure 12.11.

Table 12-1

	H (m)	T (s)	Lo (m)	d/Lo	d/L	L (m)
1	2	3.75	22.0	1.62	1.00	35.7
2	4	7	76.5	0.47	0.47	75.9
3	4	8.5	112.8	0.32	0.33	108.1
4	4	10	156.1	0.23	0.25	142.7
5	3.2	11	188.9	0.19	0.21	169.8
6	2.3	11	188.9	0.19	0.21	169.8
7	2	11.5	206.5	0.17	0.20	178.3
8	7.5	10	156.1	0.23	0.25	142.7
9	6	11	188.9	0.19	0.21	169.8
10	5	12	224.8	0.16	0.19	187.7

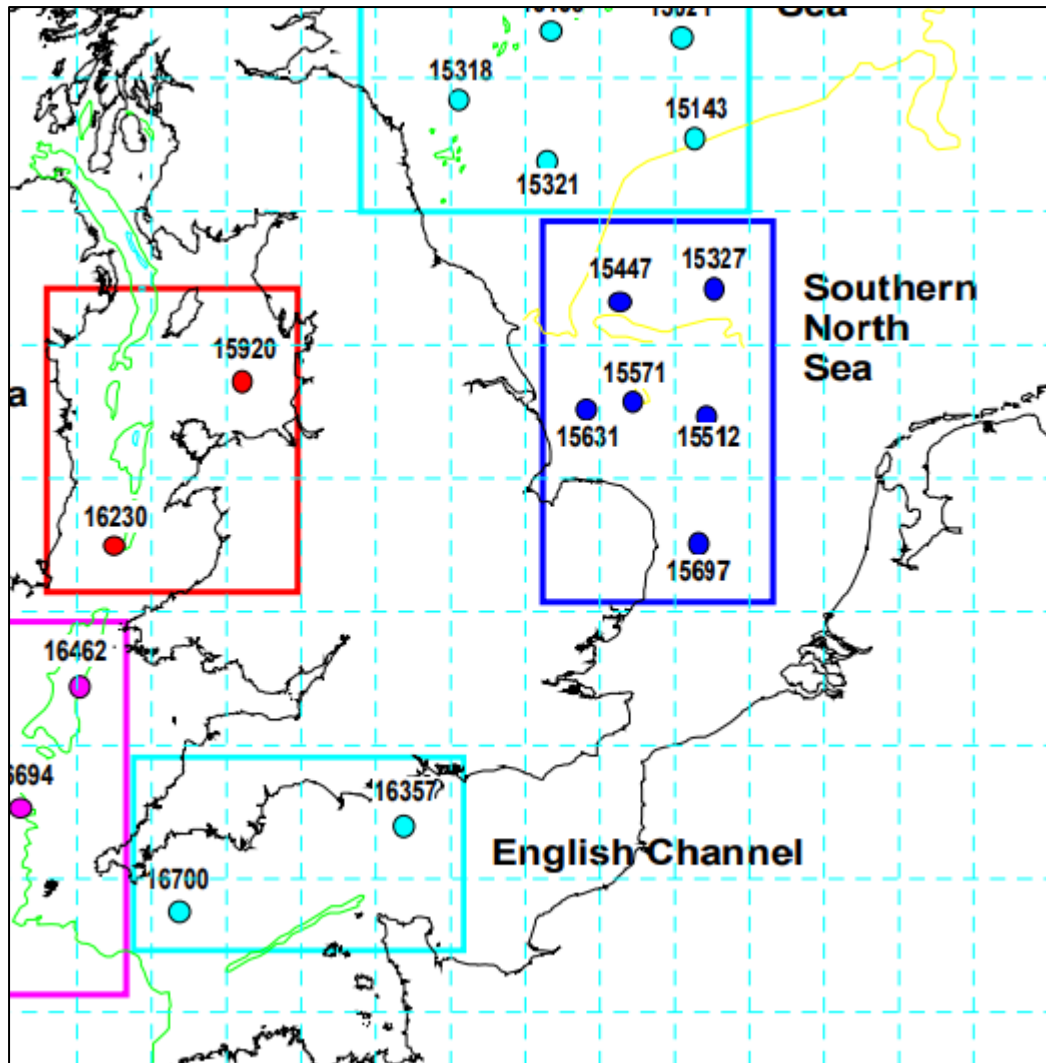


Figure 12.11

This data was then used to determine the appropriate wave theory as per Figure 12.12 with the values determined displayed in Table 12-1. Linear wave theory (Airy) was therefore used throughout.

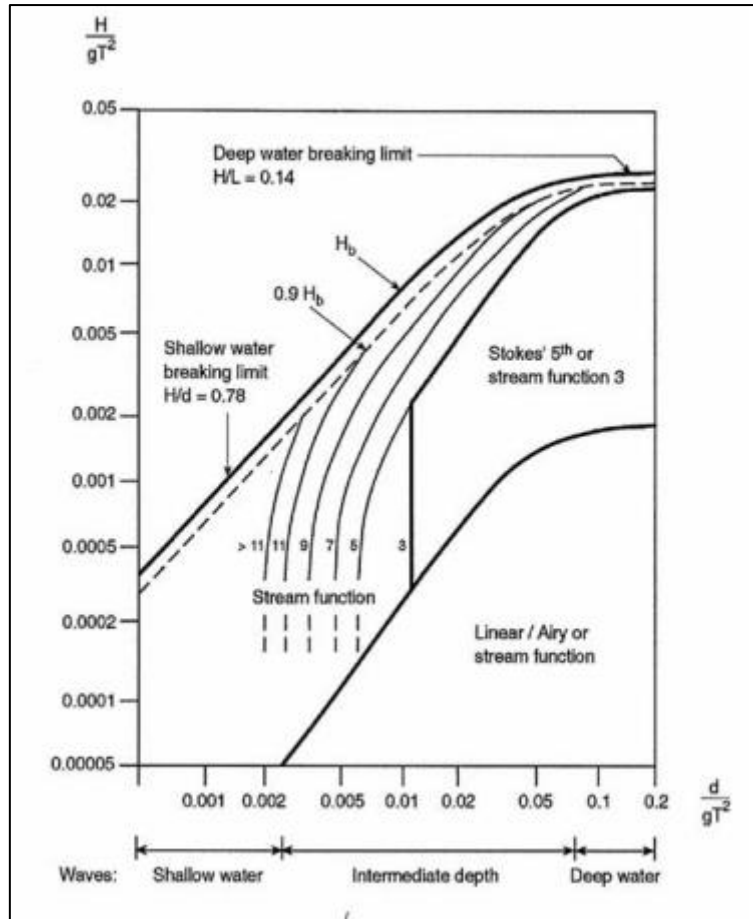


Figure 12.12; From DNV RP-C205

Deepwater wavelength, L_0 , was subsequently calculated using the following equation with results presented in Table 12-1:

$$L_0 = \frac{gT^2}{2\pi}$$

$$L_0 = (g * T^2) / (2 * \pi)$$

Wavelength, L , was then calculated using the ratio of waterdepth, d , and deepwater wavelength and the corresponding wave equation table factor (see Appendix E) with results presented in Table 12-1.

Horizontal wave velocity, u , was then calculated using the following equation:

$$U = \frac{\pi H \cosh(k(z + d))}{T \sinh(kd)} \sin(\theta)$$

Horizontal wave acceleration, u^* , is calculated using the following equation:

$$\dot{U} = \frac{-\pi^2 H \cosh(k(z+d))}{T^2 \sinh(kd)} \cos(\theta)$$

12.5. Appendix E - Wave Equation Table used for calculation

Data is obtained from the following website:

[https://www.usna.edu/Users/oceano/pguth/website/so422web/handouts/wave_tables.p](https://www.usna.edu/Users/oceano/pguth/website/so422web/handouts/wave_tables.pdf)

[df](#)

Wave Equation Tables for SO422 (9/05)													
d/L	d/L ₀	2πd/L	tanh (2πd/L)	sinh (2πd/L)	n	H/H ₀ '	d/L	d/L ₀	2πd/L	tanh (2πd/L)	sinh (2πd/L)	n	H/H ₀ '
0.010	0.0006	0.063	0.063	0.063	0.999	2.825	0.165	0.1281	1.037	0.777	1.233	0.765	0.917
0.0125	0.0010	0.079	0.078	0.079	0.998	2.528	0.170	0.1341	1.068	0.789	1.283	0.756	0.916
0.015	0.0014	0.094	0.094	0.094	0.997	2.310	0.175	0.1401	1.100	0.800	1.335	0.747	0.915
0.0175	0.0019	0.110	0.110	0.110	0.996	2.141	0.180	0.1460	1.131	0.811	1.388	0.738	0.914
0.020	0.0025	0.126	0.125	0.126	0.995	2.005	0.185	0.1520	1.162	0.822	1.442	0.730	0.913
0.0225	0.0032	0.141	0.140	0.142	0.993	1.893	0.190	0.1580	1.194	0.832	1.498	0.721	0.913
0.025	0.0039	0.157	0.156	0.158	0.992	1.799	0.195	0.1640	1.225	0.841	1.556	0.713	0.913
0.0275	0.0047	0.173	0.171	0.174	0.990	1.718	0.200	0.1700	1.257	0.850	1.614	0.705	0.913
0.030	0.0056	0.188	0.186	0.190	0.988	1.648	0.220	0.1939	1.382	0.881	1.867	0.675	0.917
0.0325	0.0065	0.204	0.201	0.206	0.986	1.586	0.230	0.2058	1.445	0.895	2.003	0.661	0.919
0.035	0.0076	0.220	0.216	0.222	0.984	1.532	0.240	0.2176	1.508	0.907	2.148	0.648	0.922
0.0375	0.0087	0.236	0.231	0.238	0.982	1.484	0.250	0.2293	1.571	0.917	2.301	0.636	0.926
0.040	0.0098	0.251	0.246	0.254	0.980	1.440	0.260	0.2409	1.634	0.927	2.464	0.625	0.929
0.0425	0.0111	0.267	0.261	0.270	0.977	1.401	0.270	0.2524	1.696	0.935	2.636	0.614	0.933
0.045	0.0124	0.283	0.275	0.287	0.974	1.365	0.280	0.2639	1.759	0.942	2.818	0.604	0.937
0.0475	0.0138	0.298	0.290	0.303	0.971	1.332	0.290	0.2752	1.822	0.949	3.012	0.595	0.941
0.050	0.0152	0.314	0.304	0.319	0.969	1.303	0.300	0.2865	1.885	0.955	3.217	0.587	0.944
0.0525	0.0167	0.330	0.318	0.336	0.965	1.275	0.310	0.2976	1.948	0.960	3.435	0.579	0.948
0.055	0.0183	0.346	0.332	0.352	0.962	1.250	0.320	0.3087	2.011	0.965	3.667	0.572	0.952
0.0575	0.0199	0.361	0.346	0.369	0.959	1.227	0.330	0.3197	2.073	0.969	3.913	0.566	0.955
0.060	0.0216	0.377	0.360	0.386	0.956	1.205	0.340	0.3306	2.136	0.972	4.175	0.560	0.959
0.0625	0.0234	0.393	0.374	0.403	0.952	1.185	0.350	0.3415	2.199	0.976	4.453	0.554	0.962
0.065	0.0252	0.408	0.387	0.420	0.948	1.167	0.360	0.3523	2.262	0.979	4.749	0.549	0.965
0.0675	0.0270	0.424	0.400	0.437	0.945	1.150	0.370	0.3630	2.325	0.981	5.063	0.544	0.967
0.070	0.0289	0.440	0.413	0.454	0.941	1.134	0.380	0.3736	2.388	0.983	5.398	0.540	0.970
0.0725	0.0309	0.456	0.426	0.471	0.937	1.119	0.390	0.3842	2.450	0.985	5.754	0.536	0.973
0.075	0.0329	0.471	0.439	0.489	0.933	1.105	0.400	0.3948	2.513	0.987	6.132	0.533	0.975
0.0775	0.0350	0.487	0.452	0.506	0.929	1.092	0.410	0.4053	2.576	0.988	6.535	0.530	0.977
0.080	0.0371	0.503	0.464	0.524	0.925	1.079	0.420	0.4157	2.639	0.990	6.963	0.527	0.979
0.0825	0.0393	0.518	0.476	0.542	0.921	1.068	0.430	0.4261	2.702	0.991	7.420	0.524	0.981
0.085	0.0415	0.534	0.488	0.560	0.916	1.057	0.440	0.4365	2.765	0.992	7.905	0.522	0.983
0.0875	0.0438	0.550	0.500	0.578	0.912	1.047	0.450	0.4469	2.827	0.993	8.421	0.520	0.984
0.090	0.0461	0.565	0.512	0.596	0.907	1.037	0.460	0.4572	2.890	0.994	8.971	0.518	0.986
0.0925	0.0484	0.581	0.524	0.614	0.903	1.028	0.470	0.4674	2.953	0.995	9.557	0.516	0.987
0.095	0.0508	0.597	0.535	0.633	0.898	1.020	0.480	0.4777	3.016	0.995	10.180	0.514	0.988
0.0975	0.0532	0.613	0.546	0.652	0.894	1.012	0.490	0.4879	3.079	0.996	10.843	0.513	0.989
0.100	0.0557	0.628	0.557	0.670	0.889	1.005	0.500	0.4981	3.142	0.996	11.549	0.512	0.990
0.110	0.0659	0.691	0.599	0.748	0.870	0.980	0.550	0.5489	3.456	0.998	15.825	0.507	0.994
0.115	0.0711	0.723	0.618	0.787	0.861	0.969	0.600	0.5994	3.770	0.999	21.677	0.504	0.997
0.120	0.0765	0.754	0.638	0.827	0.851	0.960	0.650	0.6496	4.084	0.999	29.685	0.502	0.998
0.125	0.0820	0.785	0.656	0.869	0.841	0.952	0.700	0.6998	4.398	1.000	40.647	0.501	0.999
0.130	0.0875	0.817	0.673	0.911	0.832	0.945	0.750	0.7499	4.712	1.000	55.654	0.501	0.999
0.135	0.0932	0.848	0.690	0.954	0.822	0.939	0.800	0.7999	5.027	1.000	76.200	0.500	1.000
0.140	0.0989	0.880	0.706	0.998	0.812	0.934	0.850	0.8500	5.341	1.000	104.328	0.500	1.000
0.145	0.1046	0.911	0.722	1.042	0.803	0.929	0.900	0.9000	5.655	1.000	142.837	0.500	1.000
0.150	0.1105	0.942	0.736	1.088	0.793	0.925	0.950	0.9500	5.969	1.000	195.561	0.500	1.000
0.155	0.1163	0.974	0.750	1.135	0.783	0.922	1.000	1.0000	6.283	1.000	267.745	0.500	1.000
0.160	0.1222	1.005	0.764	1.183	0.774	0.920							

12.6. Appendix F – Simulation 1

O&G - Support reactions for gravitational loads only

Support	F_x (MPa)	F_y (MPa)	F_z (MPa)	F_{res} (MPa)	M_x (KNm)	M_y (KNm)	M_z (KNm)	M_{res} (KNm)
1	0.63	5.62	-0.63	5.69	57.4	0	57.4	81.2
2	0.63	5.62	0.63	5.69	-57.4	0	57.4	81.2
3	-0.63	5.62	0.63	5.69	-57.4	0	-57.4	81.2
4	-0.63	5.62	-0.63	5.69	57.4	0	-57.4	81.2

Wind turbine – Support reactions for gravitational loads only

Support	F_x (MPa)	F_y (MPa)	F_z (MPa)	F_{res} (MPa)	M_x (KNm)	M_y (KNm)	M_z (KNm)	M_{res} (KNm)
1	0.398	3.49	-0.396	3.53	40.5	-1.16	32.1	51.7
2	0.394	3.45	0.396	3.49	-23.2	-1.16	31.6	39.2
3	-0.398	3.49	-0.396	3.53	40.5	1.16	-32.1	51.7
4	-0.394	3.45	0.396	3.49	-23.2	1.16	-31.6	39.2

Stresses in key members for gravitational loads only

Desc	Axial (MPa)	Bending Dir1 (MPa)	Bending Dir2 (MPa)	Torsional (MPa)	Von Mises (MPa)
Transition piece, front	-27.69	1.26	-1.26	0.00	29.47
Transition piece, rear	-27.71	1.45	-1.45	0.00	29.76
Leg, front, upper	-25.09	0.85	0.87	0.00	26.31
Leg, rear, upper	-25.08	-0.94	0.95	0.00	26.42
Leg, front, middle	-26.54	-0.60	-0.61	0.00	27.39
Leg, rear, middle	-26.52	0.56	-0.56	0.00	27.31
Leg, front, lower	-36.52	-0.01	-0.01	0.00	36.53
Leg, rear, lower	-36.52	0.01	-0.01	0.00	36.53
Top horizontal	-4.28	-5.33	0.00	0.00	9.61
2nd bottom horizontal	3.88	-10.44	0.00	0.00	14.32

Wind turbine – Stresses in key members for gravitational loads only

Desc	Axial (MPa)	Bending Dir1 (MPa)	Bending Dir2 (MPa)	Torsional (MPa)	Von Mises (MPa)
Transition piece, front	-13.58	6.42	-6.46	-0.01	22.69
Transition piece, rear	-13.08	6.27	-6.30	-0.01	21.97
Leg, front, upper	-13.78	0.91	0.99	-0.01	15.13
Leg, rear, upper	-13.44	-1.01	0.95	-0.01	14.84
Leg, front, middle	-15.24	-0.63	-0.64	0.00	16.14
Leg, rear, middle	-14.88	0.57	-0.58	0.00	15.70
Leg, front, lower	-22.12	-0.02	0.00	0.00	22.14
Leg, rear, lower	-21.85	-0.01	-0.01	0.00	21.86
Top horizontal	-3.41	-5.29	0.03	0.00	8.71
2nd bottom hori	1.80	-10.34	-0.01	0.00	12.14
Tower mid	-12.64	0.00	2.13	0.00	14.76
Tower lower	1.07	0.00	0.92	0.00	1.99
Tower above Transition piece	-15.34	0.00	2.13	0.00	17.47

12.7. Appendix G – Simulation 2

O&G – Transition piece reactions for full loading.

Support	F _x (MPa)	F _y (MPa)	F _z (MPa)	F _{res} (MPa)	M _x (MNm)	M _y (MNm)	M _z (MNm)	M _{res} (MNm)
1	0.0874	2.64	0.442	2.68	5.4	-0.10	-0.206	5.41
2	-0.065	5.82	0.465	5.84	5.47	-0.10	0.137	5.48
3	0.0648	5.82	0.465	5.84	5.47	0.10	-0.137	5.48
4	-0.087	2.64	0.442	2.68	5.4	0.10	0.206	5.41

OWT – Transition piece reactions for full loading.

Support	F_x (MPa)	F_y (MPa)	F_z (MPa)	F_{res} (MPa)	M_x (MNm)	M_y (MNm)	M_z (MNm)	M_{res} (MNm)
1	0.0835	-2.11	0.468	2.16	3.92	0.305	-0.215	3.94
2	-0.212	6.65	0.34	6.66	3.64	0.305	0.5	3.68
3	0.212	6.65	0.34	6.66	3.64	-0.315	-0.5	3.68
4	-0.084	-2.11	0.468	2.16	3.92	-0.305	0.215	3.94

12.8. Appendix H – Simulation 3

O&G – Support reactions for full model and full loading.

Support	F_x (MPa)	F_y (MPa)	F_z (MPa)	F_{res} (MPa)	M_x (KNm)	M_y (KNm)	M_z (KNm)	M_{res} (KNm)
1	0.266	2.28	-0.103	2.3	815	-41.6	28.6	817
2	0.995	8.97	1.16	9.1	700	-41.8	86.2	707
3	-0.995	8.97	1.16	9.1	700	41.6	-86.2	707
4	0.266	2.28	-0.103	2.3	815	41.8	-28.7	817

Support reactions for full model and full loading.

Support	F_x (MPa)	F_y (MPa)	F_z (MPa)	F_{res} (MPa)	M_x (KNm)	M_y (KNm)	M_z (KNm)	M_{res} (KNm)
1	-0.092	-1.05	0.0824	1.05	103	39.3	-13.4	111
2	0.884	7.98	0.875	8.08	39.5	39	77.1	95.1
3	-0.884	7.98	0.875	8.08	39.6	-39.3	-77.1	95.2
4	0.0918	-1.05	0.0824	1.05	103	-39	13.4	11.1

O&G – Member stresses for full loading and full model

Description	Axial (MPa)	Bending Dir1 (MPa)	Bending Dir2 (MPa)	Torsional (MPa)	Von Mises (MPa)
Transition piece, front	-16.63	-6.47	40.63	-1.63	57.78
Transition piece, rear	-38.76	45.52	-9.03	-1.64	85.17
Leg, front, upper	-7.82	42.51	0.40	1.73	50.33
Leg, rear, upper	-42.35	42.47	1.46	1.74	84.84
Leg, front, middle	-9.26	-5.60	-0.43	0.93	14.88
Leg, rear, middle	-43.80	-4.66	-0.77	0.94	48.52
Leg, front, lower	-13.96	1.05	-0.10	0.50	15.01
Leg, rear, lower	-59.08	1.07	0.08	0.50	60.15
Top horizontal	-1.90	-4.16	-3.58	0.00	7.39
2nd bottom hori	-1.72	-10.27	0.69	0.00	12.02

OWT – Member stresses for full loading and full model

Description	Axial (MPa)	Bending Dir1 (MPa)	Bending Dir2 (MPa)	Torsional (MPa)	Von Mises (MPa)
Transition piece, front	16.29	-6.38	2.97	1.44	23.33
Transition piece, rear	-42.95	13.68	-19.33	1.44	66.64
Leg, front, upper	14.08	25.90	-0.29	2.08	39.98
Leg, rear, upper	-41.31	23.99	2.24	2.08	65.40
Leg, front, middle	12.66	-1.88	-0.44	1.08	14.59
Leg, rear, middle	-42.79	-0.68	-0.82	1.09	43.85
Leg, front, lower	8.44	1.52	-0.15	0.58	9.97
Leg, rear, lower	-52.41	1.53	0.15	0.58	53.95
Top horizontal	6.50	-3.34	-6.13	0.00	13.48
2nd bottom hori	-7.49	-10.13	0.91	0.00	17.66
Tower mid	-12.64	0.00	-89.46	0.00	102.10
Tower lower	1.07	0.00	-80.88	0.00	81.95
Tower above Transition piece	-15.34	0.00	-194.66	0.00	210.00